Lehrstuhl für Raumfahrttechnik
Prof. Prof. h.c. Dr. Dr. h.c. Ulrich Walter

Technische Universität München

Masterthesis

Error Analysis for the Life Support System Model of the ISS in V-HAB

RT-MA 2018/10

Author:

B. Sc. Moritz Edelhäuser

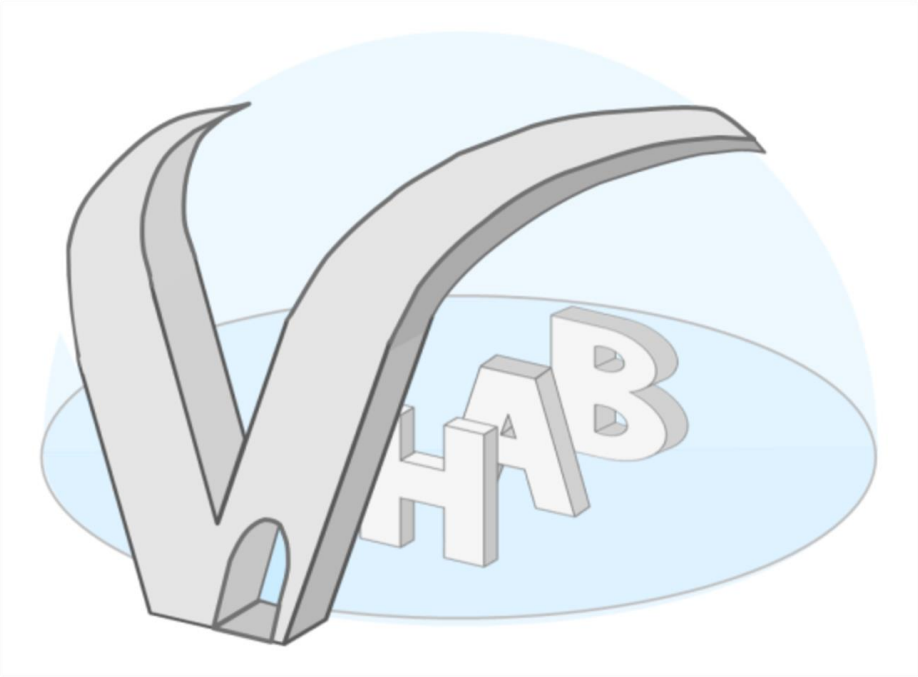

Betreuer: M. Sc. Daniel Pütz
Lehrstuhl für Raumfahrttechnik / Institute of Astronautics
Technische Universität München

Lehrstuhl für Raumfahrttechnik
Prof. Prof. h.c. Dr. Dr. h.c. Ulrich Walter

Technische Universität München

LRT-Nummer: RT-MA 2018/10

Titel der Arbeit: Error Analysis for the Life Support System Model of the ISS in V-HAB

Autor: B. Sc. Moritz Edelhäuser

Matrikelnummer: 03620616

Erklärung

Mir als vertraulich genannte Informationen, Unterlagen und Erkenntnisse werde ich nach meiner Tätigkeit am Lehrstuhl nicht an Dritte weitergeben.

Ich erkläre mich außerdem damit einverstanden, dass meine Bachelor-, Semester-, Master-/Diplomarbeit vom Lehrstuhl auf Anfrage fachlich interessierten Personen, auch über eine Bibliothek, zugänglich gemacht wird, und dass darin enthaltene Ergebnisse sowie dabei entstandene Entwicklungen und Programme vom Lehrstuhl für Raumfahrttechnik uneingeschränkt genutzt werden dürfen. (Rechte an evtl. entstehenden Programmen und Erfindungen müssen im Vorfeld geklärt werden.)

Ich erkläre außerdem, dass ich diese Arbeit ohne fremde Hilfe angefertigt und nur die in dem Literaturverzeichnis angeführten Quellen und Hilfsmittel benutzt habe.

Garching, den _____

_____

Unterschrift

Acknowledgments

First of all, I would like to thank my advisor M. Sc. Daniel Pütz, who always provides advice and support. He did not only have an open ear when it came to problems, but he was always able to give new food for thoughts, so that this work could even be created in this form. Additionally, he supports not only me, but all his students, with the basic techniques to write such a thesis in regular meetings.

Finally, I would like to thank my parents and my wife, who have supported me throughout my studies and have always been at my side with good advice.

Zusammenfassung

In dieser Masterarbeit wird eine Sensitivitätsanalyse und eine Fehlerfortpflanzungsrechnung für ein Simulationsmodell des Lebenserhaltungssystems (LSS) der Internationalen Raum Station (ISS), das in der Simulationsumgebung Virtual Habitat (V-HAB) entwickelt wurde, durchgeführt. V-HAB ist am Lehrstuhl für Raumfahrtechnik (LRT) an der Technischen Universität München (TUM) während einer langjährigen Forschungsarbeit entstanden. Die Grundlegende Aufgabenstellung ist die Untersuchung von Auswirkungen auf die Simulationsergebnisse, die durch Änderung bestimmter Simulationsparameter ausgelöst werden, wodurch der mögliche Fehler der Simulation im Vergleich zum realen System abgeschätzt werden soll. Zusätzlich wird mit den daraus folgenden Ergebnissen eine Fehlerfortpflanzungsrechnung durchgeführt.

Dafür ist es in einem ersten Schritt notwendig Simulationsparameter, die aufgrund von nicht exakt bekannten technischen Spezifikationen, natürlichen Schwankungen oder bestimmten Modellierungsannahmen eine Variation zulassen, zu identifizieren und die Simulation entsprechend zu modifizieren, sodass eine Änderung der Parameter nachvollziehbar möglich ist. Die Machbarkeit aller neu implementierten Simulationswerte wird mit Testsimulationen nachgewiesen und die Auswirkungen auf die Simulationsergebnisse mithilfe einer Sensitivitätsanalyse auf Plausibilität und Richtigkeit geprüft.

Bereits vorhandene Verfahren zur Fehlerfortpflanzungsrechnung werden vorgestellt und das für die vorliegende Problemstellung am besten Passende ausgewählt und dafür angepasst. Daraus wird für den bestehenden Fall eine Methodik zur Erstellung von Funktionen für die Berechnung von Abweichungen, aufgrund von Variationen in bestimmten Simulationsparametern, abgeleitet und eine Kurzanleitung dafür bereitgestellt (Standard Approach). Diese Methodik wird außerdem modifiziert um einen weiteren Berechnungsansatz (Advanced Approach) zu erhalten, der bessere Ergebnisse verspricht. Außerdem wird ein Ansatz zur Bestimmung der Modellierungsfehler von kompletten Subsystemen und deren Einordnung während der Fehlerrechnung beispielhaft vorgestellt. Diese beiden Methodiken werden für die Abweichung der relativen Luftfeuchtigkeit durchgeführt und Abweichungsfunktionen hierfür erstellt.

Zur Verifikation der entwickelten Funktionen werden einige Vergleichssimulationen durchgeführt, die mit den entsprechenden Ergebnissen aus den beiden Fehlerrechnungen verglichen werden und damit die Genauigkeit von diesen abgeschätzt. Der Standard Approach lieferte während diesen Vergleichssimulationen meist schlechte Ergebnisse und die guten Ergebnisse beruhten meist auf Zufall und waren nicht verlässlich. Mit dem Advanced Approach konnten bessere und vor allem nachvollziehbare Ergebnisse erzielt werden. Für die Abschätzung von Abweichungen, die von einzelnen geänderten Parametern verursacht wurden, konnten sehr genau Werte berechnet werden. Die Ergebnisse bei mehreren veränderten Parametern genügten noch zur Bestimmung der Größenordnung und Richtung der Abweichungen. Am Ende konnte ein Bereich, indem die Ergebnisse der Simulation aufgrund der Änderungen variieren, angeben werden. Daraus folgte auch eine Abschätzung der Abweichung der Simulationsergebnisse von der Realität, die aber weiterhin von noch unbekannten Fehlern, wie den Subsystemfehlern, abhängt.

Abstract

This thesis performs a sensitivity analysis and an error propagation for a simulation model of the LSS on the ISS, which has been developed in the simulation environment of V-HAB. V-HAB results from a long year research work at the LRT of the TUM. The general task is the examination of variations of certain simulation parameters, whereby the possible error of the simulation compared to the real system should be estimated. If possible, an error propagation calculation should be done thereby.

Therefore, in a first step it is necessary to identify the simulation parameters, which allow a variation because of not exactly known technical specifications, natural oscillations or certain modelling assumptions, and to modify the simulation so that a variation of the parameters is possible and comprehensible. The feasibility of the new implemented simulation values is tested with test simulations and the impact on the simulation results is proven by a sensitivity analysis for plausibility and accuracy.

Already known techniques for error propagation are investigated and the best fitted one for the existing problem is chosen and adapted. Hence a method for the creation of functions to calculate deviations because of variations in simulation parameters is developed and a short guidance for this is provided (Standard approach). Furthermore, this method is modified, to get another calculation approach (Advanced approach), which promises better results. Moreover, an approach to determine errors of the subsystem models and their classification during the error calculation is exemplary presented.

As an example, these calculating methods are performed for the deviation of the relative humidity and deviation-functions are generated.

For verification of the developed functions some comparative simulations are done, which are compared with the results from the error calculations and so the accuracy of these functions is estimated.

The Standard Approach yielded mostly poor results during these comparison simulations and the good results were usually random and not reliable. With the Advanced Approach, better and above all more comprehensible results could be achieved. For the estimating of deviations, which were caused by single changed parameters, very accurate values could be calculated. The results with several changed parameters were sufficient to determine the magnitude and direction of the deviations. In the end, an area where the results of the simulation vary due to the changes, could be specified. This also resulted in an estimation of the deviation of the simulation results from reality, which still depends on unknown error values, such as the subsystem errors.

Table of Contents

List of Figures

List of Tables

Symbols

T	Temperature
ΔT	Temperature difference
c_{sat}	Maximal absolute air moisture
R_D	Gas constant of water vapor
e_{sd}	Saturation water vapor pressure
E_m	Metabolic rate for males
E_f	Metabolic rate for females
a	Age
m	Mass
h	Height
$\bar{s}_f$	Standard Deviation
q^*_i	Equilibrium loading
m_i	Toth variable
b_i	Toth variable
q_{si}	Predefined toth parameter
m_{0i}	Predefined toth parameter
b_{0i}	Predefined toth parameter
B_i	Predefined toth parameter
m_{Ti}	Predefined toth parameter
P_i	Partial pressure of the absorbed substance
$\Delta\lambda$	Total error
$\Delta\lambda_{St.}$	Total error calculated with the standard approach
$\Delta\lambda_{Ad.}$	Total error calculated with the advanced approach
$\Delta\lambda_{mean}$	Mean error
$\Delta\lambda_{max}$	Maximal error

Abbreviations

ACLS	Advanced Closed Loop System
Adj.	Adjusted
ARS	Air Revitalization System
BMI	Body Mass Index
BPA	Brine Processor Assembly
CCAA	Common Cabin Air Assembly
CDRA	Carbon Dioxide Removal Assembly
CH_4	Methan
CHX	Condensing Heat Exchanger
CO_2	Carbon Dioxide
ExMe	Extract Merge Processor
F2F	Flow to Flow Processor
FGM	Functional Cargo Module
H_2	Hydrogen
H_2O	Water
HX	Heat Exchanger
IMV	Inter Modular Ventilation
ISS	International Space Station
JEM	Japanese Experiment Module
K	Kelvin
LRT	Institute of Astronautics
LSS	Life Support System
M	Manipulator
NaN	Not a Number
O_2	Oxygen
OGA	Oxygen Generation Assembly
P2P	Phase to Phase Processor
RMSE	Root Mean Squared Error
SCRA	Sabatier Carbon Dioxide Reprocessing Assembly
SM	Service Modul
SSE	Sum of Squares Due to Error
TUM	Technical University Munich
V-HAB	Virtual Habitat

1 Introduction

1.1 Situation

Every manned space mission, a flight to the ISS or a flight to other planets, needs, in contrast to an unmanned mission, an LSS. If you want to develop such an LSS it will be very expensive, take an immense amount of time and will be difficult to test, because of the unique environment in space. But with the computational capacity, which is available today, it opens up to build a simulation of an LSS. This would save a major part of money, because there is less need for expensive prototypes and flights into the space, a big part of time, because a simulation will be faster than real time and last but not least you can model the space environment in this simulation and a remarkable part of testing in real space can be replaced by simulations.

For these reasons a simulation environment for LSSs used during manned space missions was developed by the LRT at the TUM, called V-HAB. It can be used to build a virtual LSS for various cases of operations, like a space station or manned planetary missions. V-HAB can dynamically simulate these cases, which is a big advantage compared with current design methods for LSS. Thereby missions with changing crew behavior or random events, which influence the LSS, like a system failure or leakage, can be respected and are simulated over a whole mission [1].

Like most simulation models, V-HAB is not a perfect copy of the reality. This is owed to changing parameters, like astronauts, because every human is different or due not knowing the exact working parameters of technical instruments. This is because of a lack of public information about the systems or just because parameters can oscillate within a specified range and the exact working point is not known anytime. So, the simulation is built at a specific working point with reasonable assumptions, which cannot fit to the reality at every moment.

1.2 Motivation and Objective

The named assumptions and uncertainties were the decisive reason for this thesis. The first concern shall be to find out if the simulation will work with modified parameters and will provide comprehensible results. This will be done in a sensitivity analysis. For this it will be necessary to find the variables, which are not secured at a specific point and can be altered about their actual working value. After it is assured that this will work with the simulation, the exact impact of each change of parameters will be detected and shall lead to an error propagation.

The goal of this thesis is to estimate the error of the simulation due the unsecured working parameters or modelling deviations. Therefore, a function where all changed values are integrated to calculate the deviation of the simulation results from the results of a simulation using the currently implemented parameter values is searched. This error propagation shall determine a scope the simulation results may deviate from the real values because of such uncertainties and give the possible error of the simulation. In addition, this can make it unnecessary to simulate every case, which will take a lot of time, but to give an accurate forecast for the impact of changing one or more simulation parameters on the simulation results.

Within this a general method to develop such an error propagation function shall be evolved. This would make it possible to create an error propagation function for every simulation parameter, which is of interest.

The method shall be tested and the originated function has to be verified with different simulation results.

2 V-HAB ISS-Model

This thesis is done with a model of the ISS, which is built with V-HAB. In this chapter the model and its functions are described and the modifications to accomplish the necessary simulations are pointed out.

2.1 Main principle and structure

To give a basic understanding for the functionality of V-HAB here is a short explanation with the help of Fig. 2-1.

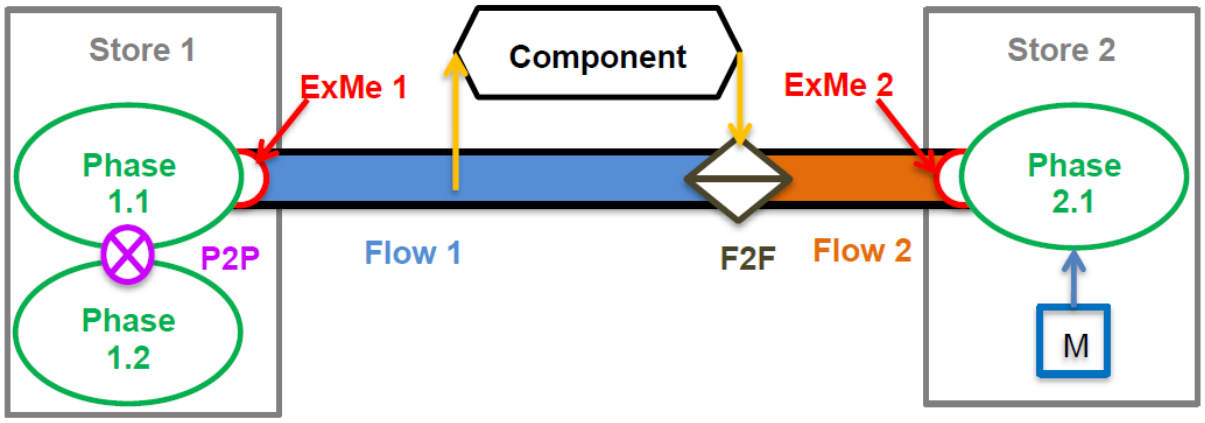

Fig. 2-1: Main components of V-HAB [2].

The basic parts of V-HAB are Stores. Each store can contain different phases with different states of aggregation. Therefore, a single store can contain more than one phase, which can swap matter with each other via a phase-to-phase processor (P2P). A single phase can also be changed in combination or modified from one phase to another with manipulators (M). To build up a more complex simulation model, it is necessary to connect phases, which are located in different stores. These links are realized via branches, which would be pipes, fans and pumps in reality. The matter flow itself, which can be found in the figure as black line around the flows, is represented by a flow object in the framework of the branch. The Extract Merge processor (ExMe) symbolizes the transition from the phase to the flow. The flow-to-flow processor (F2F) is used to change the properties, for example pressure or temperature, of the flow. The component mentioned in the figure can be some component from the V-HAB library, for example a Heat Exchanger (HX), which sets specific conditions to the connected processor [2].

The model of the ISS built in V-HAB accesses to all these methods. Every module of the ISS is represented by a store, which are connected to each other and their related subsystems. For the ISS model some new subsystems for the air revitalization system (ARS) were introduced, which are explained shortly in Tab. 2-1.

Tab. 2-1: Explanation of the ISS Subsystems.

Name of Subsystem	Explanation
Carbon Dioxide Removal Assembly (CDRA)	The CDRA uses overall four zeolite beds to remove the Carbon Dioxide (CO_2) from the cabin air. Two beds are filled with zeolite 13A to remove the humidity before the other two beds, filled with zeolite 5A, adsorb the CO_2.
Sabatier Carbon Dioxide Reprocessing Assembly (SCRA)	The SCRA uses CO_2 and hydrogen (H_2), which are both side products from other systems, to generate methane (CH_4) and water (H_2O) in a Sabatier reactor.
Condensing Heat Exchanger (CHX)	The CHX is used to condense specific substances, like H_2O, from the air. It is also used by some of the other subsystems.
Oxygen Generation Assembly (OGA)	The OGA uses water to produce oxygen (O_2) and H_2 via electrolysis. The O_2 is used to revitalize the Cabin air and the H_2 is used by the SCRA.

All these systems also use components of the V-HAB library.

A more detailed explanation of all functions of V-HAB and the subsystems of the ISS modules can be found in the Master Thesis of Daniel Pütz [2].

The composition of the ISS Model with all contained subsystems and the connection between the modules by the inter modular ventilation system (IMV) is shown in Fig. 2-2.

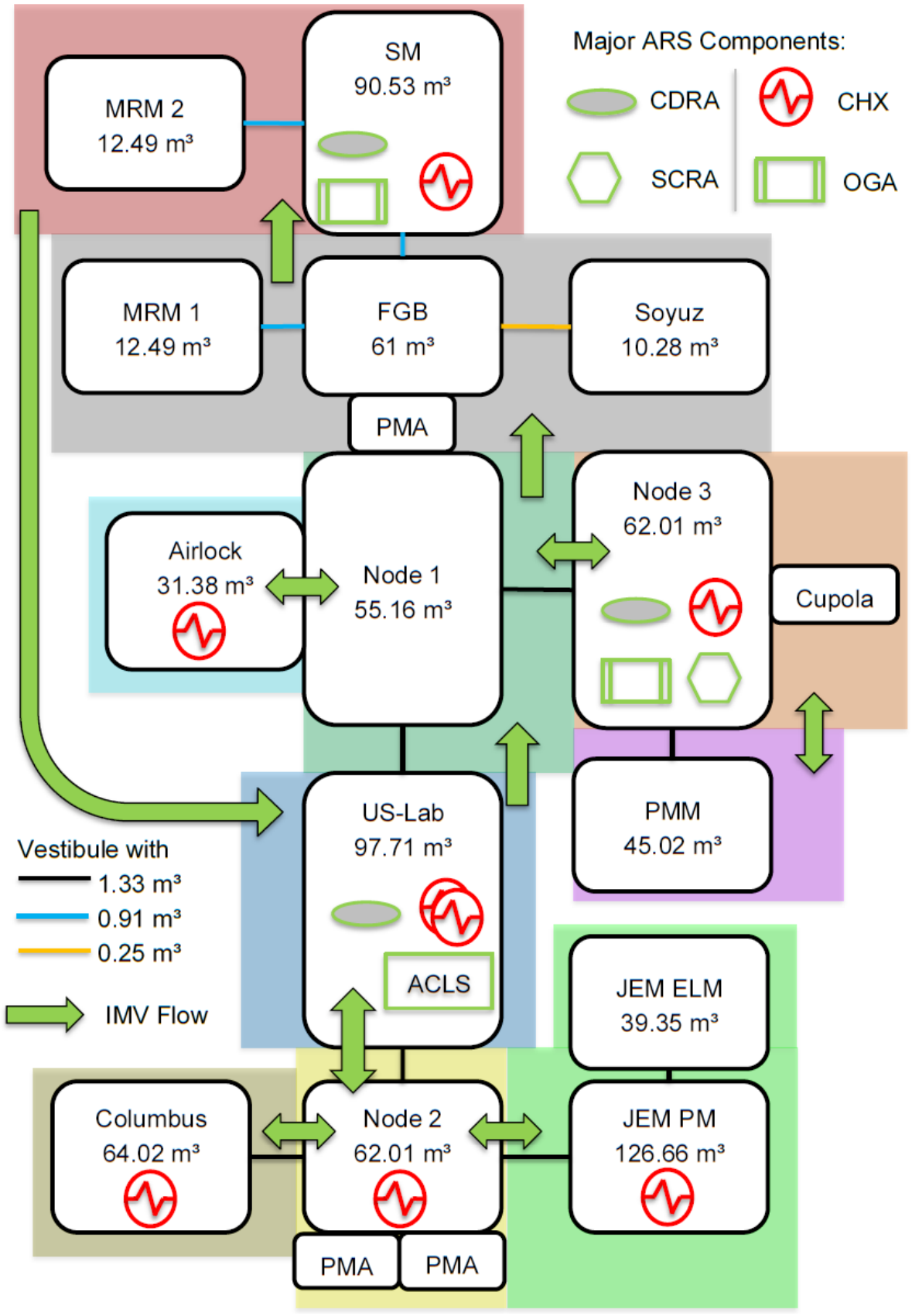

Fig. 2-2: Store Model of the ISS [2].

2.2 Modifications at the simulation model

2.2.1 Rework of the input routine

To perform all the simulations, some changes in the V-HAB code had to be done. At first, it was necessary to change the routine to execute a simulation with additional input parameters. All variables, which should be varied within this thesis, must be defined via an input parameter. That is to secure the repeatability and reliability of the simulations. Otherwise every time a simulation with a changed variable is started, you have to change it in the code, which leads to the risk of accidental code changes or losing sight of previous changes. Now there is a simple scan when performing the execution command to start a new simulation, which checks if one of the known input parameters is contained in the command. If an input parameter is mentioned in the command, V-HAB will use the given value for this parameter otherwise it will use the standard value. All currently usable input parameters are listed in Tab. 2-2.

Tab. 2-2: Input parameters for the simulation.

'ACLS'	Parameter to decide if the Advanced Closed Loop System (ACLS) should be used.
'SimpleCDRA'	Parameter to decide if the SimpleCDRA calculation should be used.
'IronRing1'	Parameter to put the whole crew in Japanese Experiment Module (JEM).
'IronRing2'	Parameter to put the whole crew in JEM and reduces the IMV from Node 2 to JEM and JEM to Node 2 To 80 cfm.
'PlantChamber'	Parameter to decide if and in which module a Plant Chamber should be used.
'CoolantTemperature'	Parameter to vary the Coolant Temperature of various systems.
'CrewValues'	Parameter to vary the metabolic values of the crew.
'SetTemperature'	Parameter to vary the cabin temperature at the ISS.
'CrewModules'	Parameter to decide if the crew stays only on one module and in which module.
'CrewMembers'	Parameter to vary the number of crew members.
'BPA_Dummy'	Parameter to decide if the influence of the Brine Processor Assembly (BPA) is included.
'ACLS_Dummy'	Parameter to decide if the influence of the ACLS is included.

The reason why exactly these input parameters were chosen to use is explained in chapter 3.1. Furthermore, it is very easy to expand the list of possible inputs for which the simulation scans at startup by just adding the name of the desired input parameter to the scanning routine. How exactly the input parameters are changed and used in the simulation is very individually for each parameter and is not explained here for

every single one. In Fig. 2-3 a typical execution command for a V-HAB ISS simulation is shown.

```
vhab.exec('puda.ISS.Setup_ISS_MultiStore', containers.Map({'tbCases'},...
{struct('SimpleCDRA',[],'CoolantTemperature',281.55,'CrewModule','Node2')}))
```

Fig. 2-3: ISS simulation execution command.

The colored marked parts are three characteristic input parameters. First you have the name of the parameter, followed by the value, which is committed with it. The yellow marked one is just a true/false parameter. So, when the name of the parameter is mentioned in the command it means true and the simulation will use, in this case, “SimpleCDRA”. Therefore, no more value is needed, and the name is just followed by an empty bracket. The green one is a parameter, which comes with a numeric value and the blue one has a value, which contains letters. These are the three common kinds of input values and how they are given to the simulation.

2.2.2 Added and modified code

Beside some small and trivial code changes to integrate the varying input parameters, like an if condition or similar, which will not further be explained here, in some cases bigger modifications were necessary. In the following these changes are explained.

CrewMembers. The simulation was designed to simulate with six crew members at every time. To change the number of crew members it was necessary to adjust the crew planer to ensure a realistic movement and activity distribution of the crew. Furthermore, there were some vectors and loops which were static for six astronauts and has been changed to adapt dynamically to the number of crew members.

CrewValues. The simulation was working with a standard human model and its metabolic data. To simulate with different types of humans**,** the metabolic properties of bigger and smaller humans than the standard model were integrated to the human model of the simulation.

BPA_Dummy & ACLS_Dummy. To implement the impact of these systems a new subsystem for each of these mechanisms was created. These subsystems were placed in and connected to the ISS module in which they should work.

Moreover, the “SimpleCDRA” system was temporary changed. Therefore, the calculation of the CO_2 absorption was modified, and a more complex function called “calculateEquilibriumLoading” was used. This modification is named “AdvancedCDRA”. A detailed explanation of this function and why it could not be used for the error propagation is given in the next chapter.

3 Sensitivity analysis

In this chapter the selection and definition of the varied parameters and their influence on the simulation results compared with the reference simulation is shown.

3.1 Selection of considered input parameters

Before the selection of the used input parameters, it was necessary to find all factors that can influence the simulation and lead to a deviation in the results. Three general points with several factors were found, which are listed in Tab. 3-1.

Tab. 3-1: Parameters influencing the simulation.

Human	Technology	External/Uncertain influences
Number of persons	Uncertain working parameter	Payloads
Metabolic rates	Realistic modeling	Accidents
Behavior		

The human factors in the first column are easy to explain, the number of persons on the ISS directly influences the cabin atmosphere of the ISS, the same counts for the metabolic rates of the crew members. Every human is different that means he needs more or less O_2, exhales a different amount of CO_2 and gives a different amount of water vapor to the cabin air. The behavior characterizes the place where a person works, sleeps or exercises and for what amount of time.

The second column describes the technical difficulties to build a simulation of a real system. Every system has working parameters, like temperature, coolant temperature mass flows and lot more, which are not always known exactly. The second difficulty is to achieve as realistic a model as possible of the real-world system with all the processes in it.

The third point specifies impacts that are not known and not predictable like leakage, fire or other accidents. Payloads are systems that are not always on the ISS and do not belong to the standard systems, like experiments or prototypes of new subsystems, which can influence the ISS atmosphere.

From these points parameters were selected to test their impact on the simulation. Therefore factors, which could be determined very exactly by documentation or measurement data, were left out. Moreover, non-predictable impacts, like accidents were ignored, to ensure a comparability to the reference simulation. After that the already mentioned input parameters in Tab. 2-2 were selected and used in the simulations.

3.2 Comparison with reference simulation

All simulations with varied parameters were tested for feasibility and then compared with a reference simulation and evaluated with the help of certain limits for the simulation values, which are defined in this chapter. The reference simulation is done with standard values for the input parameters, which are mentioned in Tab. 3-2.

Tab. 3-2: Standard values for the input parameters

CoolantTemperature	277,55 Kelvin (K).
SetTemperature	295,35 K.
CrewValues	Metabolic rates based on 41-Node Metabolic Man algorithm given by Life Support Baseline Values and Assumptions Document [3, p. 45].
CrewModules	All crew members follow the standard crew planer.
CrewMembers	6 astronauts.
BPA_Dummy	BPA system is turned off.
ACLS_Dummy	ACLS system is turned off.

All simulations last 120 hours, to reach a save steady state to guarantee a comparability between all simulations. The SimpleCDRA calculation was always used, because a more accurate mode called “ComplexCDRA” is still under development and not ready to use within this thesis. In Fig. 3-1, Fig. 3-2 and Fig. 3-3 you can see the results of the reference Simulation for the relative humidity, the partial pressure of CO_2 and of O_2. There the values are plotted, which are in each module. The graphs are arranged like the modules of the ISS are fitted together.

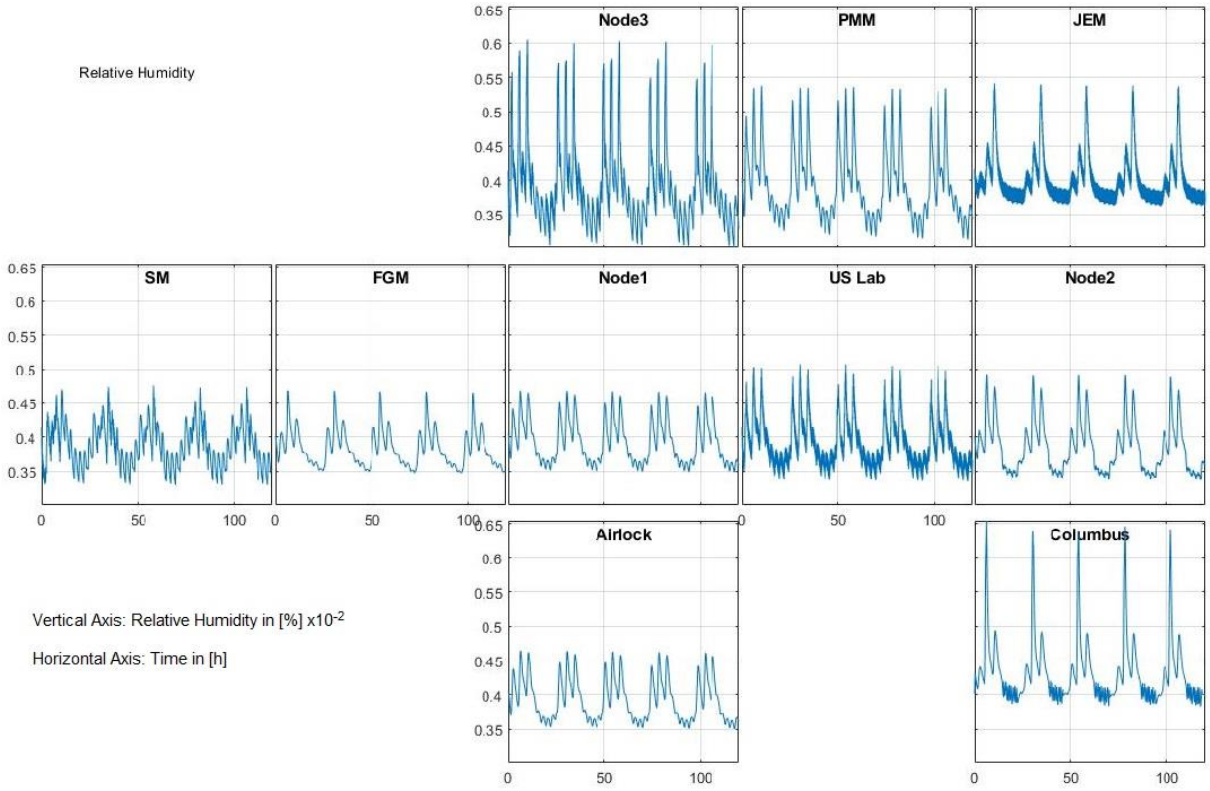

Fig. 3-1: Results for the relative humidity at the reference simulation.

The general daily oscillation of the relative humidity is caused through the sleeping and working routine of the crew. During the day there are three spikes in the curve because three times a day two out of the six crew members need to do their exercises, which

causes an extra output of humidity into the cabin air. The exercises are done in Node 3, hence there are the biggest spikes in the graph. You can also watch a bigger amplitude in single spikes in certain modules. For example, the second one in Columbus or the third one in JEM. That is the result of crew members who come back to their work places directly after finishing their exercise session in Node 3 and are still cooling down and give extra humidity to the air. So, the big differences in single spikes between modules that lay side by side can be explained. The limits for the relative humidity on the ISS are defined in [3, p. 53] and are between 25 % and 70 %. The nominal value is given there with a relative humidity of 40 %. These values are achieved by the reference simulation, which is shown in Tab. 3-3 for some example modules.

Tab. 3-3: Example values of the relative humidity for the reference case in some modules.

		Columbus	Node 3	SM
Relative humidity for reference case in [%]	Maximum	65	60	48
	Minimum	38	30	33
	Average	43	39	39

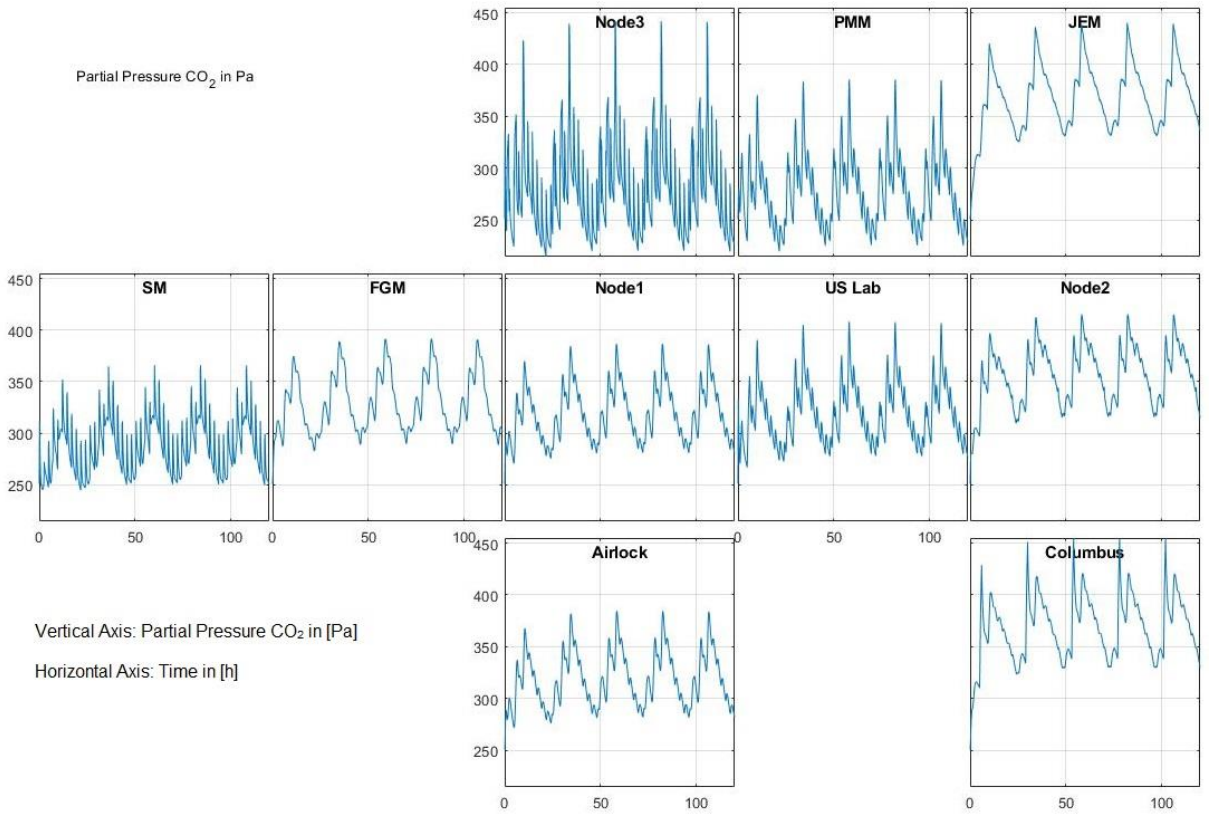

Fig. 3-2: Results for the partial pressure of CO_2 at the reference simulation.

The big and daily oscillations at the CO_2 level are also because of the sleeping and working phases of the crew. The three pikes on the ascending side of the daily oscillations is due the exercises each crew member has to do one time a day. These pikes are strongest in Node 3 because the crew moves there to do their training

sessions. The smallest pikes you can see are from the half cycle of the CDRA system that switches every 144 minutes the sorption mode. In the US Lab, Node 3 and Service Modul (SM) these pikes are best to see, because in these modules a CDRA system is active. In the SM these spikes appear more often because the Russian equivalent to the CDRA, the Vozdukh, has a shorter half cycle time of 30 minutes between adsorbing and desorbing. It needs some time to vent the air via the IMV from these modules to the other ones, so the effect disappears in the other modules. In the Columbus and JEM modules the CO_2 partial pressure is the highest, because the next module with an CDRA is two modules away. As it is shown in Tab. 3-4,the limit of the maximum CO_2 level of 706 Pa for a 180 day period [3, p. 53], which is a typical mission time for an ISS crew member, is achieved in the reference case as well as the limit of 506 Pa, which is the limit value for a 1000 day mission [3, p. 53].

Tab. 3-4: Example values of the partial pressure of CO_2 for the reference case in some modules.

	Columbus	Node 3	SM
Maximum partial pressure of CO_2 in the reference case [Pa]	455	442	366

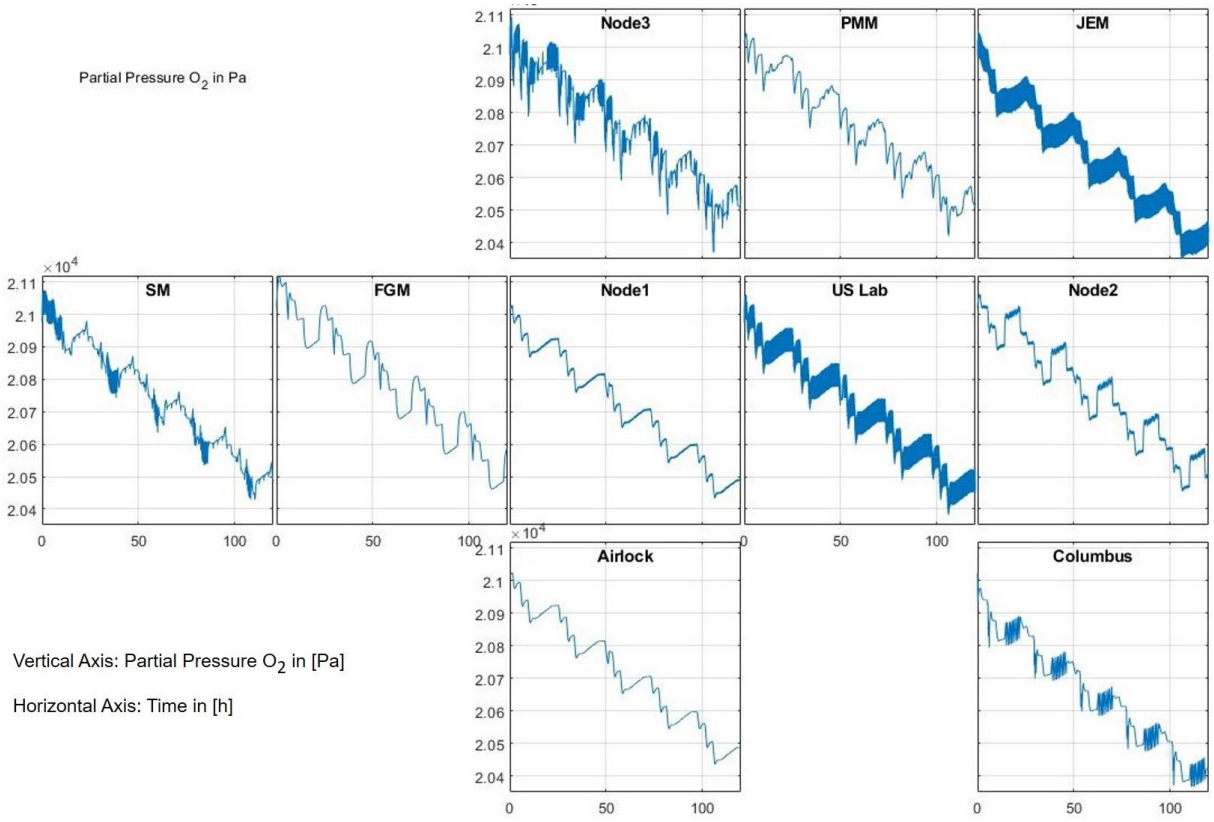

Fig. 3-3: Results for the partial pressure of O_2 at the reference simulation.

The partial pressure of O_2 is descending, because the OGA is only running at 35% of its maximum performance, but it never reaches the lower limit for the O_2 concentration, at which the control logic increases the O_2 production. The general profile of the curve is stamped by the sleeping and working phases of the crew. In the night less O_2 is used by the crew and the partial pressure can increase slowly. During the day and especially during the exercising sessions, identifiable by the three small spikes during a working

phase, the crew needs more O_2 than is produced and the O_2 level drops. In Node 3 these spikes are more pronounced, because during the training sessions the crew needs the most O_2. Because the lower limit of the O_2 level was never reached in any simulation, the results never show the full performance of the OGA system. So, it is only a trend observable if the O_2 is dropping faster, slower or even rises when the need for O_2 changes due some modifications at the simulation parameters. For this reason, the results for partial pressure of O_2 are not shown here for every single input parameter but the comparison with the reference simulation can be found in B.1.

3.2.1 SetTemperature

The temperature in the ISS cabin can be set by the crew members. The standard value of 295,5 K is varied from 291,65 K to 299,65 K [4].

$$c_{sat} = \frac{e_{sat}}{R_D \times T} \qquad \textbf{Eq. (3-1) [5]}$$

With equation Eq. (3-1) the maximal absolute air moisture $\mathbf{c_{sat}}$, which is the maximal water vapor a certain volume of air can carry, can be calculated. In this equation $\mathbf{e_{sat}}$ is the saturation water vapor pressure, $\mathbf{R_D}$ is the gas constant of water vapor and **T** is the temperature of the air. So, the maximal air moisture depends on the temperature. The diagram in Fig. 3-4 shows $\mathbf{c_{sat}}$ over the temperature.

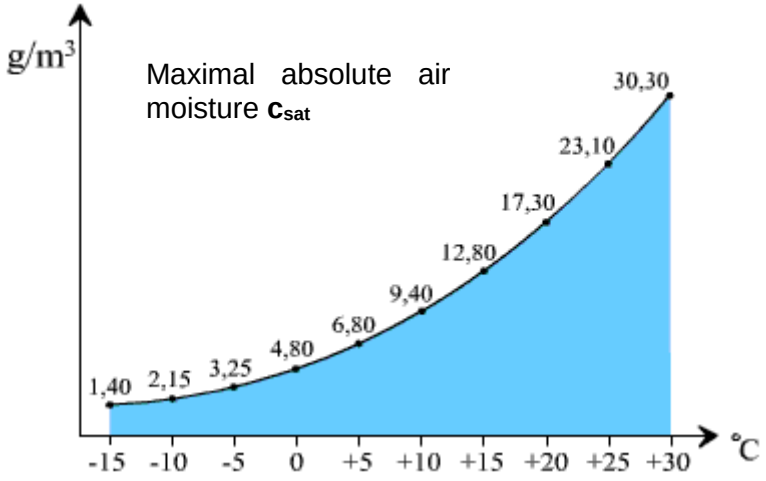

Fig. 3-4: Diagram for the temperature dependency of the maximal absolute air moisture [6].

The higher the temperature the more water vapor can be in the air. If the air is cooled down the water vapor needs to condense to liquid water. The more the air is cooled down, the more water will condense.

Therefore, with a higher air temperature the air will be cooled down over a higher ΔT and more condensation occurs and as a result a lower relative humidity can be expected. In Fig. 3-5 the results of a simulation with a cabin temperature of 298,15 K compared to the standard values are plotted.

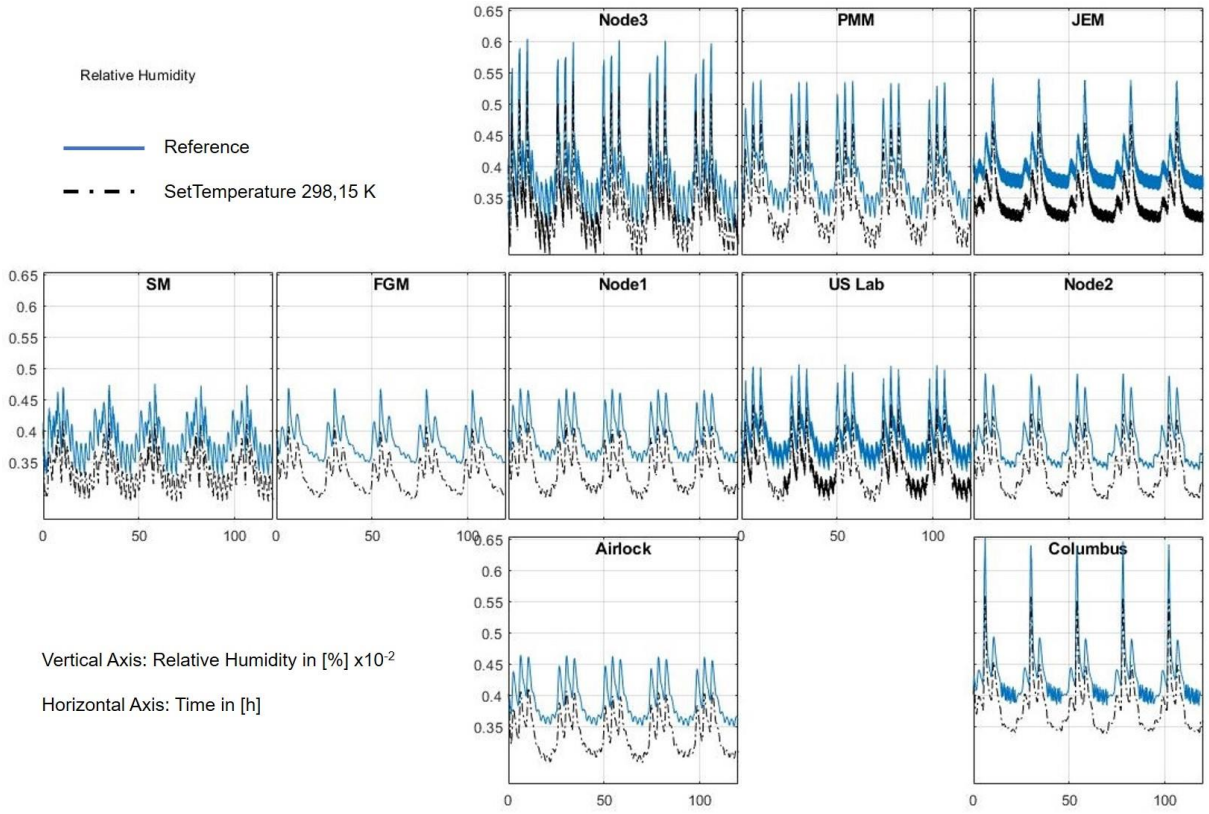

Fig. 3-5: Results of the relative humidity simulated with higher air temperature compared to the reference.

The results show a significant drop of the relative humidity using a higher cabin air temperature. But the principal profile of the graph stays the same. This is exactly what was expected before and shows that the simulation works fine with these changes. The relative humidity is also still in the limits. The nominal value for the relative humidity is only reached by the simulation with the higher cabin temperature during the exercise sessions of the crew (Tab. 3-5).

Tab. 3-5: Values of the relative humidity in some modules for a higher cabin temperature.

		Columbus	Node 3	SM
Relative humidity for the SetTemperature case with 298.15 K in [%]	Maximum	56	53	41
	Minimum	34	26	29
	Average	38	34	34

Fig. 3-6 shows the results with a cabin temperature of 292,15 K. Here, according to Eq. (3-1) a lower ΔT should produce less condensation and consequently a higher humidity level over all modules.

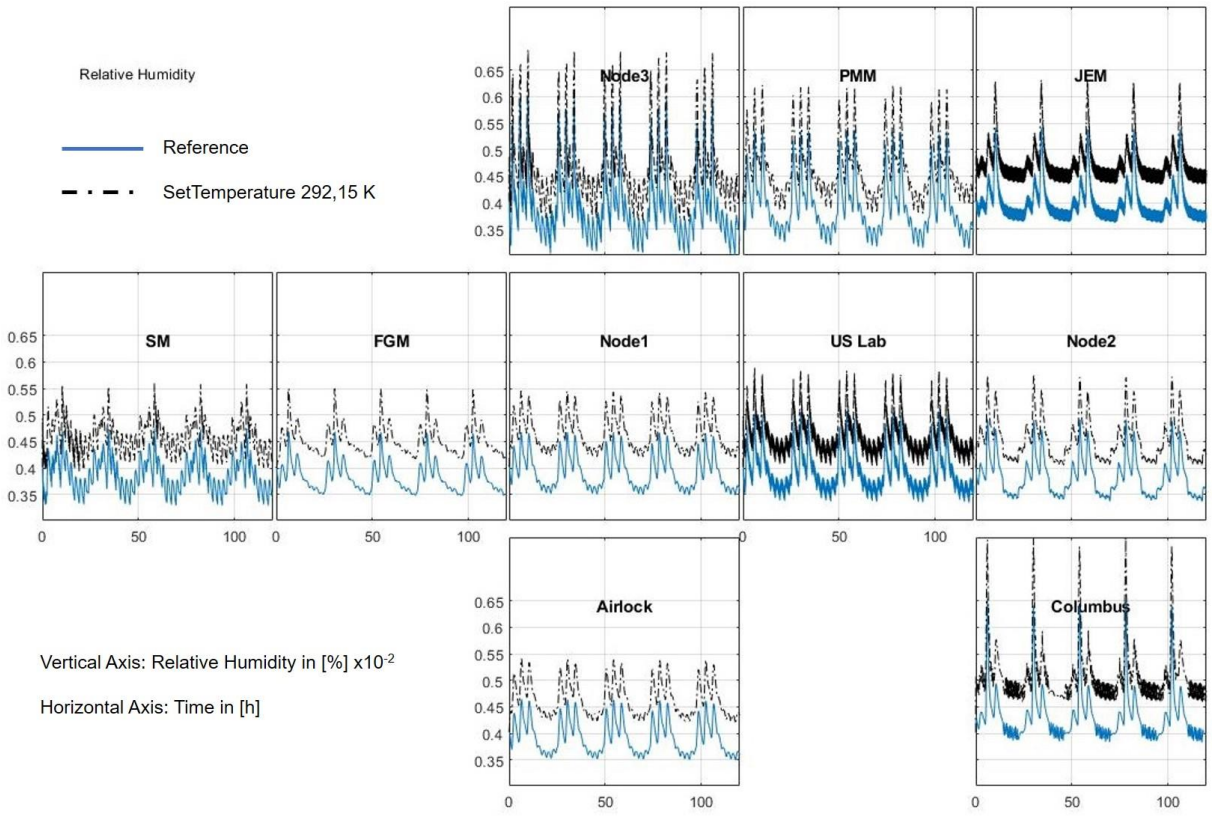

Fig. 3-6 Results of the relative humidity simulated with lower air temperature compared to the reference.

The impact of this change in the simulation is also exactly what was expected before. The profile of the curve stays the same, but the relative humidity is overall on a higher level. The simulation here works just as well as in the case before. The limits for the relative humidity are met, disregarding from some very short spikes in Columbus. But the results do not stick to the nominal value of 40%, which should be hit over long term (Tab. 3-6).

Tab. 3-6: Values of the relative humidity in some modules for a lower cabin temperature.

		Columbus	Node 3	SM
Relative humidity for the SetTemperature case with 292.15 K in [%]	Maximum	77	68	56
	Minimum	46	37	40
	Average	50	46	46

In all other simulations that were done with a varied cabin air temperature in the range from 291,65 K to 299,65 K the results were as good as the two examples shown here. So, we can say the simulation delivers comprehensible results for the considered temperatures and works fine with it.

3.2.2 CoolantTemperature

The coolant is used in all Condensing Heat Exchangers (CHX), which are built in the Common Cabin Air Assemblies (CCAA) and the SCRA to control the relative humidity

in the cabin air and to retrieve usable water. The working temperature of the coolant can vary from 277,15 K [7] to 282,55 K [4]. According to Eq. (3-1) and Fig. 3-4 varying the coolant temperature should have the same influence on the relative humidity like changing the air temperature, because the ΔT the air is cooled down will change.

To increase the coolant temperature will result in a lower ΔT and therefore in less condensation and a higher relative humidity. In Fig. 3-7 the results of the simulation with a coolant temperature of 281,55 K are shown.

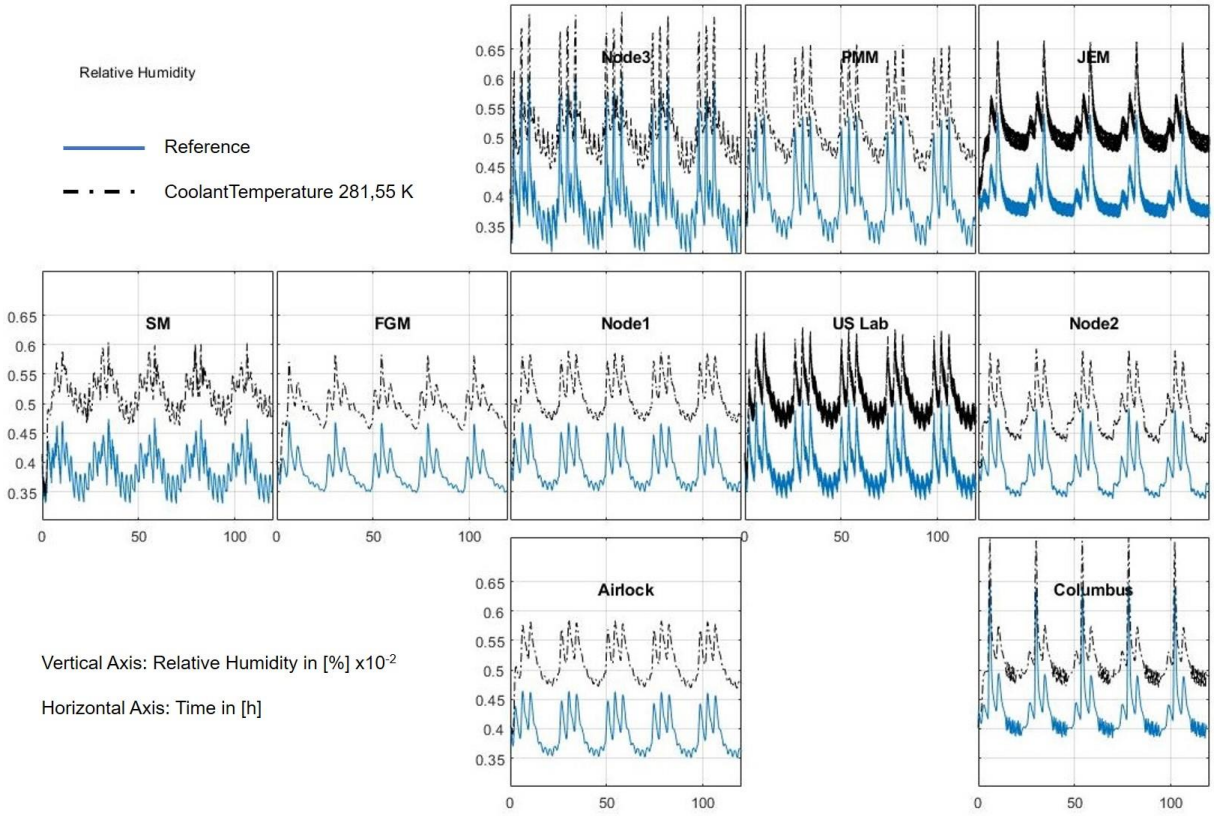

Fig. 3-7: Results of the relative humidity simulated with higher coolant temperature compared to the reference.

Like expected, the behavior of the relative humidity with a higher coolant temperature is similar to the results with a lowered air temperature. The curve stays the same but on a significant higher level. The nominal value of 40 % relative humidity is not reached anymore and in the Columbus module and in Node 3 the upper limit of 70 % is slightly exceeded (Tab. 3-7).

Tab. 3-7: Values of the relative humidity in some modules for a higher coolant temperature.

		Columbus	Node 3	SM
Relative humidity for the CoolantTemperature case with 281.55 K in [%]	Maximum	73	71	60
	Minimum	47	44	46
	Average	51	52	52

With a lower coolant temperature, ΔT is getting bigger and consequently, like raising the air temperature, a lower humidity is expected. But it can be doubted, if there will

be a visible effect in the test simulation, because the coolant temperature is lowered only by 0,4 K. The results are posted in Fig. 3-8.

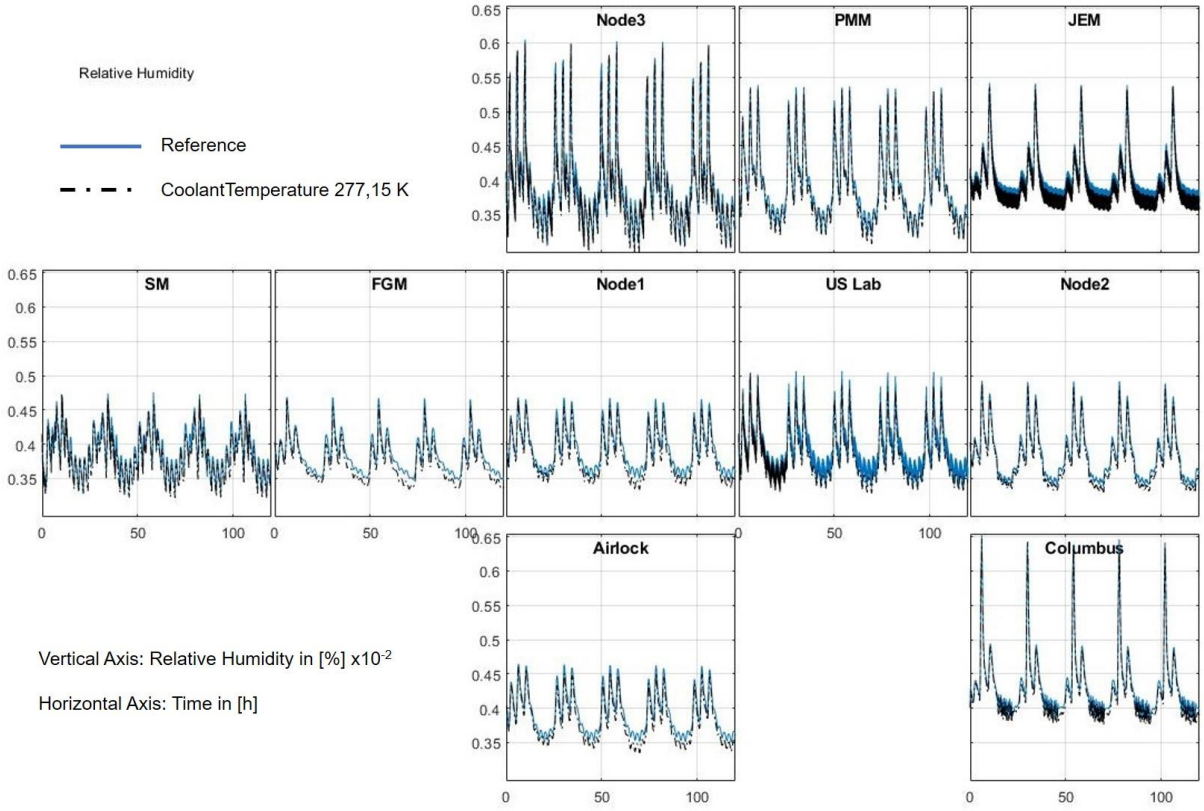

Fig. 3-8: Results of the relative humidity simulated with lower coolant temperature compared to the reference.

Although the coolant temperature was only lowered for 0,4 K compared to the reference a slight reduction of the lower humidity values is visible in the Functional Cargo Module (FGM), Node 1, Node 2 and the Airlock. The limits and nominal values are met by the relative humidity like expected (Tab. 3-8).

Tab. 3-8: Values of the relative humidity in some modules for a lower coolant temperature.

		Columbus	Node 3	SM
Relative humidity for the CoolantTemperature case with 277.15 K in [%]	Maximum	64	60	47
	Minimum	38	30	32
	Average	42	39	38

3.2.3 CrewValues

The crew members body functions, like metabolic rate, CO_2 exhausting, O_2 consumption and sweat runoff rate, are listed in [3, p. 45] for a male with a bodyweight of 82 kg. These values are used for all crew members as an average value. In this case, so named “CrewValues”, two simulations were run, one with a crew consisting

of members with body functions at the upper edge of the allowed level for ISS astronauts and one with a crew consisting of members with body functions at the lower edge of the allowed level. These simulation cases are called “small crew” and “big crew”. This is because the small crew case consists of a crew from six females with the minimum weight of 53 kg and the big crew case consist of a crew from six males with the maximum weight of 110 kg. All crew members are in all cases 40 years old. These borders are mentioned in [3, p. 43]. With the equation Eq. (3-2) for males and Eq. (3-3) for females, which are given in [3, pp. 43,44] for the metabolic rates $\mathbf{E_f}$ and $\mathbf{E_m}$, the values for this simulation case were calculated and are listed together with the value for the reference model and the deviation from it in Tab. 3-9.

$$E_m = \frac{622 - 9.53 \times a + 1.25(15.9 \times m + 539.6 \times h)}{0.238853 \times 10^3} \qquad \textbf{Eq. (3-2)}$$

$$E_f = \frac{354 - 6.91 \times a + 1.25(9.36 \times m + 726 \times h)}{0.238853 \times 10^3} \qquad \textbf{Eq. (3-3)}$$

In this equitation **a** is the age of the specific crew member, **m** is her or his mass and **h** is her or his height. The high of the crew members is calculated with the help of the Body Mass Index (BMI)(Eq. (3-4)).

$$BMI = \frac{m}{h^2} \qquad \textbf{Eq. (3-4)}$$

The **BMI** is calculated with the mass **m** and the height **h** of a person. The BMI of all crew members in all cases are taken for the same. So, because the BMI of the crew member for the reference case is known, it is 24.5 kg/m^2, it is easy to calculate the height for the other cases.

Tab. 3-9: Metabolic rates for different crews.

	Metabolic Rates [kJ/day]	Percentage from Reference [%]
Reference Values	12000	0
Small Crew Values	8620	72
Big Crew Values	15809	132

With the help of the fraction mentioned in Tab. 3-9 all other body functions for the two extreme cases were calculated, too. It is expected that the change of metabolic rates leads to a reduction of the relative humidity and the CO_2 levels with the small crew case and to an increase with the big crew case. The results for the small crew case are in Fig. 3-9 and in Fig. 3-10.

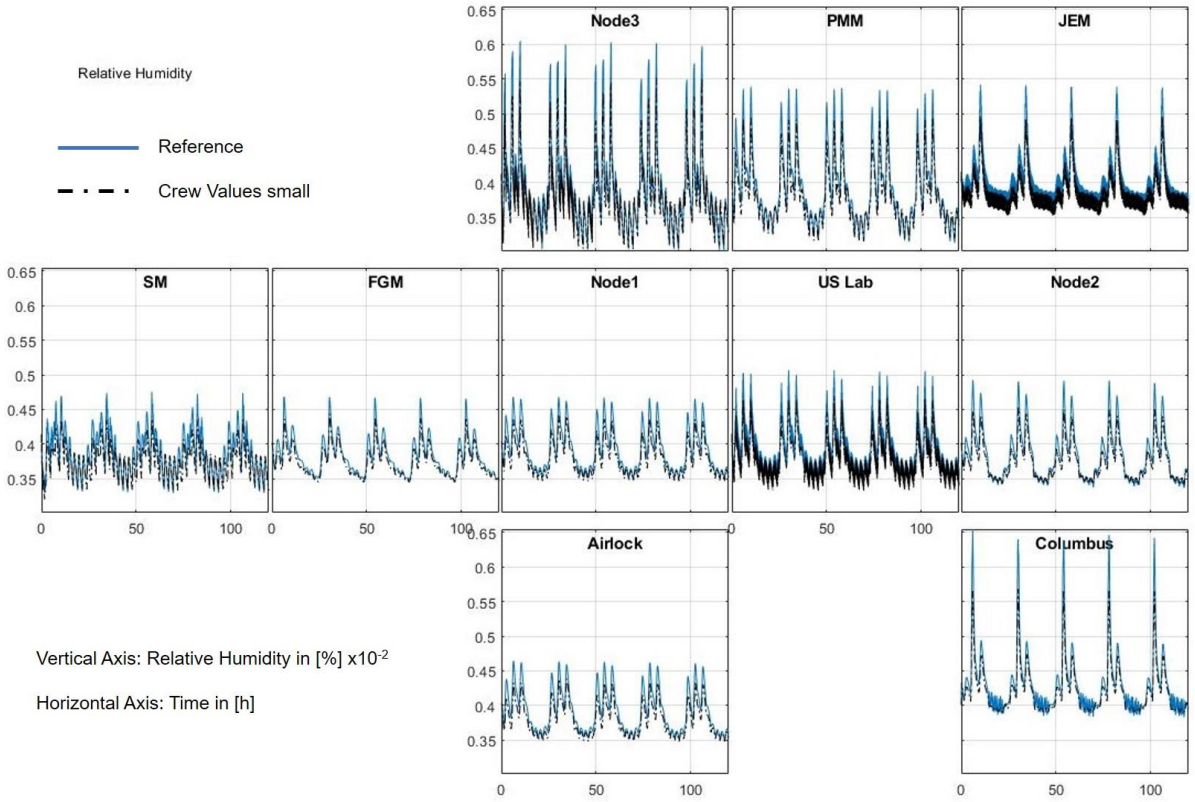

Fig. 3-9: Results of the relative humidity simulated with a small crew compared to the reference.

The simulation worked fine with the changed parameters. Here only a very small impact of the metabolic changes on the relative humidity is diagnosable. The pikes are in all modules lower than the reference values but overall the minimal and the average values stay nearly at the same level. So, the values meet the given limits and hit the nominal level (Tab. 3-10).

Tab. 3-10: Values of the relative humidity in some modules for a small crew.

		Columbus	Node 3	SM
Relative humidity for the small crew case in [%]	Maximum	57	55	44
	Minimum	39	30	33
	Average	42	38	38

The impact of the changed crew values on the CO_2 level is clearly higher, as is shown in Fig. 3-10.

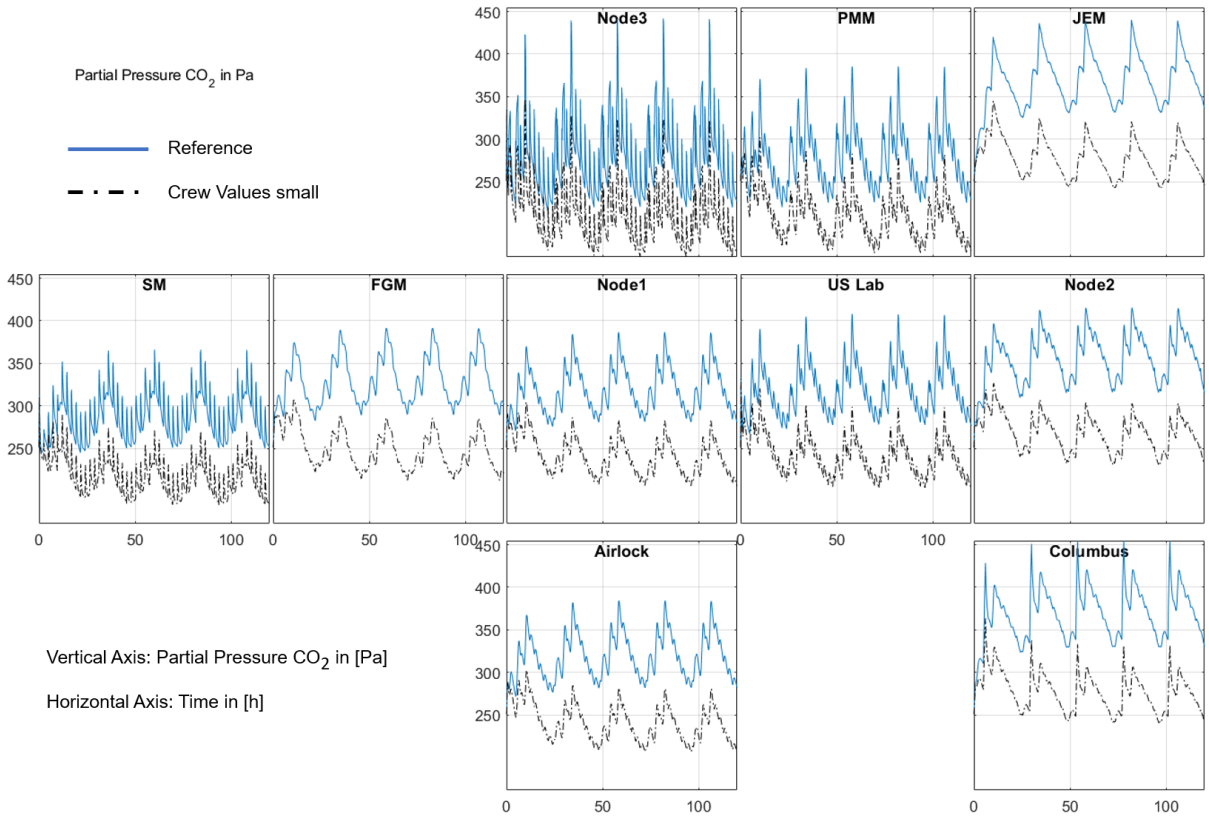

Fig. 3-10: Results of the partial pressure CO_2 simulated with a small crew compared to the reference.

The values for the partial pressure of CO_2 are significantly lower than in the reference simulation. Also, the peaks after exercises have a lower amplitude. In this simulation case the maximum CO_2 level of 706 Pa for a 180 day is not reached, actually the simulation sticks to the limit of 506 Pa for a 1000 day mission (Tab. 3-11).

Tab. 3-11: Values of the partial pressure of CO_2 in some modules for a small crew.

	Columbus	Node 3	SM
Maximum partial pressure of CO_2 in the small crew case [Pa]	332	323	270

The simulation with the big crew values did not go without any trouble. In this case the simulation stopped with an error in the SCRA, which could not be fixed within this thesis. So, there are only results till the point this error occurs, which was approximately after 106 hours. Consequently, the last 14 hours of the simulation are missing. The results of the relative humidity for the big crew are in Fig. 3-11.

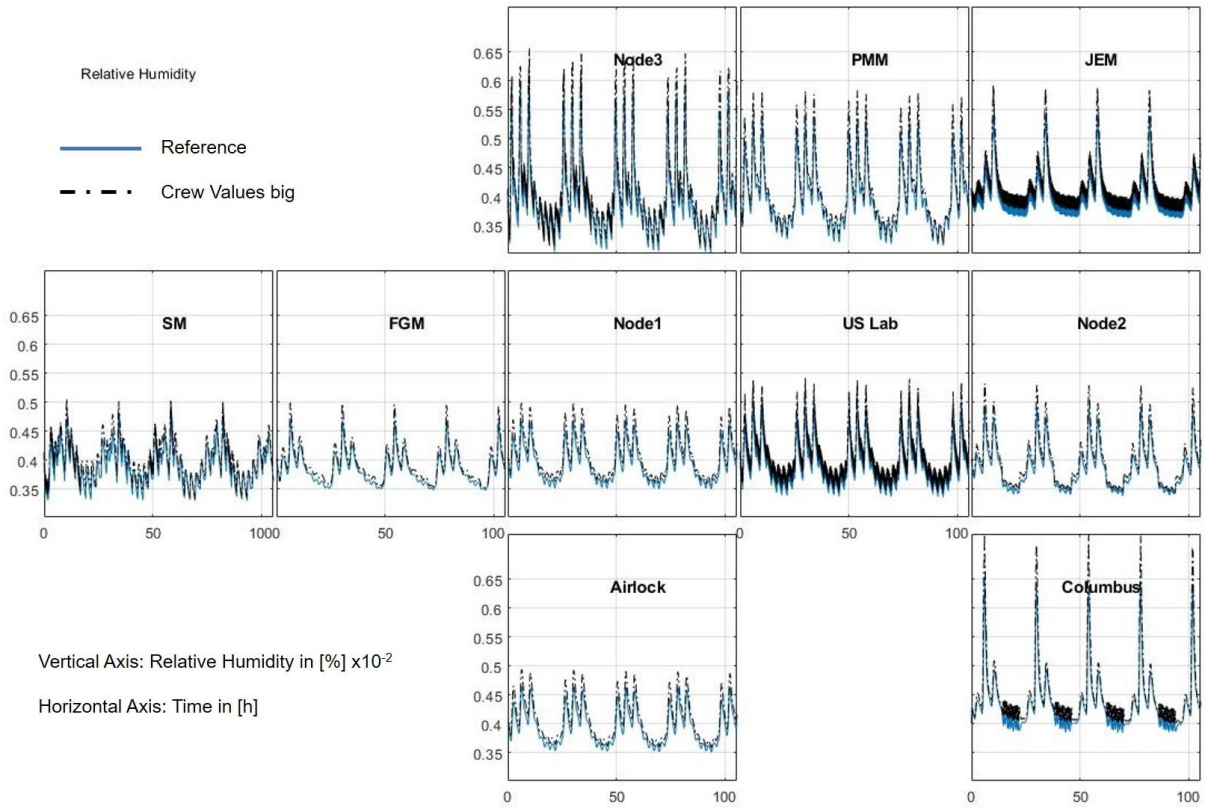

Fig. 3-11: Results of the relative humidity simulated with a big crew compared to the reference.

In this case, like at the small crew simulation, no significant change over the whole curve is noticeable. Here the pikes are significantly higher than to the reference simulation and in the Columbus module the 70 % limit is exceeded, but in all other modules the limits are met, and the nominal value is hit. In both cases the CCAA can regulate the relative humidity to hold them into the required level, besides from the outliner in the Columbus module, and does not reach its limit of capacity in both cases, so there is hardly a change in the curves compared to the reference case visible (Tab. 3-12).

Tab. 3-12: Values of the relative humidity in some modules for a big crew.

		Columbus	Node 3	SM
Relative humidity for the big crew case in [%]	Maximum	72	65	50
	Minimum	40	31	33
	Average	45	42	40

As well as in the CO_2 results for the small crew simulation, in the big crew simulation are clear changes in the curve for the partial pressure for CO_2, which are shown in Fig. 3-12.

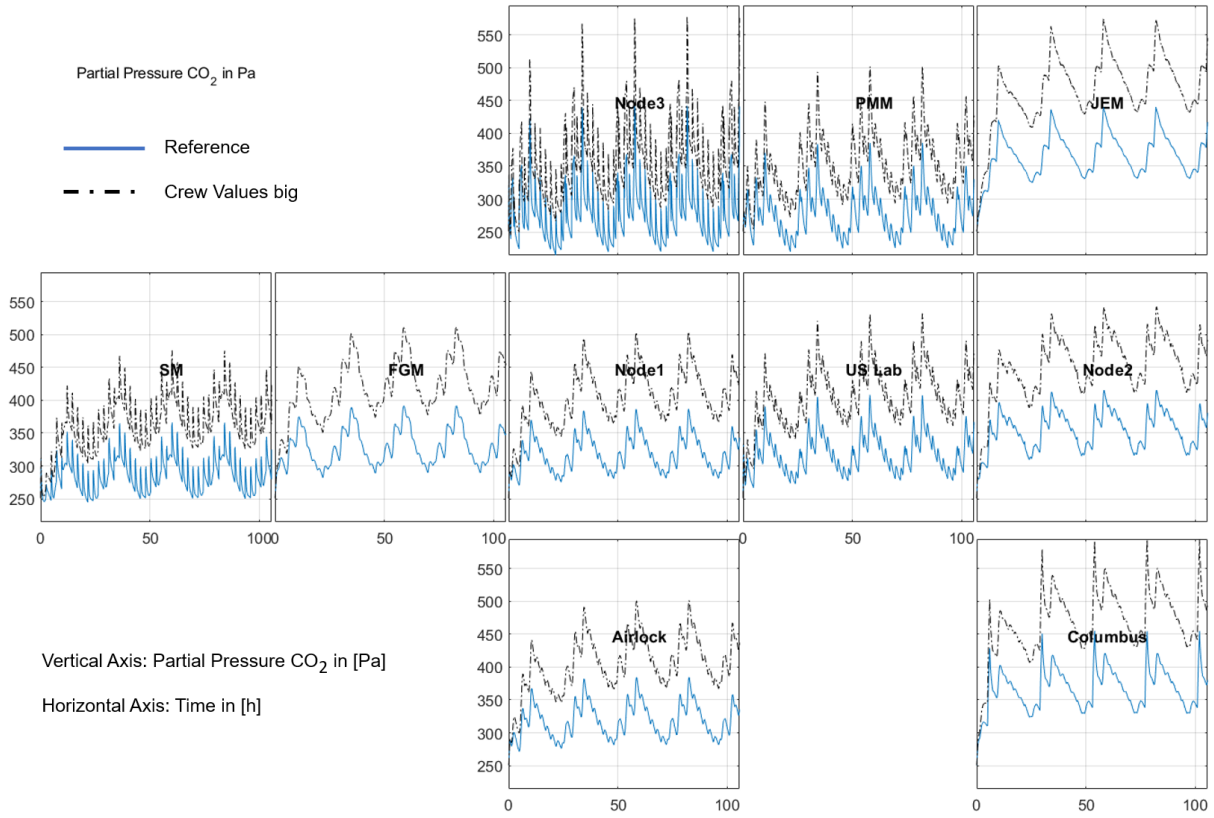

Fig. 3-12: Results of the partial pressure CO_2 simulated with a big crew compared to the reference.

The partial pressure levels and also the pikes of the CO_2 are higher than in the reference model and rather high for the ISS but still hold the limit for a 180 day mission. But in contrast to the reference and the small crew case the partial pressure is too high for a 1000 day mission. Especially the modules without an own CDRA and far away to the next module with an active CDRA system, like Columbus, Node 3 and JEM, reach CO_2 levels that are rather too high for an ISS mission (Tab. 3-13).

Tab. 3-13: Values of the partial pressure of CO_2 in some modules for a big crew.

	Columbus	Node 3	SM
Maximum partial pressure of CO_2 in the big crew case [Pa]	594	577	475

3.2.4 CrewModules

To test the simulation and the LSSs reaction on extreme situations this simulation case was implemented. In this simulation all crew members can be put together in one ISS module for the whole simulation time. It can be chosen in which module the crew should stay, and all cases with every module were tested. Here two representative examples are shown. The first one is the US Lab, which has an own CDRA. The second one is the Columbus module, which does not have an own CDRA and additionally is two modules away from the next module with an active CDRA. Additionally, the results for the relative humidity in the FGM module are shown, because there is an abnormality compared to the other modules. The results for the other modules can be found in B.2.

In the first case, the US-Lab, an increase of the partial pressure of CO_2 in this module is expected, but slighter than in the Columbus module, because of the CDRA in the module. The relative humidity should rise, too, but also slighter as in Columbus, because the air is vented to more attached modules. Fig. 3-13 shows the relative humidity for the US-Lab case.

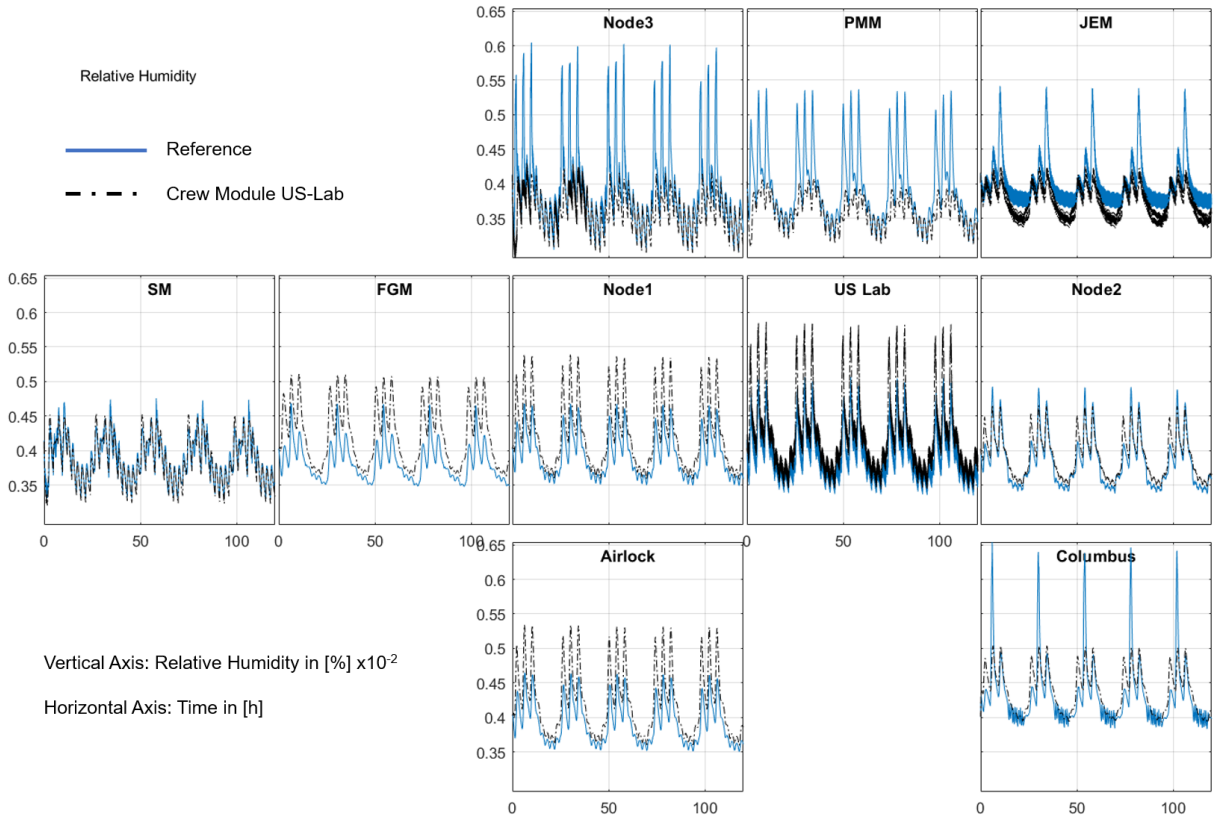

Fig. 3-13: Results of the relative humidity simulated with all crew members in US-Lab compared to the reference.

The general level of the relative humidity is very similar here to the reference case. But the spikes in the US-Lab are now visible for every training session and clearly higher. These spikes are also very obvious in Node 1 and FGM, because the air is vented to there from the US-Lab and these modules do not have an own CHX. In the other modules these spikes, compared to the reference simulation, are missing, because no crew member is there anymore. Therefore, the significant change in this case is the variation at the spikes of the relative humidity, but the overall level, even in the US-Lab, stays nearly the same and met the limits (Tab. 3-14).

Tab. 3-14: Comparison of the relative humidity in the US-Lab.

	Maximum	Average	Minimum
Relative humidity for reference case [%]	50	39	33
Relative humidity for crew in the US-Lab [%]	58	42	34

The results for the Partial Pressure of CO_2 are visible in Fig. 3-14.

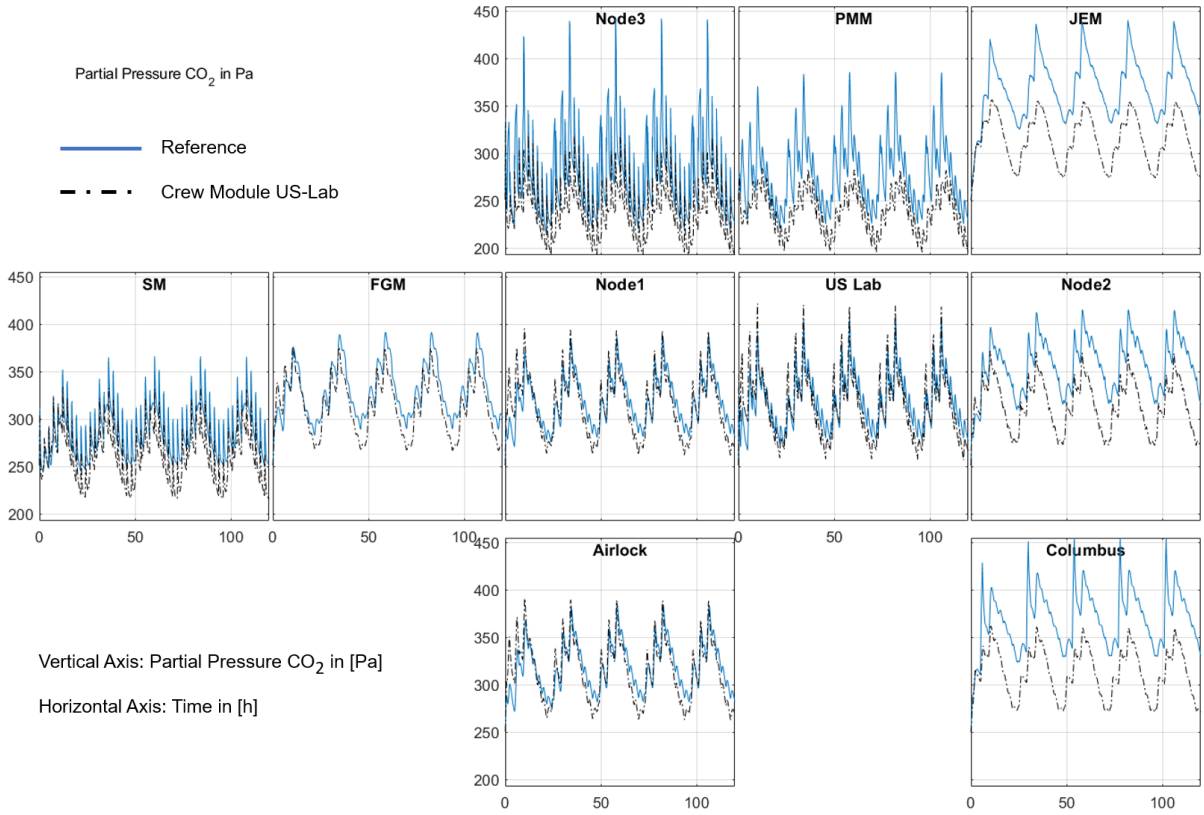

Fig. 3-14: Results of the partial pressure CO_2 simulated with all crew members in US-Lab compared to the reference.

The Partial Pressure of CO_2 is surprisingly not really increased in the US-Lab. The spikes after the training are higher, but only marginal. This means, the CDRA system in the US-Lab can compensate the higher CO_2 production in this module very well. In the modules the air from the US-Lab is vented to, like Node 1, FGM and Airlock, the curve nearly remains identical to the reference (Tab. 3-15). In the other modules a significantly lower CO_2 level is detectable. In all modules the limit of 506 pascal for the partial pressure of CO_2 is met.

Tab. 3-15: Comparison of the partial pressure of CO_2 for modules air is vented to from US-Lab.

		Node 1	FGM	Airlock
Maximum CO_2 partial pressure [Pa]	Reference case	387	391	384
	Crew in US-Lab	392	374	388
Average CO_2 partial pressure [Pa]	Reference case	321	332	321
	Crew in US-Lab	312	312	312

In the second case, the Columbus module, a heavy increase of the partial pressure of CO_2 in this module is expected, because of the distance to the next CDRA. Furthermore, the relative humidity should increase there too, although there is a CHX in the module, because there are now 6 persons for all the time and not only 1 person

during the daytime, which means in this module is more than 6 times more humidity produced by the crew, than in the reference case. The following figure Fig. 3-15 shows the relative humidity for this case.

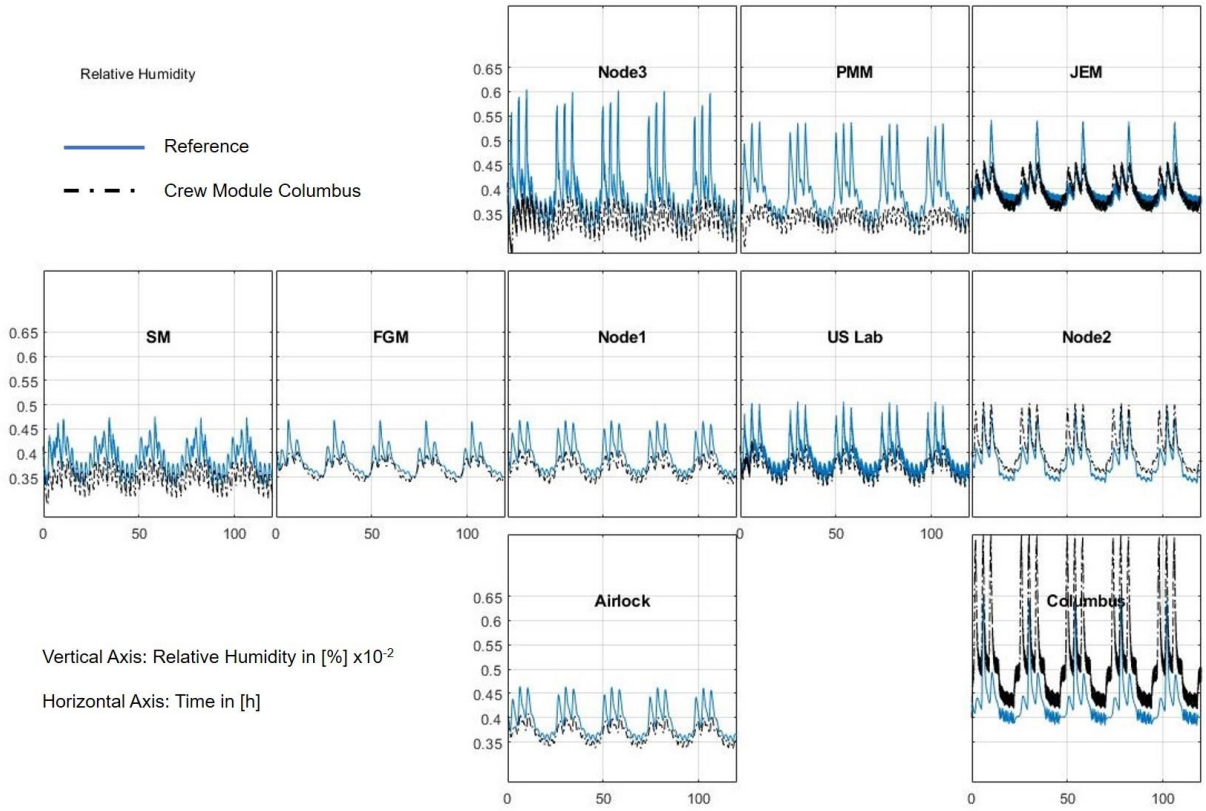

Fig. 3-15: Results of the relative humidity simulated with all crew members in Columbus compared to the reference.

The level of the relative humidity in all modules beside Columbus, Node 2 and JEM fits between the limits and the average values perfectly meet the nominal value of 40%. In JEM the humidity level is higher as in the other modules but very similar to the reference except for the spike after the exercise because nobody goes there after the training, but instead all three spikes of the exercise session are clearly visible on a general lower level. In Node 2 the humidity level is also higher than in the other models, but moreover there are the spikes from all exercises clearly visible and at the level of the reference. The reason for the higher humidity level in these two modules and the visibility of all three spikes is the neighborhood to Columbus, where now all training sessions take place, from where the humidity comes through the IMV. In the US-Lab no increased humidity level can be observed, though it has the same distance to Columbus like JEM. The reason for this is that the module gets air from other modules too and not only from one with a higher humidity level, like JEM does. The relative humidity in Columbus is permanent over the nominal level of 40% and the spikes are far over the upper limits of 70% (Tab. 3-16). Here the CCAA is no longer able to regulate the humidity to acceptable levels.

Tab. 3-16: Comparison of the relative humidity in the Columbus module.

	Maximum	Average	Minimum
Relative humidity for reference case [%]	65	43	38
Relative humidity for crew in Columbus [%]	78	52	42

The results for the partial pressure of CO_2 in this case are pictured in Fig. 3-16.

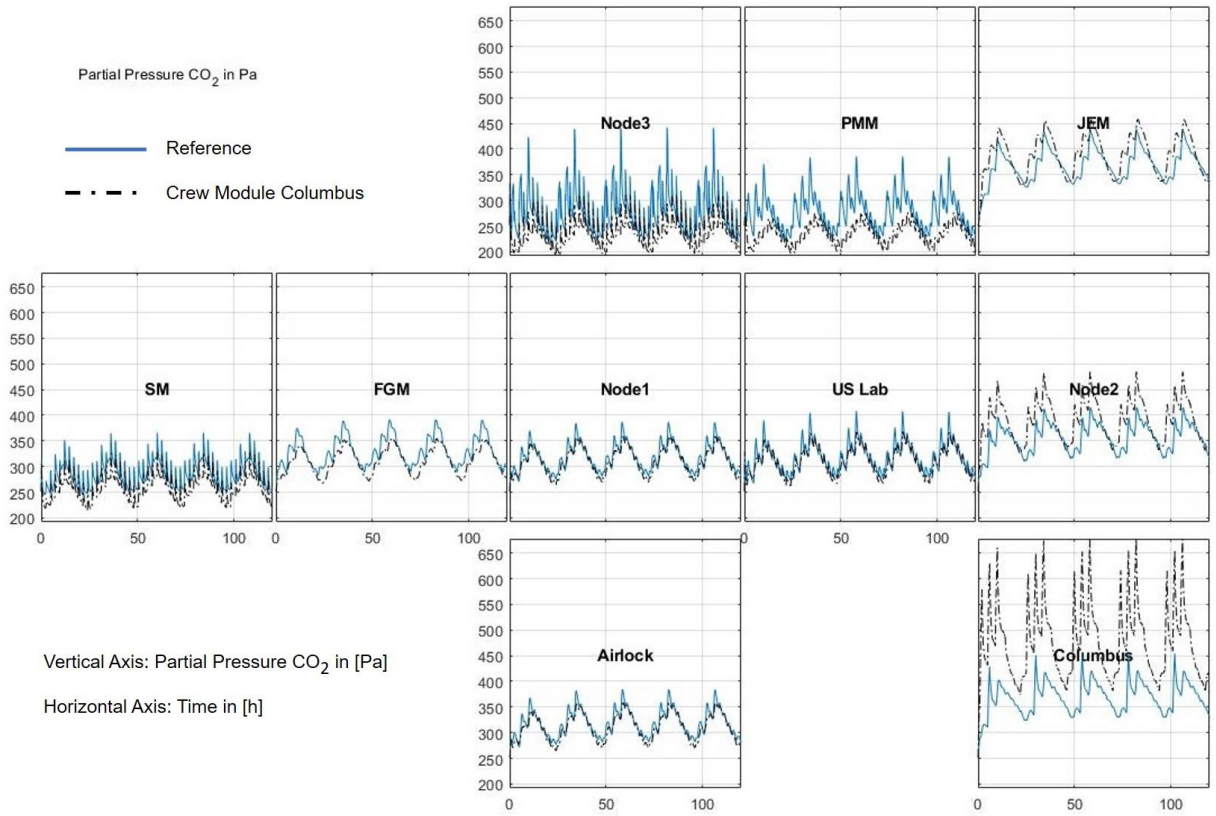

Fig. 3-16: Results of the partial pressure CO_2 simulated with all crew members in Columbus compared to the reference.

The behavior of the CO_2 partial pressure is very similar to the results of the relative humidity. In all modules beside Columbus, Node 2 and JEM the CO_2 level stays easily under 400 Pa and in Node 3 and PMM it is clear lower than the reference and nearly the whole time under 300 Pa. The CO_2 partial pressure in JEM and Node 2 is higher for the same reason how the humidity is. Additionally, these both modules do not have an CDRA. But the CO_2 levels are anyway similar to the reference simulation and even conform to the limits of a 1000 day mission. In Columbus the average CO_2 level is at 500 Pa and during the training sessions nearly reaches the 700 Pa, which is the limit for a 180 day mission. Indeed, this limit is still maintained, it is very high for the ISS and not recommendable (Tab. 3-17).

Tab. 3-17: Comparison of the partial pressure of CO_2 for some modules.

		Columbus	Node 2	Node 3
Maximum CO_2 partial pressure [Pa]	Reference case	455	415	442
	Crew in Columbus	678	485	311
Average CO_2 partial pressure [Pa]	Reference case	371	360	292
	Crew in Columbus	479	394	249

In the FGM, compared to the other modules simulated in this case, no CHX is installed. Therefore, a higher relative humidity than in the examples before is expected. The result for the relative humidity in the FGM is shown in Fig. 3-17.

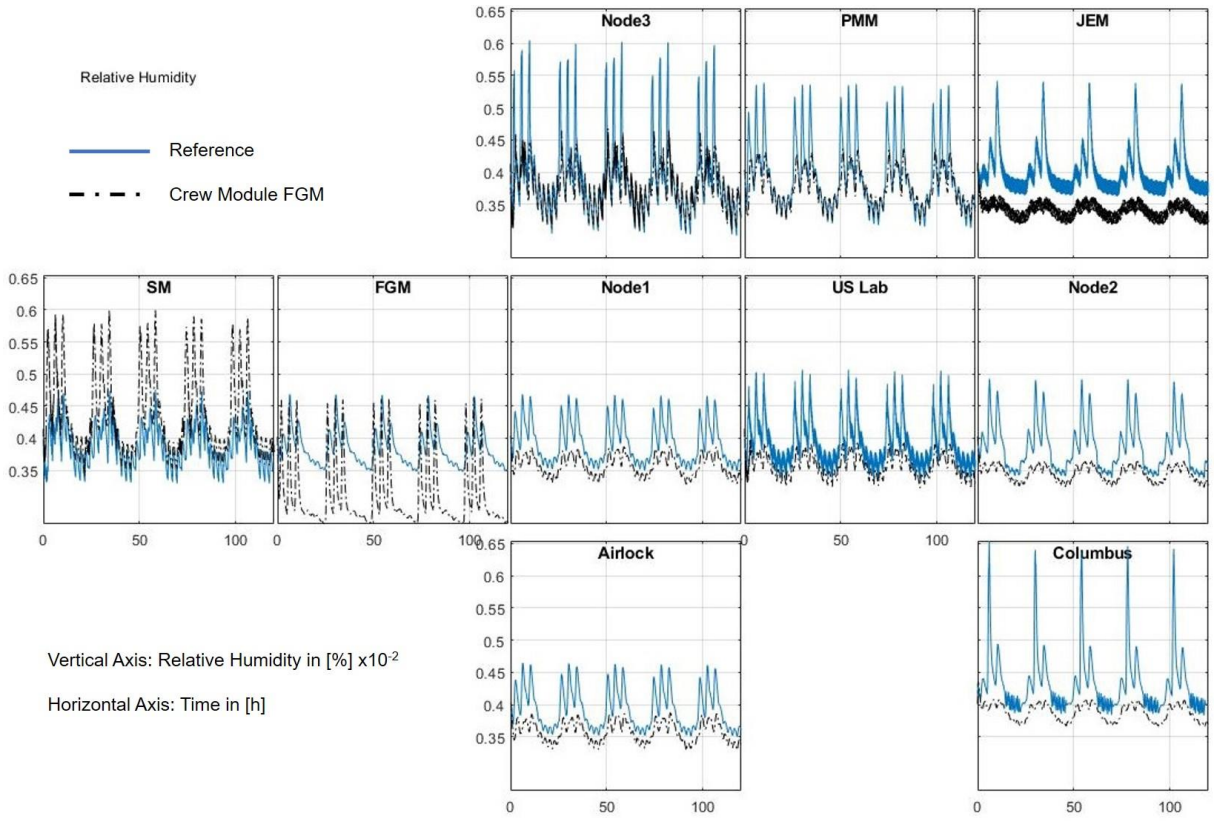

Fig. 3-17: Results of the relative humidity simulated with all crew members in FGM compared to the reference.

In contrast to the expectations the relative humidity in the FGM is significantly lower than in the reference case and also lower than in all other modules. But the pikes, which are caused through the training sessions of the crew, are clearly visible. In the SM, the air is vented to from the FGM, the relative humidity level is higher and all three spikes from the training sessions are visible compared to the reference case, like it is expected. (Tab. 3-18)

Tab. 3-18: Comparison of the relative humidity for some modules.

		SM	FGM	Columbus
Maximum relative humidity in [%]	Reference case	47	47	65
	Crew in FGM	59	46	41
Average relative humidity in [%]	Reference case	39	38	42
	Crew in FGM	44	31	39

The discrepancy in the FGM can be explained with the absence of not only a CHX, but also the CCAA in this module. Because of the absence of the CCAA, which should regulate the cabin temperature, the temperature in the FGM can rise because of the heat output from the crew members there. In all other modules, simulated in this case, a CCAA is installed and the cabin temperatures stick to the specified value of 295.35 K. The cabin temperatures for this case are shown in the following figure (Fig. 3-18).

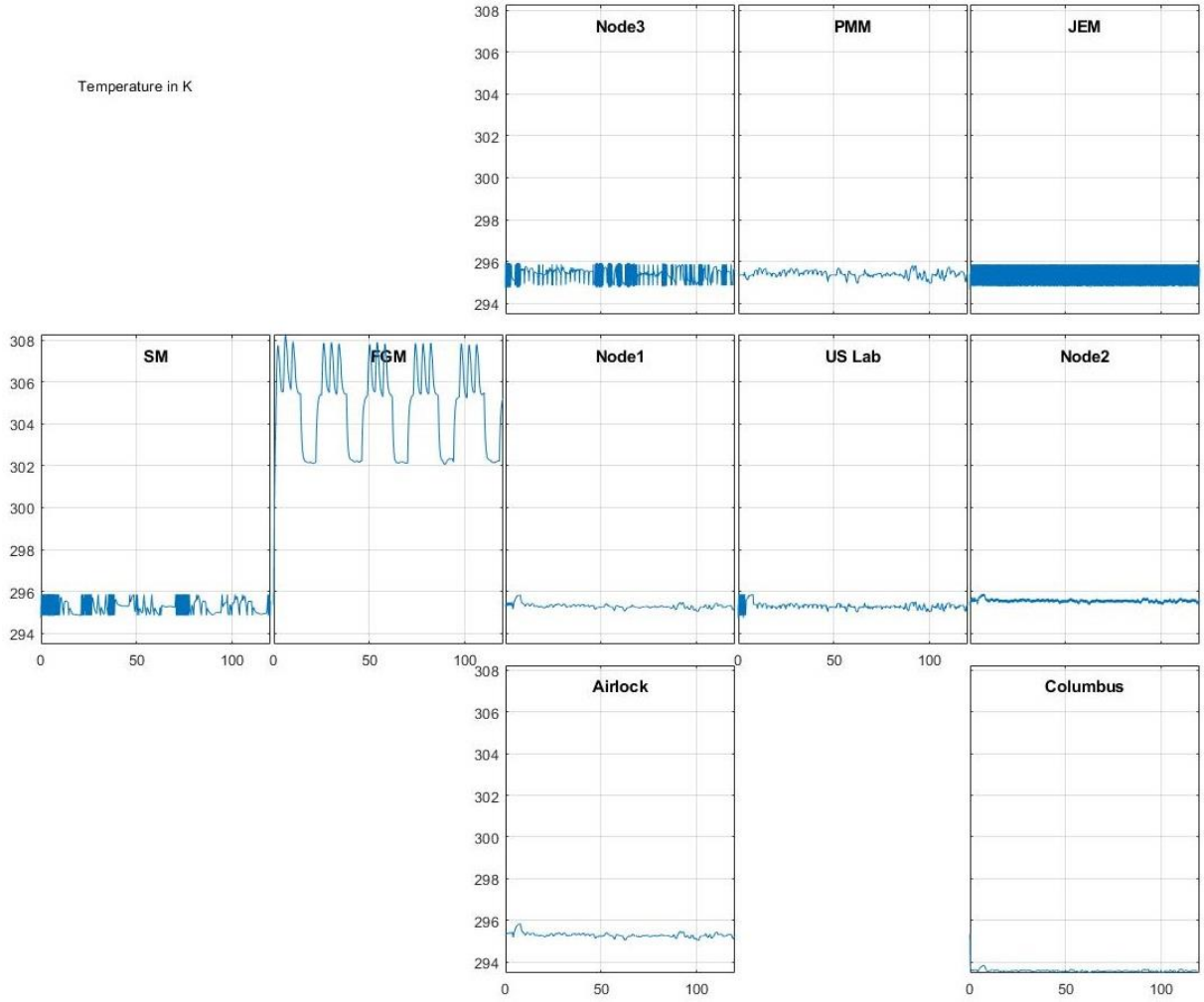

Fig. 3-18: Cabin air temperatures in the modules for all crew members in the FGM.

As can be seen in the figure the temperature in the FGM rises up to 308 K. Relating to Eq. (3-1) and Fig. 3-4 the maximal absolute air moisture increases exponentially with a higher air temperature. Hence, though the humidity in the FGM is higher than to the

reference case and to the other modules, because 6 persons are in there, the relative humidity is lower due of the higher maximal absolute air moisture.

3.2.5 CrewMembers

Within these simulations the number of crew members is varied. Thereby not only the number of persons is varied but also the location, where they sleep and work, respectively the number of crew members is working and sleeping in a module. With the necessary changes in the code, it is now possible to vary the number of crew members from 0 to 10. The changes in working (Tab. 3-19) and sleeping (Tab. 3-20) space allocation are specified in the following tables.

Tab. 3-19: Number of persons working in each module.

Persons on ISS	US Lab	Node 2	Columbus	JEM	Node 3	FGM	SM
0	-	-	-	-	-	-	-
1	1	0	0	0	0	0	0
2	1	0	1	0	0	0	0
3	1	0	1	1	0	0	0
4	1	0	1	1	1	0	0
5	1	0	1	1	1	1	0
6	1	0	1	1	1	1	1
7	2	0	1	1	1	1	1
8	2	0	2	1	1	1	1
9	2	0	2	2	1	1	1
10	2	0	2	2	1	1	2

Tab. 3-20: Number of crew member sleeping in each module.

Persons on ISS	Sleeping spaces
0 - 4	All in Node 2
0 - 7	4 in Node 2; others in SM
0 -10	4 in Node 2; 3 in SM; others in Node 3

Node 3 remains the place where all crew members perform their exercises.

Simulations with every possible number of crew members were tested and some of them did not work well and stopped with the same error in the SCRA, which was already mentioned in chapter 3.2.3. Because of this there are only results with 3 to 7 crew members available. The other simulations with 0,1,2,8,9 and 10 persons did not finish.

In these cases, a similar result as in the simulation with modified metabolic rates is expected, because these changes should have the same impacts beside of the distribution of the crew members over the ISS modules. So, in some modules a bigger variation in the measured values should be observable than in the ones, where no change in the crew presence takes place. The two simulations with the most and the fewest crew members are discussed in the following to see the biggest changes in the results. The curves for the relative humidity and for the partial pressure of CO_2 resulting from the simulation with 3 crew members are visible in Fig. 3-19 and in Fig. 3-20.

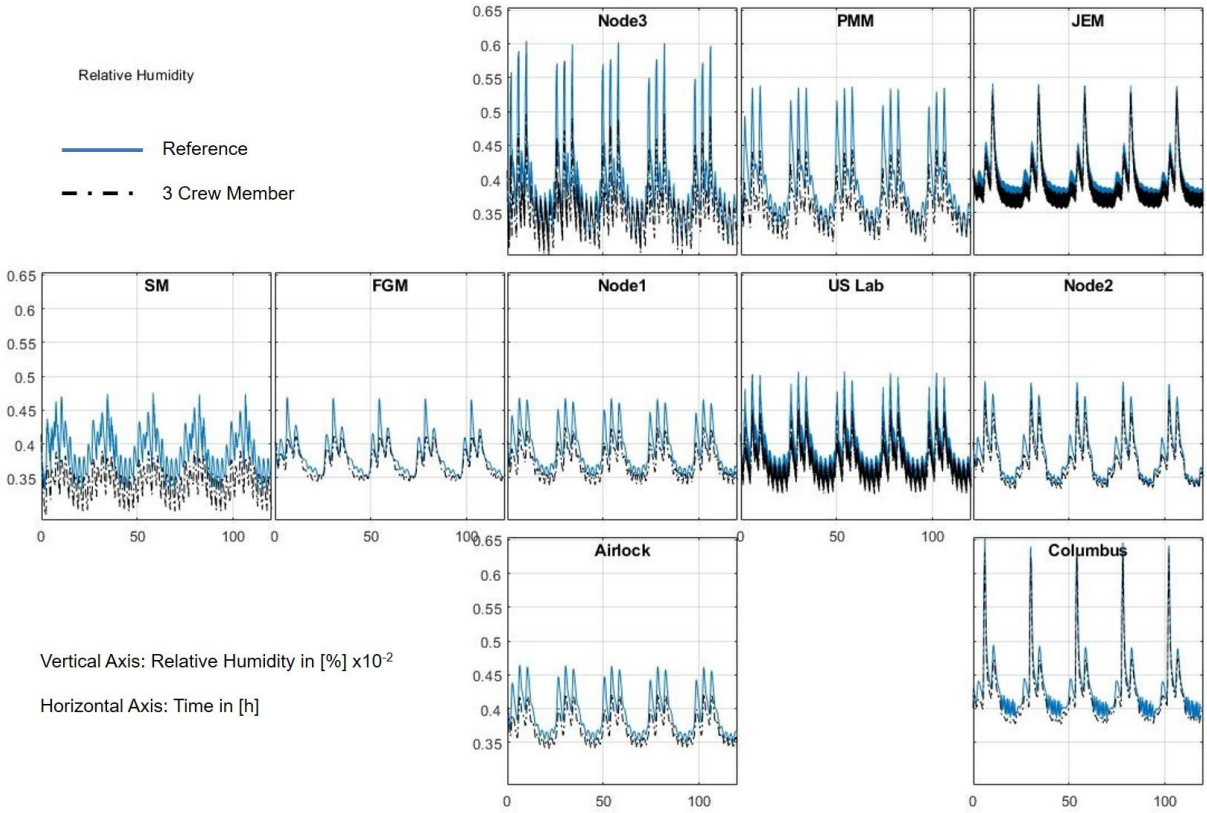

Fig. 3-19: Results of the relative humidity simulated with 3 crew members compared to the reference.

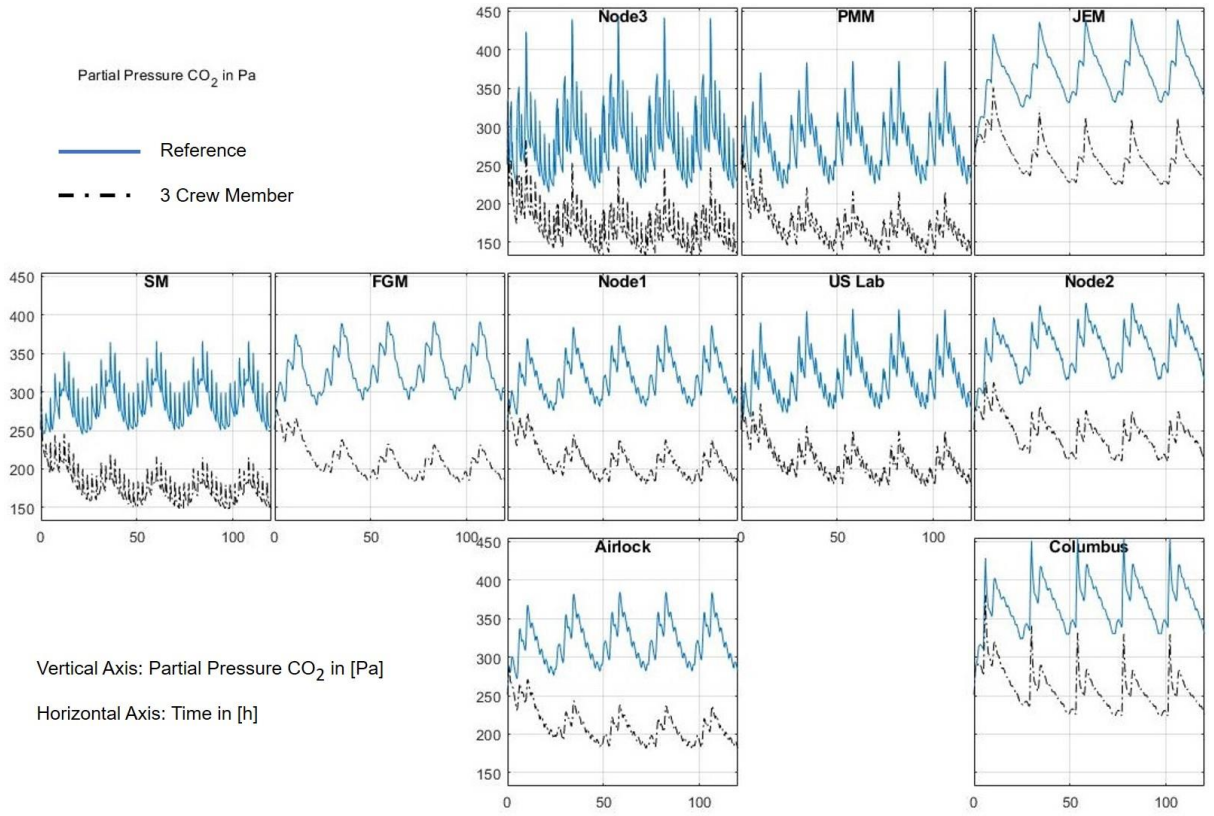

Fig. 3-20: Results of the partial pressure CO_2 simulated with 3 crew members compared to the reference.

Here the level of the relative humidity is generally a bit lower in all modules compared to the reference, but the biggest change can be observed in the SM, because nobody is working or sleeping there anymore. So, the main level of the humidity is significant lower and spikes after training are missing there, too. The absence of these spikes is also visible in the FGM, also because nobody is working there anymore. In Node 3 this change is not really visible because, besides this working space is also empty, the crew comes here for exercises. But overall the humidity levels still fit all limits and guidelines (Tab. 3-21).

Tab. 3-21: Values of the relative humidity in some modules for 3 crew members.

		Columbus	Node 3	SM
Relative humidity for 3 crew members in [%]	Maximum	64	50	39
	Minimum	38	29	30
	Average	41	36	35

The partial pressure of CO_2 shows a significant drop in all modules. As in the case of the humidity the lowest values are visible in SM where no crew member stays over the whole time. Here and in the FGM module no spikes are showing anymore and the spikes in the other modules are obviously smaller compared to the reference. Of course, the CO_2 values follow all limits (Tab. 3-22).

Tab. 3-22: Values of the partial pressure of CO_2 in some modules for 3 crew members.

	Columbus	Node 3	SM
Maximum partial pressure of CO_2 for 3 crew members [Pa]	330	247	215

In Fig. 3-21 and Fig. 3-22 the results for the simulation with 7 crew members are shown.

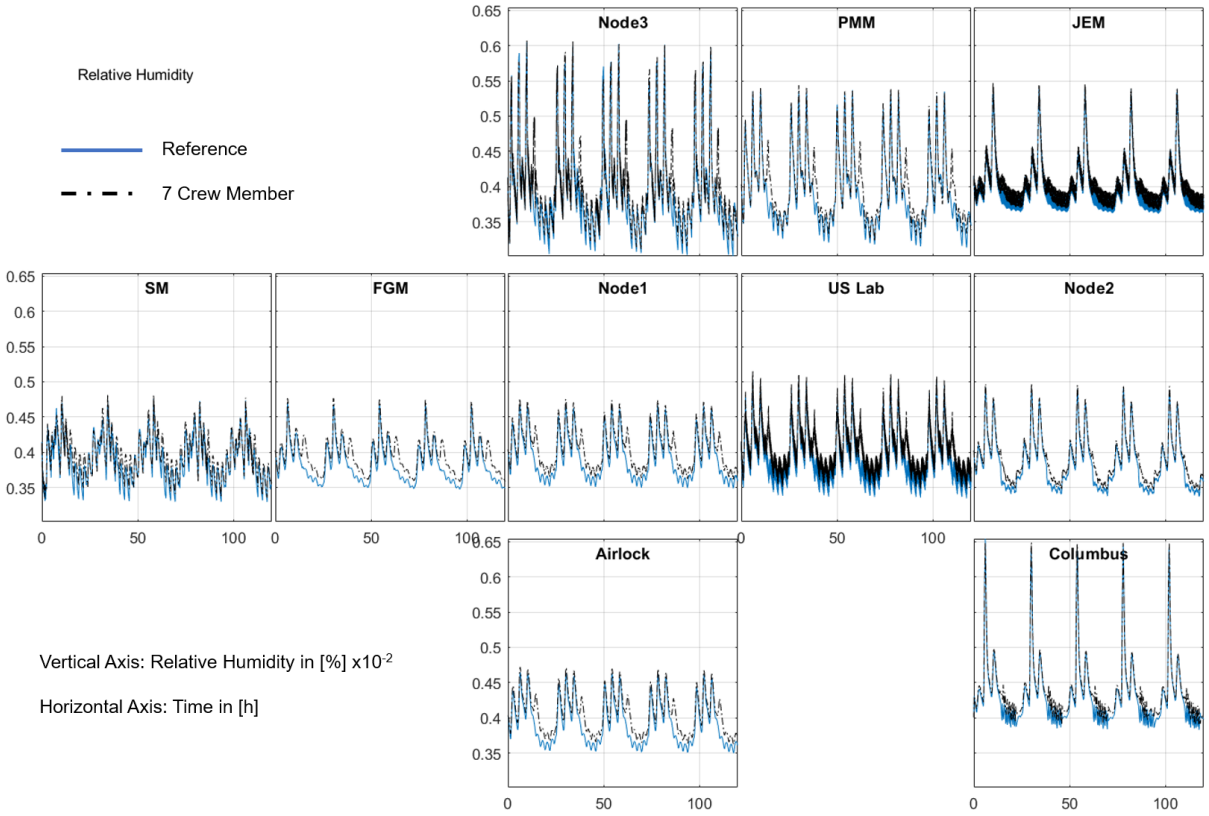

Fig. 3-21: Results of the relative humidity simulated with 7 crew members compared to the reference.

The relative humidity nearly stays at the same level as in the reference case, only in SM a small increase of the lower limit of the humidity is identifiable because one more crew member is sleeping there. But in nearly all modules, except for Columbus, JEM and Node 2, the emergence of a fourth spike is clearly noticeable. This is because the seventh crew member does the training session at an extra time slot, which did not exist before. In Columbus, JEM and Node 2 this spike is hard to see because the CCAAs from the other modules balance the humidity in the air before the air can reach these modules. The overall humidity limits are still met, and the extra crew member has no negative impact on the general humidity level (Tab. 3-23).

Tab. 3-23: Values of the relative humidity in some modules for 7 crew members.

		Columbus	Node 3	SM
Relative humidity for 7 crew members in [%]	Maximum	65	60	48
	Minimum	39	32	34
	Average	43	40	40

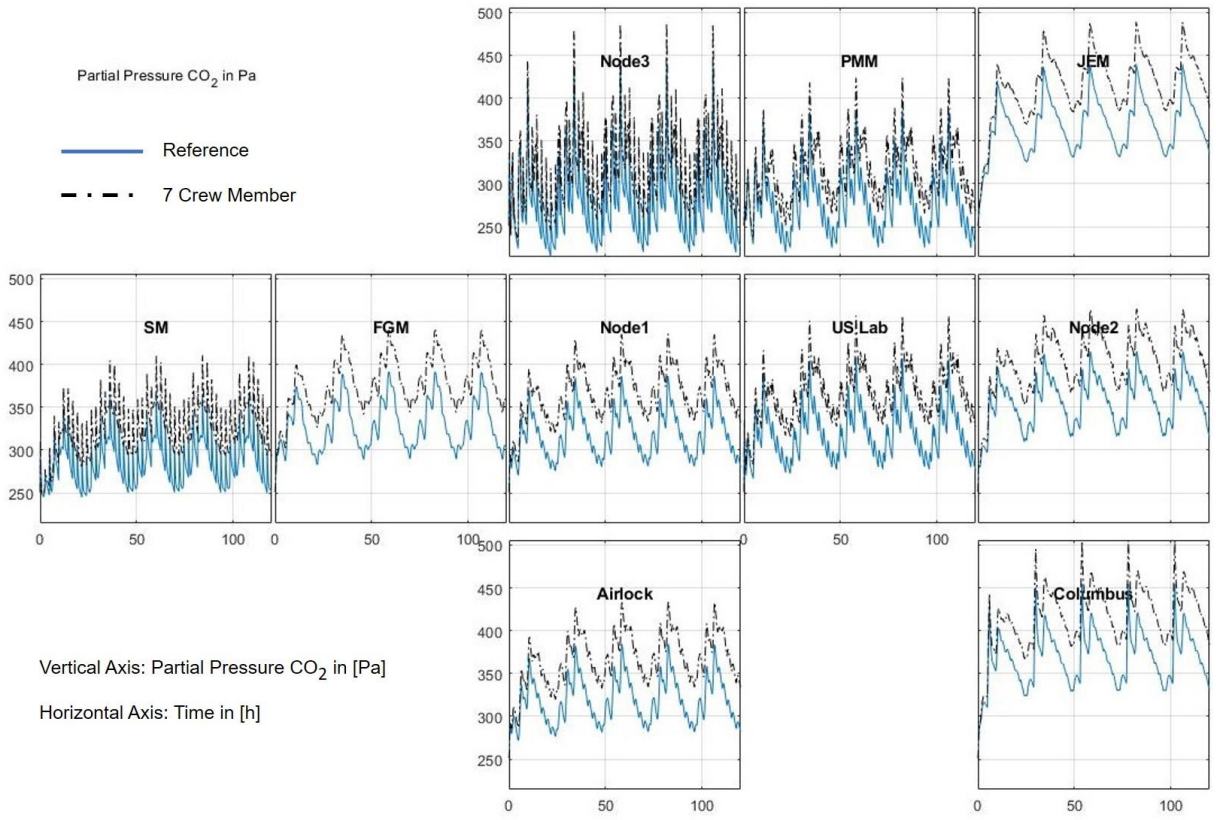

Fig. 3-22: Results of the partial pressure CO_2 simulated with 7 crew members compared to the reference.

One extra crew member hast clearly a bigger impact on the partial pressure of CO_2 level as on the relative humidity. This is especially noticeable in modules without an own CDRA, like FGM, Node 1, JEM and Columbus. In contrast the influence of the extra training session is hardly visible. Only in the US Lab and Node 3, which are used by the extra crew member and more less in their adjacent modules a small extra step in the curve appears. The general CO_2 values are still in accordance with the limit for a 180 day mission, but the limits for an 1000 day mission are reached, for example in the Columbus module (Tab. 3-24).

Tab. 3-24: Values of the partial pressure of CO_2 in some modules for 7 crew members.

	Columbus	Node 3	SM
Maximum partial pressure of CO_2 for 7 crew members [Pa]	506	486	411

3.2.6 BPA_Dummy

The BPA_Dummy represents a payload, which will be sent to the ISS in 2019. It does not simulate the real function of the system, but the influence it will have on the cabin air. According to [8] it will give 1,74 kg of water to the ISS atmosphere per day and will be in Node 3. Hence an increase of the main humidity level, especially in Node 3, is expected. In Fig. 3-23 the comparison with the reference simulation is given.

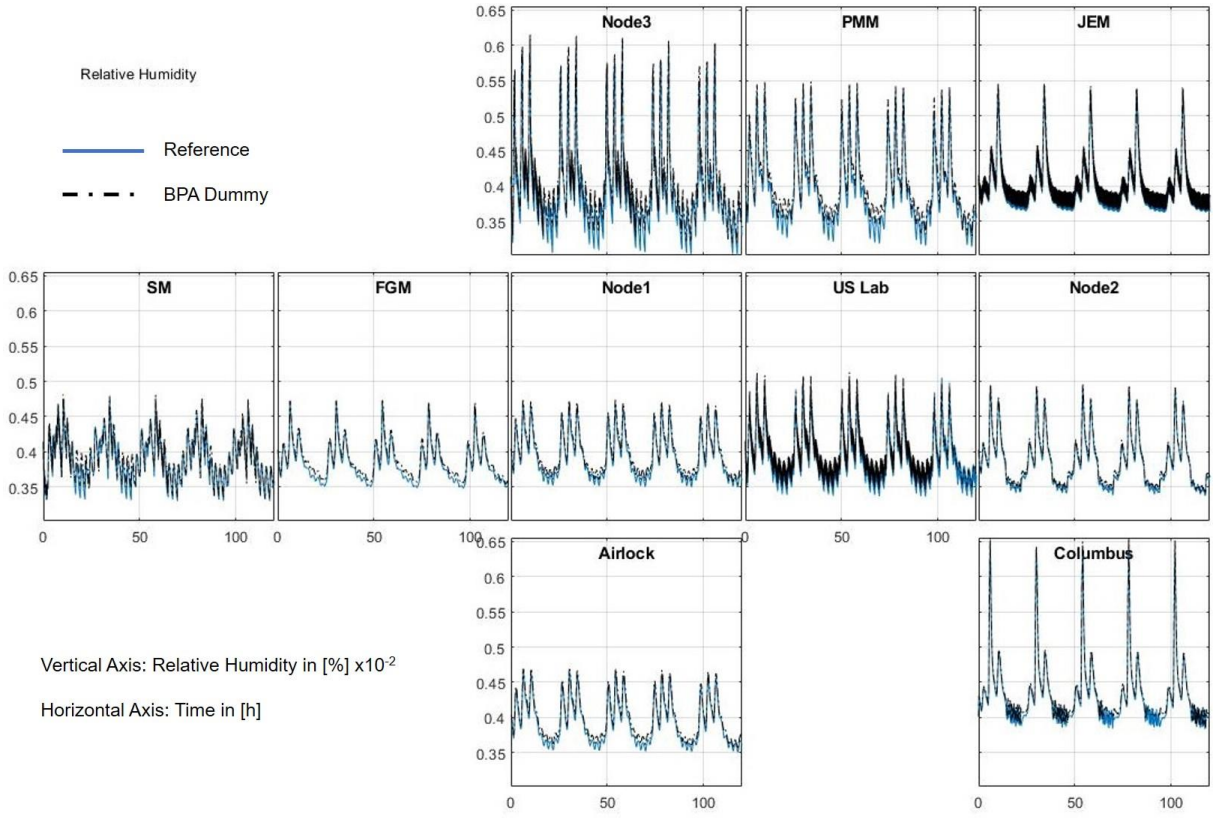

Fig. 3-23: Results of the relative humidity simulated with the BPA_Dummy compared to the reference.

The impact of the BPA is very weak on the humidity level of the ISS atmosphere. In some modules like PMM, Node 1, FGM and SM a slight increase of the lower humidity values is noticeable and the spikes in Node 3, where the system is located, are slightly higher. But overall there is no significant change in the relative humidity (Tab. 3-25). This shows again that the CCAAs of the modules are able to regulate additional humidity very well.

Tab. 3-25: Values of the relative humidity in some modules for the BPA_Dummy case.

		Columbus	Node 3	SM
Relative humidity for the BPA_Dummy case in [%]	Maximum	66	61	48
	Minimum	39	32	33
	Average	43	40	39

3.2.7 ACLS_Dummy

The ACLS_Dummy represents a payload, which is sent to the ISS in summer 2018. It does not simulate the real function of the system, but the influence it will have on the cabin air. According to [9] it will give 4,9 kg of H_2O and 2,52 kg of O_2 to the ISS atmosphere and remove 3 kg of CO_2 from the ISS atmosphere per day and will be installed in the US Lab. Hence an increase of the main humidity level and a decrease of the partial pressure of CO_2, especially in the US Lab, is expected. In Fig. 3-24 and Fig. 3-25 the comparison with the reference simulation is given.

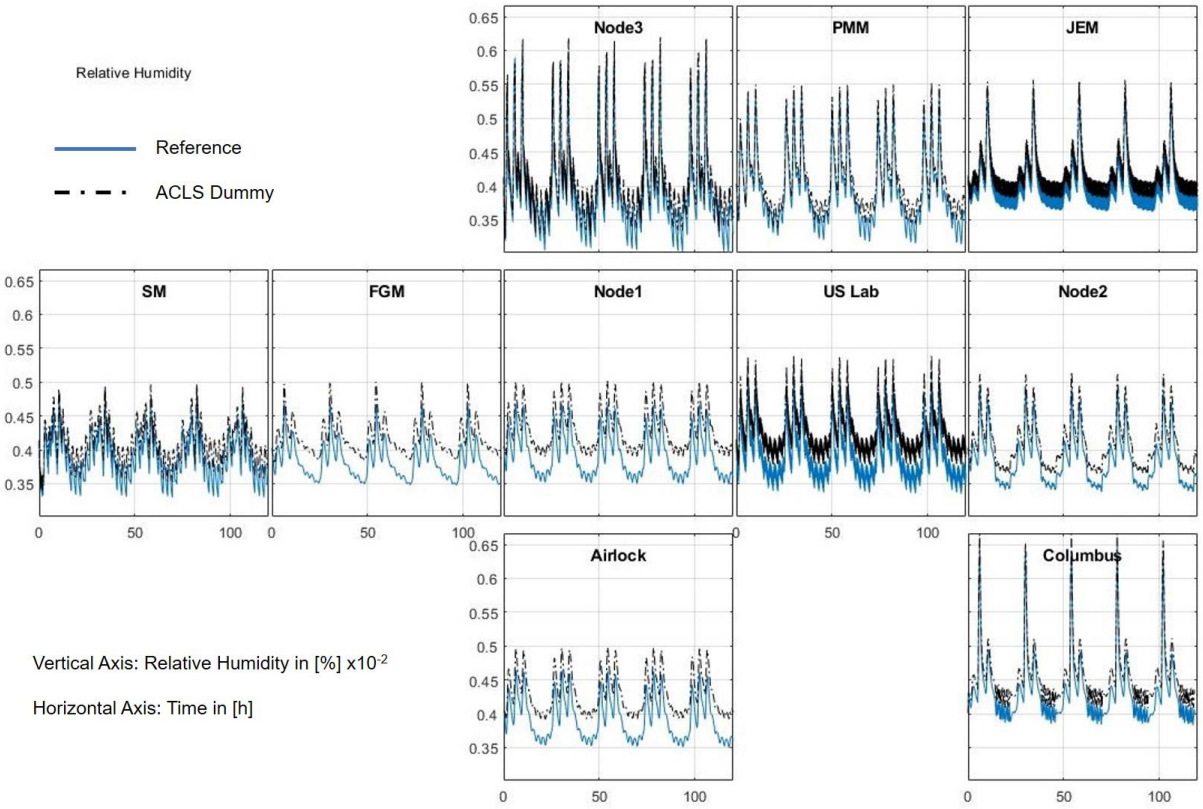

Fig. 3-24: Results of the relative humidity simulated with the ACLS_Dummy compared to the reference.

The relative humidity level reaches a higher value than in the reference simulation, but it is still acceptable and follows the same pattern. In all modules the increase is similar and in the US-Lab, where the ACLS system is located, no special increase is noticeable. The spikes of the relative humidity climb at the same level how the overall values, so there is no exceeding of any limits. The nominal value of 40 % is just achieved by the lower limit of the relative humidity in the most modules, but in the Columbus module this value is never reached anymore (Tab. 3-26).

Tab. 3-26: Values of the relative humidity in some modules for the ACLS_Dummy case.

		Columbus	US-Lab	SM
Relative humidity for the ACLS_Dummy case in [%]	Maximum	67	54	50
	Minimum	41	38	36
	Average	45	43	41

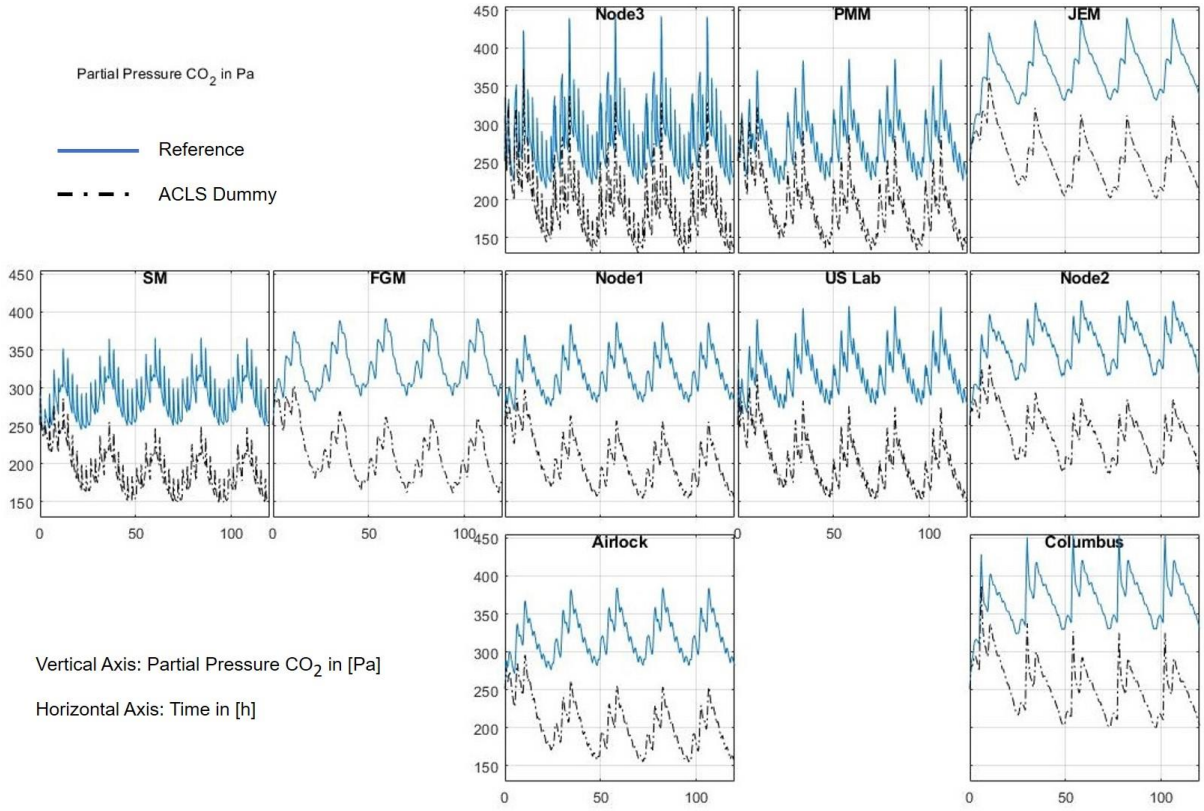

Fig. 3-25: Results of the partial pressure CO_2 simulated with ACLS_Dummy compared to the reference.

The partial pressure of CO_2 is remarkable lower in all modules with the ACLS Dummy and nearly reaches 60% of the reference value in some modules, meanwhile the profile of the curve stays the same. But an especially strong decline in the US Lab cannot be determined. Of course, the CO_2 values follow all limits (Tab. 3-27).

Tab. 3-27: Comparison of the partial pressure of CO_2 for some modules.

		Columbus	US-Lab	SM
Maximum CO_2 partial pressure [Pa]	Reference case	455	408	365
	ACLS_Dummy	325	274	249
Average CO_2 partial pressure [Pa]	Reference case	371	323	298
	ACLS_Dummy	243	194	188

3.2.8 Advanced SimpleCDRA

The SimpleCDRA system was temporary modified with the calculateEquilibriumLoading function. This function is also implemented in the ComplexCDRA and uses the toth equitation Eq. (3-5) to calculate the capacity of the zeolite to adsorb the CO_2. In the SimpleCDRA function an interpolation of a given table with zeolite capacities is used.

$$q_i^* = \frac{b_i P_i q_{si}}{[1 + (\sum_j b_j P_j)^{m_i}]^{\frac{1}{m_i}}} \qquad \textbf{Eq. (3-5)}$$

$$b_i = b_{0i} \exp(\frac{B_i}{T}) \qquad \textbf{Eq. (3-6)}$$

$$m_i = m_{0i} + (\frac{m_{Ti}}{T}) \qquad \textbf{Eq. (3-7)}$$

The equilibrium loading $\mathbf{q^*_i}$ is calculated by the toth variables $\mathbf{m_i}$, $\mathbf{b_i}$ and the predefined toth parameter $\mathbf{q_{si}}$. $\mathbf{P_i}$ represents the partial pressure of the absorbed substance and the summation is over all substances of the system. The toth variables $\mathbf{b_i}$ (Eq. (3-6)) and $\mathbf{m_i}$ (Eq. (3-7)) are calculated with the predefined toth Parameters $\mathbf{b_{oi}}$, $\mathbf{m_{oi}}$, $\mathbf{B_i}$ and $\mathbf{m_{Ti}}$. Both variables are also dependent from the temperature **T** [10]**.** With usage of the toth equation a more realistic calculation of the capacity is possible, and it should be used to vary the parameters $\mathbf{m_{0i}}$, $\mathbf{b_{0i}}$, $\mathbf{B_i}$, $\mathbf{m_{ti}}$ and $\mathbf{q_{si}}$, which model the zeolite isotherms [11] and examine their impact on the CO_2 absorption. After some tests and modifications, the basic function went to work. In the following figures you can see two test simulations.

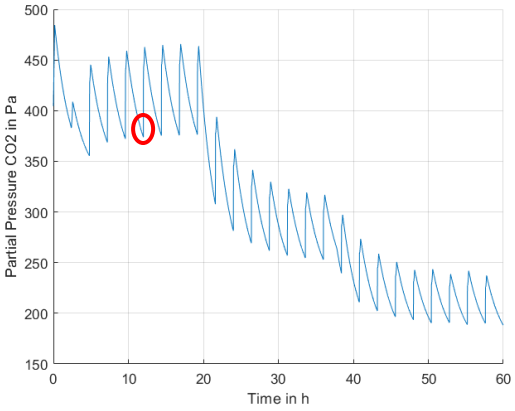

Fig. 3-26: Results with SimpleCDRA

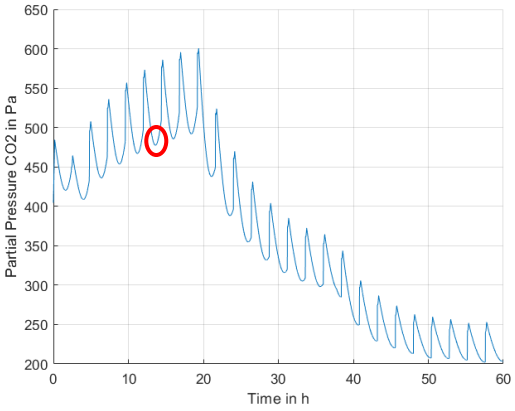

Fig. 3-27:Results with Advanced SimpleCDRA

In both cases the CDRA Tutorial was simulated, which is a test simulation to prove the function of the CO_2 absorption ability of the CDRA system. In this test the first 19,4 hours a system with six crew members, the next 18,5 hours a system with 4 crew members and the last 22,2 hours a system with three crew members is simulated. Thereby the partial pressure of CO_2 drops in both cases step by step. The results of the SimpleCDRA function is pictured in Fig. 3-26 and the results of the Advanced SimpleCDRA in Fig. 3-27. As you can see, the Advanced SimpleCDRA provides a nearly 150 Pa higher CO_2 Partial Pressure when simulating with six crew members. Moreover, the graph shows a difference in the marked parts. The sharp corners in the left picture are typically for this simulation and indicates the switch from absorbing to desorbing in the zeolite beds. In the right figure these sharp corners are missing, instead you can see a rather round curve. This can be explained with zeolite absorbers, which reached their maximum loading. That difference in the CDRA functions is because of a lower zeolite capacity, calculated by the calculateEquilibriumLoading

function of the Advanced SimpleCDRA, which also explains the higher CO_2 partial pressure. To fix this problem the whole SimpleCDRA system must be remodeled, what will lead to the ComplexCDRA function, which is already under development but not finished yet. Because of this, the influence of the toth parameters could not be tested.

4 Error propagation

Error propagation is a branch of the mathematical error calculation. It is used to calculate the deviation of a result, which has been calculated with values that already showed some errors in their results. In this chapter the mathematical principle of error propagation is presented and how it needs to be adapted to use it with the ISS V-HAB model to create a function, which calculates the deviation of the results to the reference model when using varied input parameters.

4.1 Method

4.1.1 Mathematical basic principles [12] [13]

For better understanding the two kinds of errors, which are considered in error propagation, are explained shortly.

Random errors. These errors typical vary top and bottom from the real value. The deviation can be caused through different effects. For example, it can be a reading error because of a small scale or a varying value over the time.

Systematic errors. These errors affect the result always in the same direction. For example, that can be caused by a wrong justified measurement equipment. If you have a thermometer, which always shows two degrees colder than it is in reality, all your measurement points are two degrees too low.

There are two principles of error propagation that can be used to investigate the influence of defective values on the result, which is calculated with these values.

The first principle is the **linear error propagation.** This approach consists of the development of a Taylor series, which is stopped after the first element, to calculate the searched error. From this results the following Equation.

$$\Delta\lambda = \frac{\delta f}{\delta x_1} \times \Delta x_1 + \frac{\delta f}{\delta x_2} \times \Delta x_2 + \ \ldots \qquad \textbf{Eq. (4-1)}$$

In this equation **Δλ** is the total error, $\frac{\delta f}{\delta x_{1,2\ldots}}$ symbolizes the partial derivative from **f** after $x_{1,2\ldots}$ and $\Delta x_{1,2\ldots}$ are the known errors from $x_{1,2\ldots}$. To get the final equation for the maximal error (Eq. (4-2)) or the mean error (Eq. (4-3)) some changes have to be done to Eq. (4-1) because with this equation it is possible that the errors will compensate each other.

$$\Delta\lambda_{max} = \left|\frac{\delta f}{\delta x_1} * \Delta x_1\right| + \left|\frac{\delta f}{\delta x_2} * \Delta x_2\right| + \cdots \pm \frac{\delta f}{\delta x_{1,2\ldots}} * \Delta x_{1sys,2sys,\ldots} \qquad \textbf{Eq. (4-2)}$$

$$\Delta\lambda_{mean} = \sqrt{\left(\frac{\delta f}{\delta x_1} * \Delta x_1\right)^2 + \left(\frac{\delta f}{\delta x_2} * \Delta x_2\right)^2 + \ \ldots \pm \frac{\delta f}{\delta x_{1,2\ldots}} * \Delta x_{1sys,2sys,\ldots}} \qquad \textbf{Eq. (4-3)}$$

At both equations the last part was added to respect eventually appearing systematic errors. The linear error propagation is used when the single errors $x_{1,2,\ldots}$ are known through measurements or similar.

The second principle is the **Gaussian error propagation.** Compared to the linear approach, the Gaussian error propagation is based on statistical considerations. It can be used to calculate the standard deviation $\bar{s}_f$ (Eq. (4-4)) based on statistical determined errors.

$$\bar{s}_f = \sqrt{\left(\frac{\delta f}{\delta x_1} * \bar{s}_{x1}\right)^2 + \left(\frac{\delta f}{\delta x_2} * \bar{s}_{x2}\right)^2 + \ \dots} \qquad \textbf{Eq. (4-4)}$$

The principle of this equation is similar to the equation for the mean error, but you do not use the known errors $\boldsymbol{\Delta x_{1,2\dots}}$ from $\boldsymbol{x_{1,2\dots}}$ but the mean values $\bar{s}_{x1,x2,\dots}$ of the dependent variable.

4.1.2 Adaption of the principle to the ISS simulation

To perform an error propagation for the ISS simulation only the linear error propagation is a possibility, because the deviations of the single values $\boldsymbol{x_{1,2\dots}}$ are exactly known in this case, since they are the variations, which are determined with the input parameters of the simulation. Furthermore, it does not matter if the equation for mean or maximal error is used, because all variations, which are performed in the simulations are equal to systematic errors. So the part in the equations for random errors falls away (Eq. (4-5)) and only Eq. (4-6)is left over.

$$\Delta\lambda_{max} = \left|\frac{\delta f}{\delta x_1} * \Delta x_1\right| + \left|\frac{\delta f}{\delta x_2} * \Delta x_2\right| + \dots \pm \frac{\delta f}{\delta x_{1,2\dots}} * \Delta x_{1sys,2sys,\dots} \qquad \textbf{Eq. (4-5)}$$

$$\Delta\lambda = \pm\frac{\delta f}{\delta x_{1,2\dots}} * \Delta x_{1sys,2sys,\dots} \qquad \textbf{Eq. (4-6)}$$

As the errors of the single values are known, the more complicated part is to find the function **f** to provide the partial derivative for every single value.

To find this general function, for every input parameter, which can be varied over a specific range, a single function needs to be known. The variables of these functions must be the particular varied parameters and the output can be the deviating value to the reference simulation or directly the deviation in percent to the reference. Of course, for every possible output value, like partial pressure CO_2 or relative humidity, an individual function needs to be created.

To build the necessary functions for every parameter, simulations over the whole range of these input parameters have to be done. With the results it is possible to plot a curve over the input range and the considered result. The corresponding function to the data points is the function needed. After this procedure is done for each input parameter, it is possible to give the function **f** for the particular considered result.

The first step at the selection of the best fitted function is the visual examination of the curve. There can be parts of the curve that differ explicitly from the expected course. If there are more than one good fitted curves, there are four statistics provided by MATLAB, which evaluate the goodness-of-fit. These statistics are explained in Tab. 4-1.

Tab. 4-1: Statistics to prove the goodness-of-fit.

The sum of squares due to error (SSE)	“This statistic measures the total deviation of the response values from the fit to the response values. A value closer to 0 indicates that the model has a smaller random error component, and that the fit will be more useful for prediction.” [14]
R-square	“R-square is the square of the correlation between the response values and the predicted response values. R-square can take on any value between 0 and 1, with a value closer to 1 indicating that a greater proportion of variance is accounted for by the model.” [14]
Adjusted (Adj.) R-square	“This statistic uses the R-square statistic defined above, and adjusts it based on the residual degrees of freedom. The adjusted R-square statistic can take on any value less than or equal to 1, with a value closer to 1 indicating a better fit.” [14]
Root mean squared error (RMSE)	“This statistic is also known as the fit standard error and the standard error of the regression. It is an estimate of the standard deviation of the random component in the data. A RMSE value closer to 0 indicates a fit that is more useful for prediction.” [14]

In Fig. 4-1 an example for such data points and how they can be fitted to a suitable function is given.

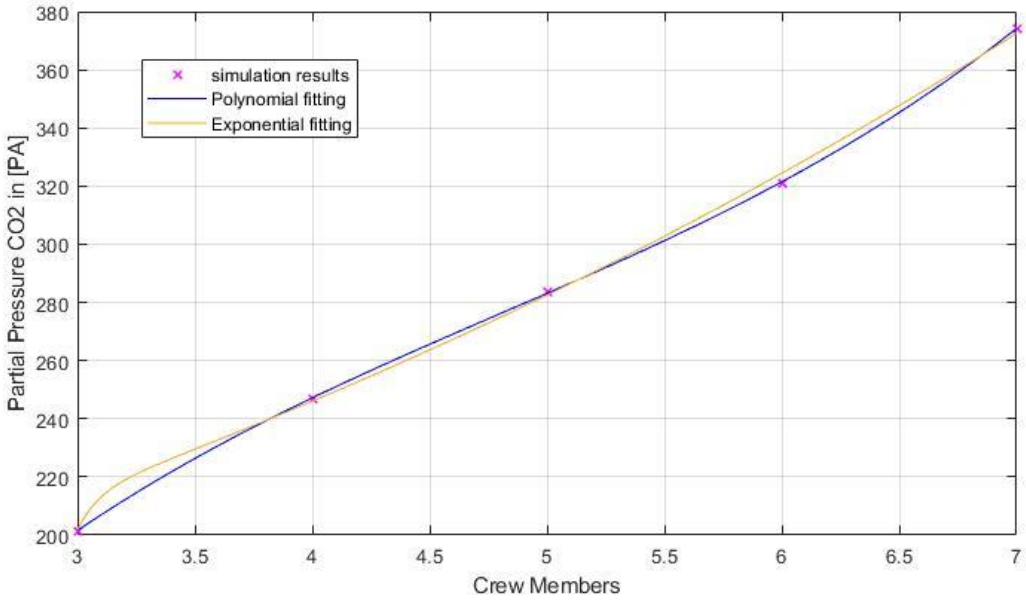

Fig. 4-1: Simulation results with two fitted functions.

It is visible to the naked eye that the yellow curve, fitted with an exponential function, has a spot between 3 and 3,5 on the x-Axis, which does not fit the data points very well. But to give a complete example of the selection process the goodness-of-fit statistics are given for both fitted functions in Tab. 4-2.

Tab. 4-2: Comparison of the goodness-of-fit statistics for both functions.

	SSE	R-square	Adjusted R-square	RMSE
Polynomial function	0,3691	1,0	0,9999	0,6075
Exponential function	15,5375	0,9991	0,9965	3,9417

The statistics clearly confirm, what was visible in the graph. The Polynomial function is better than the Exponential function in every statistic value. Especially the SSE and the RMSE are way lower at the Polynomial function.

In the following a short guidance is given how to get to a function to calculate the deviation of any value, which is influenced by a change of the simulation parameters, without the need of doing an extra simulation.

1. The value, from which the deviation should be calculated, must be determined, for example CO_2, O_2 or relative humidity. After that, all parameters, which influence the chosen value in the simulation and are not clearly defined with an exact value, need to be found.

2. Simulations for every single parameter over the whole range the parameter can be varied have to take place. The more simulations within the specified range are done, the better will be the fitted function for this parameter in the end. But it also will take more time.

3. With the received data points from the simulations, functions for every varied parameter are created via curve fitting. The best fitted functions will be chosen like mentioned before.

4. By adding up the functions, which were chosen for every parameter, the function **f** mentioned in Eq. (4-6) is formed. Now the function **f** must be derived after every variable appearing in the function. After that the partial derivation is done.

5. Now the deviation for the value chosen at the beginning can be calculated. Therefore, the condition of the system, of which the behavior should be examined, is defined by choosing the deviation of the input parameters.

4.1.3 Changes to the principle to improve accuracy

The introduced principle is rather used for small errors. So, it is expected the bigger the errors get the more inaccurate the deviation results will be. This is because the equation uses the derivation of the functions for the deviations, which is the gradient of the function in a particular point. For small errors the gradient of the function does not change significantly in the deviation range. But unfortunately, in the case of the ISS simulation the deviation is rather bigger. So, the idea is, not to use the gradient in one point but the mean gradient over the whole part of the function from the reference value to the value of the deviation. The mean gradient between two points of a function can be calculated with the equation Eq. (4-7).

$$m = \frac{f(x_2) - f(x_1)}{x_2 - x_1} \qquad \textbf{Eq. (4-7)}$$

In this equation **m** is the mean gradient of the function **f** in the interval from $\mathbf{x_1}$ to $\mathbf{x_2}$. This can be put in Eq. (4-6) instead of the partial deviation for every function. Then the equation for the total error **Δλ** looks like in Eq. (4-8).

$$\Delta\lambda = \frac{f_{1,2,\dots}\left(x_{2,(1,2,\dots)}\right) - f_{1,2,\dots}\left(x_{1,(1,2,\dots)}\right)}{x_{2,(1,2,\dots)} - x_{1,(1,2,\dots)}} \times \Delta x_{1sys,2sys,\dots} \qquad \textbf{Eq. (4-8)}$$

In this equitation $\mathbf{f_{1,2,\dots}}$ are the functions found by curve fitting for the different input parameters. $\mathbf{X_{1,(1,2,\dots)}}$ and $\mathbf{x_{2,(1,2,\dots)}}$ are the reference and the deviation value for the parameter belonging to the function mentioned in the brackets in the index. Because $\mathbf{\Delta x_{1sys,2sys,\dots}}$ is the same like the difference under the break mark the equation simplifies to Eq. (4-9).

$$\Delta\lambda = f_{1,2,\dots}\left(x_{2,(1,2,\dots)}\right) - f_{1,2,\dots}\left(x_{1,(1,2,\dots)}\right) \qquad \textbf{Eq. (4-9)}$$

The difference in the results of this approach, in the following named “advanced approach”, and the “standard approach” mentioned before will be evaluated in chapter 5.3. The procedure to obtain a deviation function with this approach is the same in the first three points compared to the standard approach but the following step divers from it.

1. See 4.1.2.
2. See 4.1.2.
3. See 4.1.2.
4. Now the fitted functions can be used to build the function for the deviation in Eq. (4-9). After that the deviation for the value chosen at the beginning can be calculated. Therefore, the parameters of the two cases, which should be compared, need to be put in the function.

4.2 Example calculation for relative humidity

The approaches mentioned in the chapter before are now performed to find a function to calculate the deviation of the relative humidity. Therefore, the points in the instruction in 4.1.2 and in 4.1.3 will be processed on by one.

4.2.1 Determination of the used input parameters

At first all parameters, which can reasonable influence the relative humidity of the ISS atmosphere, need to be found. Furthermore, the values these parameters can take are determined. In Tab. 4-3 all parameters, which will go down in the derivation function, are listed with the range of values they will be simulated.

Tab. 4-3: Selected input parameters with variation area.

Input parameter	Simulated range
SetTemperature	291,65 K to 299,65 K
CoolantTemperature	277,15 K to 282,55 K
CrewMembers	3 to 7 crew members
BPA_Dummy	On or off (1 or 0)
AClS_Dummy	On or off (1 or 0)

4.2.2 Simulations with the determined parameters

It is difficult to give a deviation function for the whole ISS, because the results between the modules have particulate strong variations. For this example, only the results for the Node 1 module are used and a function for this module is given. The simulations will last 5 days so that the last 2 days of the simulation represent a steady state, which can be used to calculate comparable values. Over the last two days of the simulation the mean value for the relative humidity is calculated and the results for all simulated cases are then used to find the function for each parameter. In Tab. 4-3, an example for the relative humidity in Node 1 over a 5-day simulation is given and the used steady state area is marked as well as the calculated mean value.

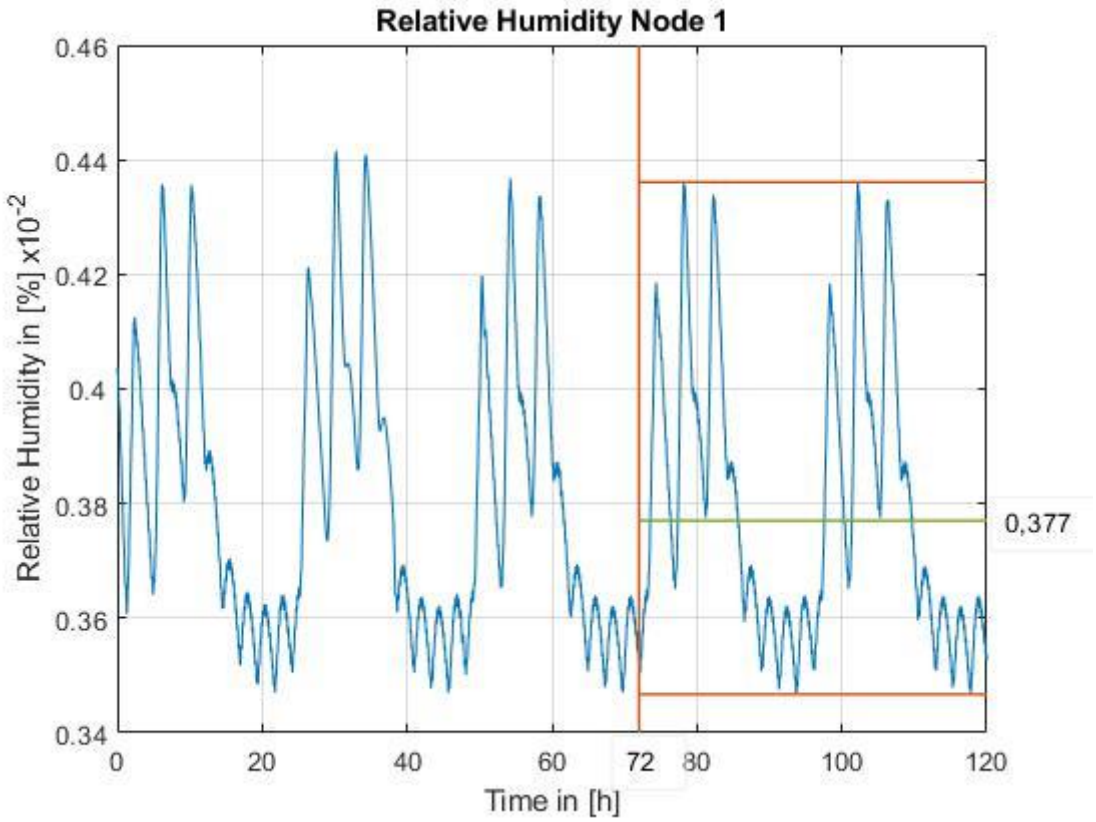

Fig. 4-2: Used area to calculate the mean value of the relative humidity.

In this case a deviation function, which gives the deviation in percent, should be generated. So, the data points, which characterize the relative humidity of each

simulation, must be converted to a deviation value in percent from the reference simulation. It is also possible to develop the function with the original data points. Then a function is generated, which gives the difference of the reference value and the calculated value as percentage of the relative humidity. It is no problem to convert these two types of deviation into each other, when the value of the relative humidity for the reference case is known. The diagrams for the direct simulation results and the converted deviation are given for each parameter in the following figures.

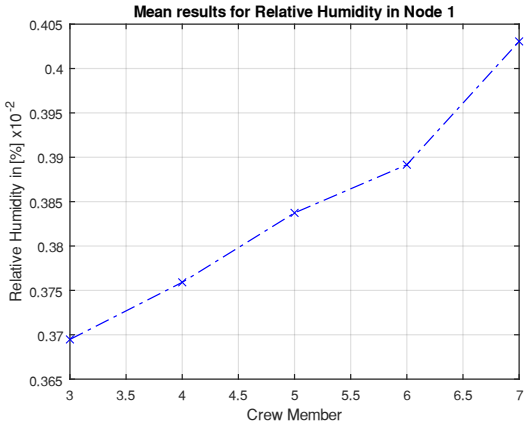

Fig. 4-3: Results with varied CrewMembers

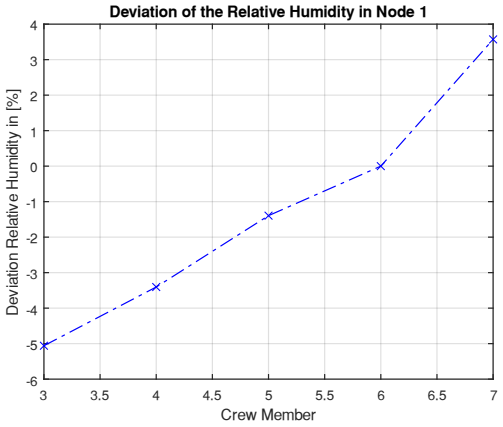

Fig. 4-4: Deviation with varied CrewMembers

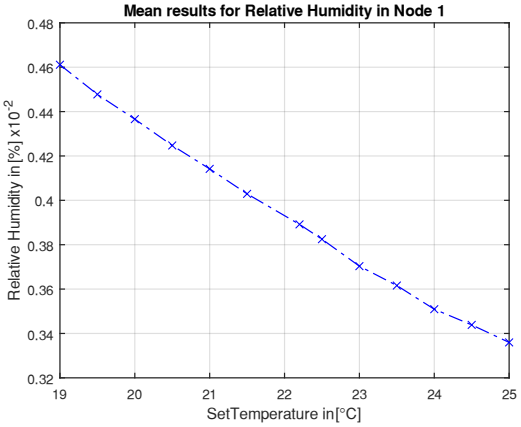

Fig. 4-5: Results with varied SetTemperature

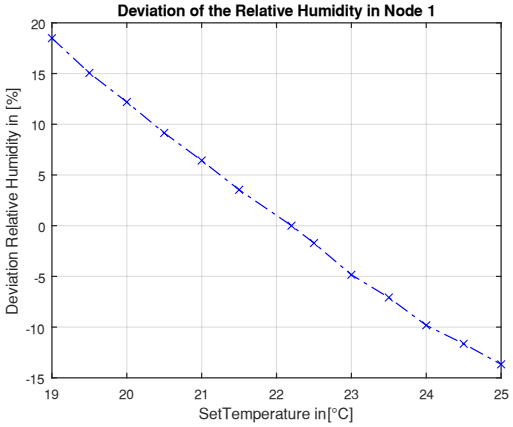

Fig. 4-6: Deviation with varied SetTemperature

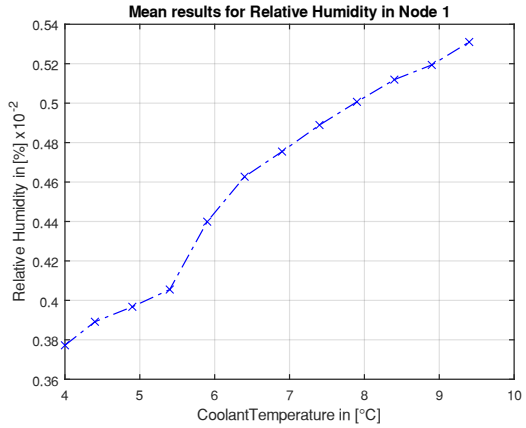

Fig. 4-7: Results with varied CoolantTemperature

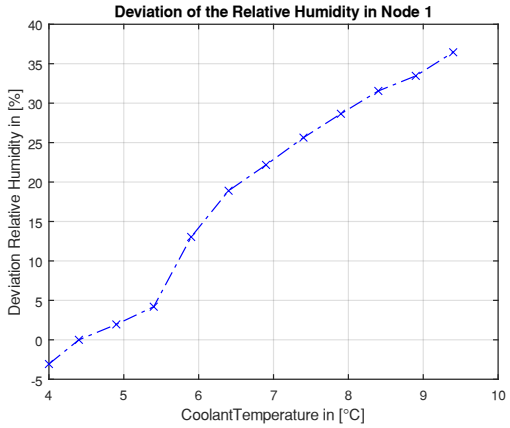

Fig. 4-8: Deviation with varied CoolantTemperature

For the BPA_Dummy and the ACLS_Dummy it is not possible to create a function, because the only possible variation is if the systems are working or not. So, the deviation whit the reference simulation can be calculated directly and is given in Tab. 4-4.

Tab. 4-4: Deviation of the relative humidity caused by extra payloads.

	Reference	BPA_Dummy	ACLS_Dummy
Rel. Humidity in [%]	38,92	39,50	42,02
Difference to Ref. in [%]	-	0,58	3,1
Deviation from Ref. in [%]	-	1,49	7,96

4.2.3 Curve fitting to create necessary functions

Now for the three parameters SetTemperature, CoolantTemperature and CrewMembers the corresponding functions are generated via curve fitting with the simulation results. The index each input parameter will have in the final function is given in Tab. 4-5.

Tab. 4-5: Indices of the different input parameters.

SetTemperature	X_1
CoolantTemperature	X_2
CrewMembers	X_3
BPA_Dummy	X_4
ACLS Dummy	X_5

For the simulation results of the SetTemperature input five functions come in the nearer selection. The Functions are plotted in Fig. 4-9.

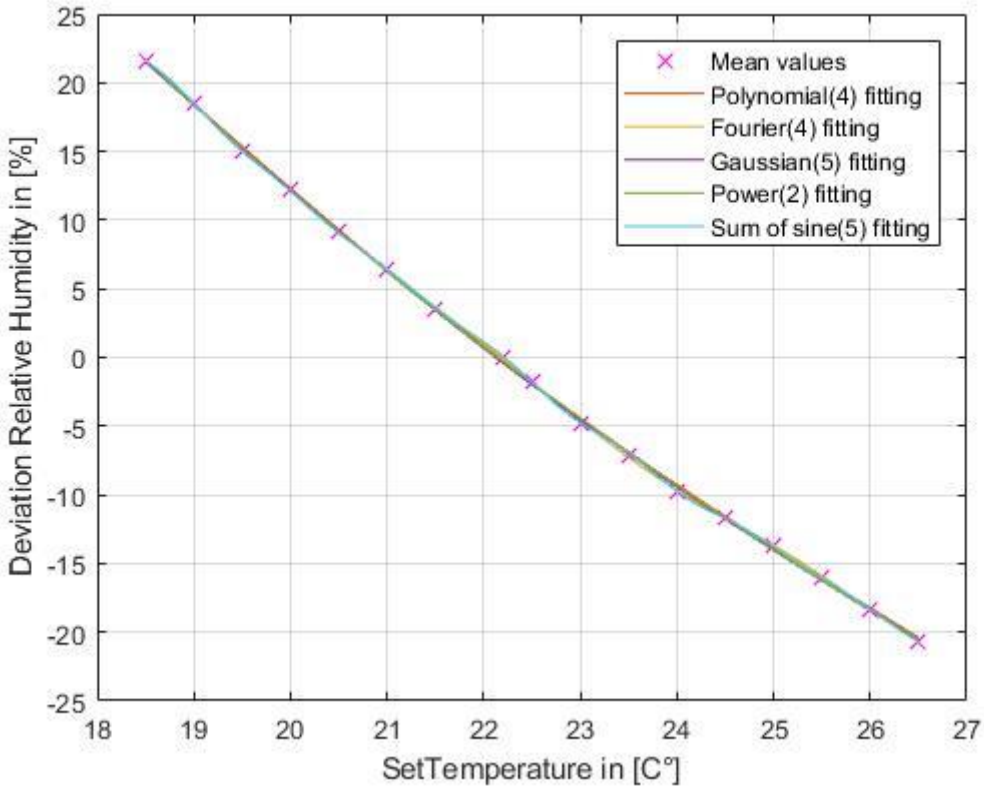

Fig. 4-9: Comparison of the fitted functions for the SetTemperature variation.

All plotted functions look good by visual examination. There is hardly a difference to discover and therefore, the goodness-of-fit statistics in Tab. 4-6 are consulted to make a decision.

Tab. 4-6: Comparison of the goodness-of-fit statistics for the SetTemperature functions.

Function	SSE	R-squared	Adj. R-square	RMSE
Polynomial 4th degree	0,7333	0,9997	0,9997	0,2472
Fourier 4 terms	0,2180	0,9999	0,9998	0,1765
Gaussian 5 terms	0,7499	0,9997	0,9986	0,5
Power 2 terms	0,7982	0,9997	0,9997	0,2388
Sum of sine 5 terms	0,0546	1,0	0,9998	0,1653

The Function fitted with a sum of sine term is the best in all statistics, so it seems clear to choose this one. But on a second view it is also a possibility to take the function fitted with power series, because it is obviously simpler with only two terms than the sum of sine function with 5 terms. More examination revealed that the maximum difference in the results at particulate input values of the functions is 0,5 percent. Because the accuracy of the error propagation should be evaluated in this case, the

sum of sine function is selected. But if it is necessary to look after complexity and effort the function fitted with power is also an option.

For the simulation results of the CoolantTemperature input six fitted functions come in the nearer selection. The Functions are plotted in Fig. 4-10.

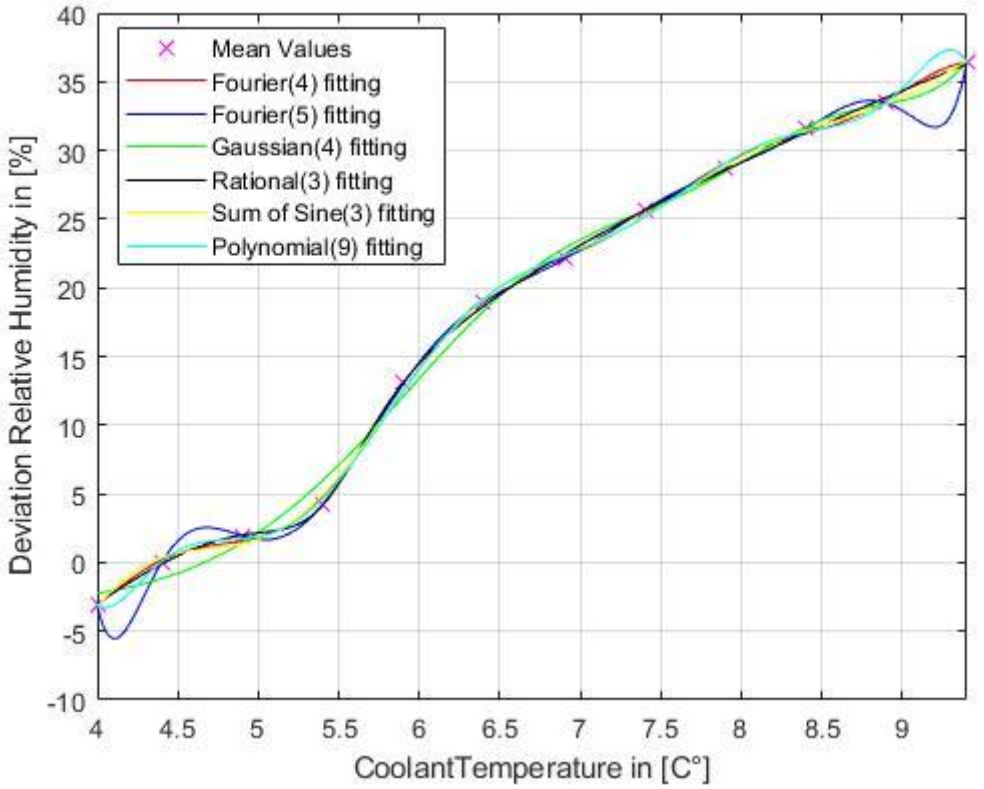

Fig. 4-10: Comparison of the fitted functions for the CoolantTemperature variation.

There a three functions, which show visual deviations that do not stick to the data points. The Fourier fitted function with 5 terms shows heavy oscillations from 4 C° to 5 C° and from 8.5 C° to 9.4 C° on the x-axis. The Polynomial fitted function wit 9 terms shows also a deviation from 8.5 C° to 9.4 C°. The Gaussian fitted function with 4 terms has no heavy oscillations, but from 4 C° to 6.5 C° the function rather does fit to mean values of the simulation results and is too far away from the data points. The final selection of the used function is done with the goodness-of-fit statistics in Tab. 4-7.

Tab. 4-7: Comparison of the goodness-of-fit statistics for the CoolantTemperature functions.

Function	SSE	R-squared	Adj. R-square	RMSE
Fourier 4 terms	1,2831	0,9994	0,9968	0,8010
Fourier 5 terms	0,0198	1,000	NaN	NaN
Gaussian 4 terms	7,2408	0,9967	NaN	NaN
Rational 3 degree	0,3955	0,9998	0,9996	0,2813

Sum of sine 3 terms	1,6247	0,9993	0,9973	0,7359
Polynomial 9th degree	1,1801	0,9995	0,9970	0,7681

It is interesting that the two statistics, which are available for the function fitted with 5 Fourier terms, are the best with distance to the other ones. This is the proof that you should not rely on the goodness-of-fit statistics alone, because by visual examination this function was already rejected. The rational fitted function is in these two statistics the second best and has also a clear distance to the next one. In the other two statistic values the rational function is even the overall best. Because it also had no conspicuousness by visual examination this function was chosen to symbolize the deviation by varying the coolant temperature.

For the simulation results of the CrewMembers input four fitted functions come in the nearer selection. The Functions are plotted in Fig. 4-11.

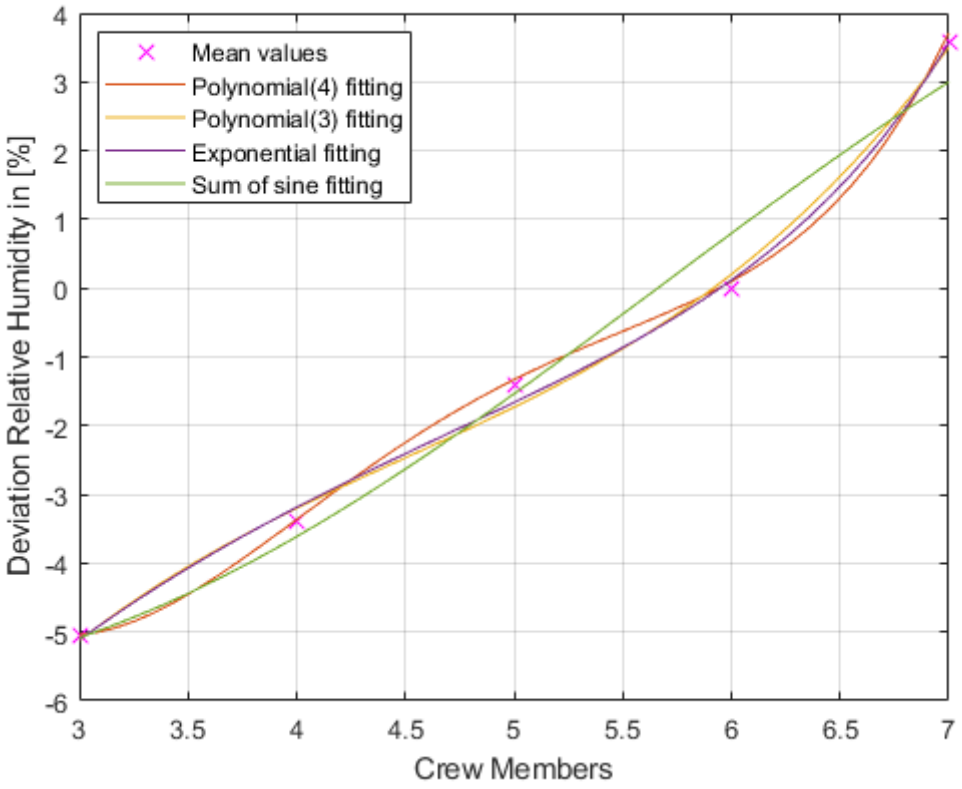

Fig. 4-11: Comparison of the fitted functions for the CrewMembers variation.

By visual examination the green function fitted with a sum of sine seems the worst, because especially the values right from five crew members are clearly farer away from the simulation results than the other ones. But the other three functions make a good impression. In Tab. 4-8 the goodness-of-fit statistics are given for the four functions.

Tab. 4-8: Comparison of the goodness-of-fit statistics for the CrewMembers functions

Function	SSE	R-squared	Adj. R-square	RMSE
Polynomial 4th degree	4,0116x10-26	1	Not a Number (NaN)	NaN
Polynomial 3th degree	0,2022	0,9944	0,9816	0,4497
Exponential	0,1357	0,9969	0,9877	0,3684
Sum of sine	1,0274	0,9766	0,9533	0,7167

Here are two functions that are the best in two out four statistic points each. The function fitted with a polynomial of the 4th degree was chosen in the end, because for this function it is important to fit on the whole numbers of the x-Axis. This is because the simulation will always run with whole crew members and not with four and a half or similar. The SSE and R-squared statistics give an indication how good the function fits at the whole numbers, because these also were the points the function was fitted around.

As already mentioned for the input parameters BPA_Dummy and ACLS_Dummy no function fitting is possible. So, in Tab. 4-9 the developed functions for all input parameters, SetTemperature $\mathbf{f_1}$, CoolantTemperature $\mathbf{f_2}$, CrewMembers $\mathbf{f_3}$, BPA_Dummy $\mathbf{f_4}$ and ACLS_ Dummy $\mathbf{f_5}$ are given.

Tab. 4-9: Functions developed for each parameter.

$f_1(x_1) =$	$4.828 * \sin(1.06 * x_1 + 13.65) + 3.043 * \sin(1.268 * x_1 + 24.63) - 0.1445 * \sin(5.234 * x_1 - 42.72) - 0.09991 * \sin(3.979 * x_1 - 19.85) + 19.97 * \sin(0.3483 * x_1 + 7.951)$
$f_2(x_2) =$	$(120.0005 * x_2^3 + -1794.2 * x_2^2 + 8926.4 * x_2 - 14765) / (x_2^3 - 2.5836 * x_2^2 + -60.1359 * x_2 + 246.3549)$
$f_3(x_3) =$	$0.1568 * x_3^4 - 2.984 * x_3^3 + 20.78 * x_3^2 + -60.82 * x_3 + 58.27$
$f_4(x_4) =$	$1{,}49 * x_4$
$f_5(x_5) =$	$7{,}96 * x_5$

4.2.4 Partial derivation and build of the standard approach function

After creation of the functions for all input parameters the derivations of them are required to assemble the final function for the deviation. In Tab. 4-10 all derivations needed are listed. In this case the derivation of every single function $\mathbf{f_{1,..,5}}$ can be taken, because all functions are independent from each other. If the functions are not independent, all functions have to be added up to the function **f** and a partial derivation must be performed, like it is described in Eq. (4-6).

Tab. 4-10: Derivation of the functions developed for each parameter.

$\frac{\delta f_1}{\delta x_1} =$	$5.11768 * \cos(1.06 * x_1 + 13.65) + 3.85852 * \cos(1.268 * x_1 + 24.63) - 0.756313 * \cos(5.234 * x_1 - 42.72) - 0.39754189 * \cos(3.979 * x_1 - 19.85) * 6.955551 * \cos(0.3483 * x_1 + 7.951)$
$\frac{\delta f_2}{\delta x_2} =$	$\left((-3 * x_2^2 + 5.1671 * x_2 + 60.1359) * (120.0005 \times x_2^3 - 1794.2 * x_2^2 + 8926.4 * x_2 - 14765)\right) / (-x_2^3 + 2.5836 * x_2^2 + 60.1359 * x_2 - 246.3549)^2 - (360.0014 * x_2^2 - 3588.3 * x_2 + 8926.4)/(-x_2^3 + 2.5836 * x_2^2 + 60.1359 * x_2) - 246.3549)$
$\frac{\delta f_3}{\delta x_3} =$	$(0{,}6272 * x_3^3) - (8{,}952 * x_3^2) + (414{,}56 * x_3) - 60{,}82$
$\frac{\delta f_4}{\delta x_4} =$	1,49
$\frac{\delta f_5}{\delta x_5} =$	7,96

Now the derivations can be inserted in the equation for the deviation and as result the final equation (Eq. (4-10)) is ready to calculate $\Delta\lambda_{St.}$.

$$\Delta\lambda_{St.} = \frac{\delta f_1}{\delta x_1} * \Delta x_1 + \frac{\delta f_2}{\delta x_2} * \Delta x_2 + \frac{\delta f_3}{\delta x_3} * \Delta x_3 + \frac{\delta f_4}{\delta x_4} * \Delta x_4 + \frac{\delta f_5}{\delta x_5} * \Delta x_5 \qquad \textbf{Eq. (4-10)}$$

4.2.5 Built of the advanced approach function

The built of the function for the advanced approach is very simple now, because the functions $\mathbf{f_{1,2,3,4,5}}$ have already been developed and that is all what is needed for this approach. In Eq. (4-11) the final Equation to calculate $\Delta\lambda_{Ad.}$ is given.

$$\Delta\lambda_{Ad.} = (f_1(x_{2,1)}) - f_1(x_{1,1})) + (f_2(x_{2,2}) - f_2(x_{1,2})) + (f_3(x_{2,3}) - f_3(x_{1,3})) + 1{,}49 * x_4 + 7{,}96 * x_5 \qquad \textbf{Eq. (4-11)}$$

In the next chapter (5) the equations for $\Delta\lambda_{Ad.}$ and $\Delta\lambda_{St.}$ will be used to calculate some deviations, which will be compared to each other and to the real simulation results.

4.3 Subsystem error

In the following an approach to examine the error caused by a subsystem model, which is not fitted 100 percent to the reality, should be showed. The problem with the error propagation and the subsystem error is that if the quality of the subsystem model is not known, it is hard to say if the deviation of the simulation results compared to the reality is caused by a wrong simulation parameter, like the Coolant Temperature, or an error in the whole subsystem model. Therefore, real test data with known specifications are necessary. Because of the lack of such data for the relative humidity, this is exemplary showed for the CDRA subsystem with the CO_2 partial pressure.

4.3.1 CDRA subsystem

For the CDRA and the CCAA real test data can be found for the CO_2 concentration in a store similar to the US-Lab. The test cases mentioned in “International Space Station Carbon Dioxide Removal Assembly Testing” [15] simulated the behavior of the CDRA system with 6, 4 and 3 crew members. Therefore, exact CO_2 injection rates were defined, and the parameters Coolant Temperature, Set Temperature and cabin pressure are specified, too. The exact parameters are shown in Tab. 4-11.

Tab. 4-11: Test specifications for the CDRA test case in reality.

	Coolant Temperature	Set Temperature	6 Crew Member	4 Crew Member	3 Crew Member	Cabin pressure
CDRA test case	279.261 [K]	291.483 [K]	6 [kg/day]	4 [kg/day]	3 [kg/day]	102732 [Pa]

The real test proceeding was reproduced with the CDRA tutorial, which was already mentioned in 3.2.8. Therefore, the specifications for the Coolant Temperature, Set Temperature, Cabin Pressure and CO_2 injection rates mentioned in Tab. 4-11 are used for the CDRA tutorial. In Fig. 4-12 a comparison of the test results mentioned in [15] and the results of the CDRA tutorial, using the same parameters, is shown.

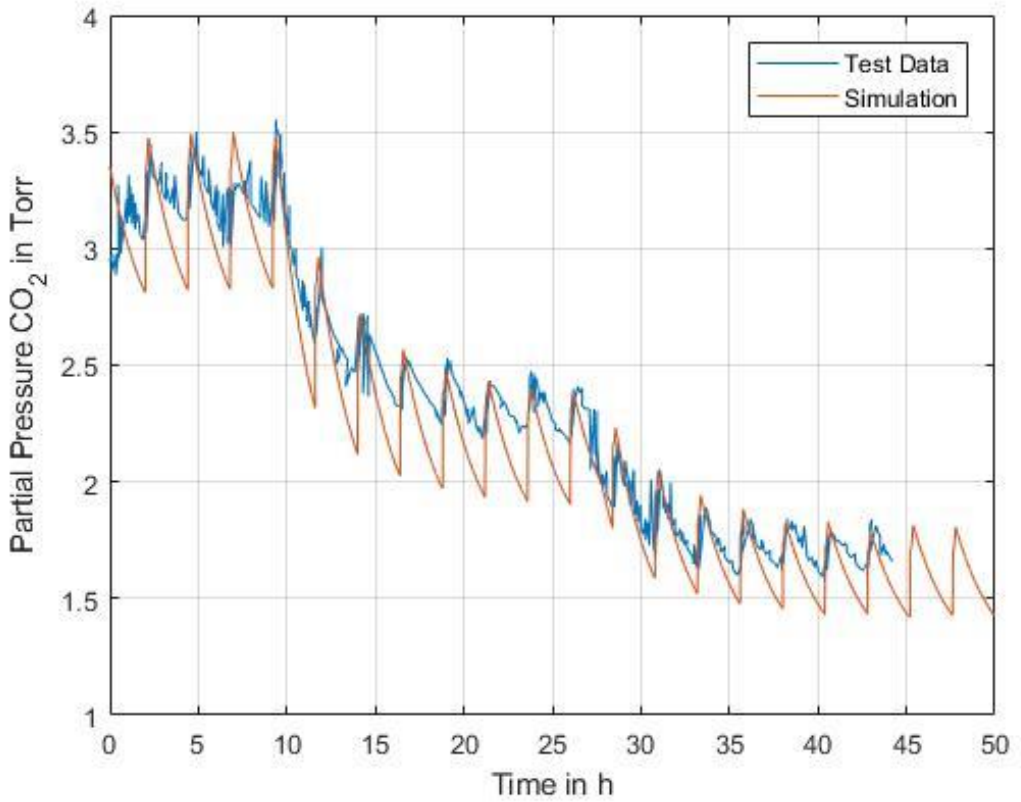

Fig. 4-12: Partial pressure of CO_2 for test [15] and simulation data.

The three steps in the diagram symbolize the transition from 6 crew members in the beginning to 4 crew members in the middle and 3 crew members in the end. So, each case can be examined individually. With knowing the exact values for the Cabin Temperature, Cabin Pressure, Coolant Temperature and CO_2 injection rates, there are

only 2 variables left, which can cause an error. The overall subsystem model or the zeolite material. Because there was no variation of the zeolite possible (3.2.8), this parameter remains unvalued. It is clearly visible in the figure above that the amplitude of the partial pressure is bigger in the simulation than in the test results. The inhomogeneity of the curve from the test date is due the bad quality of the picture the data is taken from. To examine the differences in the three cases with a varying number of crew members, sections of the diagram, where a steady state is visible, were selected and are shown in Fig. 4-13 to Fig. 4-15.

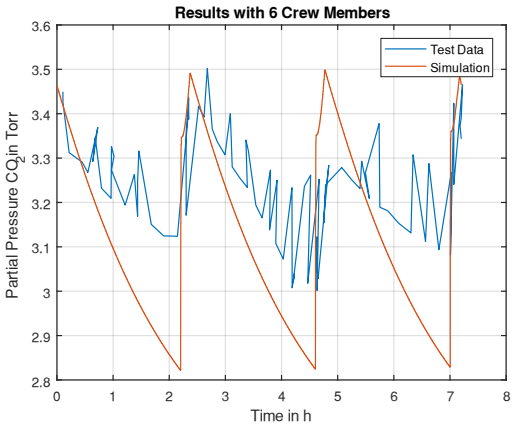

Fig. 4-13: Comparison of test and simulation.

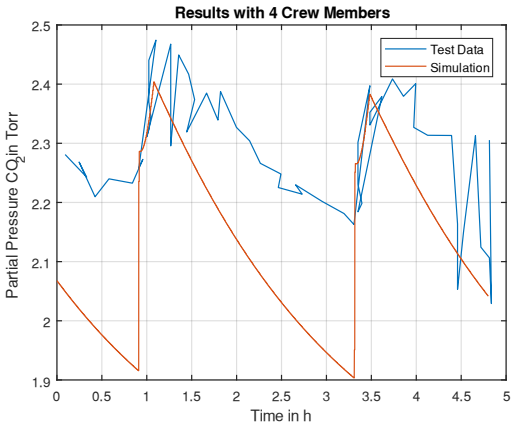

Fig. 4-14: Comparison of test and simulation.

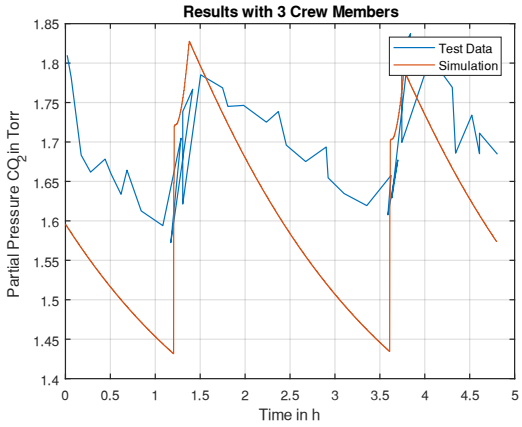

Fig. 4-15: Comparison of test and simulation.

As already mentioned the simulation results show a bigger amplitude in the CO_2 values. In Tab. 4-12 the deviations of each case for the maximal, minimum and average values of the simulation compared to the test data are estimated.

Tab. 4-12: Deviations of the simulation cases compared to the test data.

	6 Crew Members	4 Crew Members	3 Crew Members
Maximal Values	0 % to 3.6 %	1 % to 2.7 %	0.5 % to 2.5 %
Minimum Values	6.4 % to 10.9 %	12 % to 13.7 %	8.9 % to 11.1 %
Average Values	1.1 %	5 %	3.4 %

The deviation of the maximal values shows the smallest difference between the test and the simulation, but the minimal values deviate clearly. Hence the deviation of the average values is mostly caused by the difference in the minimal values, which has been seen by the naked eye in the diagrams. Now the question is, if this error of the simulation is caused by the zeolite used in the simulation, which could have a better adsorption ability than the one in the real test, or the CDRA model does not conform to the real test system. With the existing results it can only be said, that the system deviates about in average 1.1 % to 5 %, dependent from the simulation case, to the real system. When the subsystem error can be specified more exactly, its deviation can be respected in the error calculation. Then it is known that the simulation and also the error calculation results generally deviate about the error of the subsystem compared to the reality, and the influence of the varied input parameters and the deviation from the real system can be estimated more accurate. With the functions given in Eq. (4-10) and Eq. (4-11) only the deviation of one simulation case to another simulation case is calculated. When the error of the simulation to the reality should be calculated, the error of the subsystems must be respected, too. As the subsystem errors are systematic errors and not dependent from a function they can be handled like the BPA or ACLS Dummy. This would lead to the modified terms for the standard (Eq. (4-12)) and the advanced approach (Eq. (4-13)).

$$\Delta\boldsymbol{\lambda}_{\mathbf{St.}} = \frac{\delta f_1}{\delta x_1} * \Delta x_1 + \frac{\delta f_2}{\delta x_2} * \Delta x_2 + \frac{\delta f_3}{\delta x_3} * \Delta x_3 + \frac{\delta f_4}{\delta x_4} * \Delta x_4 + \frac{\delta f_5}{\delta x_5} * \Delta x_5 + \frac{\delta f_{subsys.}}{\delta x_{subsys.}} * \Delta x_{subsys.} \qquad \textbf{Eq. (4-12)}$$

$\frac{\delta f_{subsys.}}{\delta x_{subsys.}}$ is the derivation of the function for the particular subsystem. As it is like with the BPA or with the ACLS Dummy, this is just one term with one value. $\Delta x_{subsys.}$ can also just be 0 or 1 and determines, if the subsystem should be respected in the calculation.

$$\Delta\boldsymbol{\lambda}_{\mathbf{Ad.}} = (f_1(x_{2,1)}) - f_1(x_{1,1})) + (f_2(x_{2,2}) - f_2(x_{1,2})) + (f_3(x_{2,3}) - f_3(x_{1,3})) + 1{,}49 * x_4 + 7{,}96 * x_5 + \Delta y_{subsys.} * x_{subsys.} \qquad \textbf{Eq. (4-13)}$$

$\boldsymbol{\Delta y_{subsys.}}$ is the deviation, which is determined for the subsystem, like it is the 7.96 for the ACLS Dummy in this term. $\boldsymbol{x_{subsys.}}$ is also similar to the ACLS Dummy and can only be 0 or 1, which determines if the subsystem should be respected in the calculation.

In both equations every desired subsystem can be added on this way. With these terms it would be possible to calculate deviations from the simulation results to the reality, presupposed the working parameters and the subsystem errors are known.

This chapter should only be an example how to evaluate and respect errors of whole subsystems. Because of no real test data is available, this cannot performed for the example calculation of the relative humidity. But when the new Complex CDRA subsystem is introduced, which promises considerable better results and allows a variation of the zeolite isotherms, it might be possible to give a more exact assumption for the quality of the CDRA subsystem model and do an error calculation for the partial pressure of CO_2.

5 Verification

The functions for the deviation of the relative humidity, which were developed in the chapter before, are now used to calculate some test cases. The results of them are compared with the results of the real simulations with the same parameters. Thus, the validity of the error propagation calculation can be evaluated.

5.1 Definition of the test cases

In Tab. 5-1 all test cases are specified, and the varied input values are given.

Tab. 5-1: Definition of all test cases.

Reference: $case_0$	According to Tab. 3-2.
1 changed parameter: $case_1$	CoolantTemperature: 6.7 °C.
1 changed parameter: $case_2$	SetTemperature: 19.2 °C.
1 changed parameter: $case_3$	CrewMembers: 7.
2 changed parameters: $case_4$	CoolantTemperature: 6.7 °C. SetTemperature: 19.2 °C
3 changed parameters: $case_5$	CoolantTemperature: 6.7 °C. SetTemperature: 19.2 °C. CrewMembers: 7.
2 changed parameters: $case_6$	CoolantTemperature: 7.4 °C. SetTemperature: 24 °C.
3 changed parameters: $case_7$	CoolantTemperature: 7.4 °C. SetTemperature: 24 °C. CrewMembers: 3.
4 changed parameters: $case_8$	CoolantTemperature: 7.4 °C. SetTemperature: 24 °C. CrewMembers: 3. BPA_Dummy: On.
5 changed parameters: $case_9$	CoolantTemperature: 7.4 °C. SetTemperature: 24 °C. CrewMembers: 3. BPA_Dummy: On. ACLS_Dummy: On.
Minimal Rel. Humidity: $case_{10}$	CoolantTemperature: 4 °C. SetTemperature: 26.5 °C.

	CrewMembers: 3.
Maximal Rel. Humidity: $case_{11}$	CoolantTemperature: 9.4 °C. SetTemperature: 18.5 °C. CrewMembers: 7. BPA_Dummy: On. ACLS_Dummy: On.
1 changed parameter: $case_{12}$	CoolantTemperature: 5.9 °C.
1 changed parameter: $case_{13}$	CoolantTemperature: 8.9 °C.

$Case_0$ is the reference case all other cases are compared with. $Case_1$ to $case_3$ are considered to evaluate how exact the two calculation approaches work, when only varying one parameter. This is not done for the BPA_Dummy and the ACLS_Dummy, because there is no function behind to calculate, but only one fixed value, which is the same for both calculation methods. $Case_4$ and $case_5$ are used to prove the behavior of the error propagation when more than one parameter is varied. Here the same values are used as in the cases before to watch the influence on the simulation when more than one parameter is changed, and how they influence each other. Therefore, the parameters were chosen so that they all will cause an increase in the relative humidity to eliminate a compensation of the deviations. In $case_6$ to $case_9$ the parameters were chosen to deviate the relative humidity in both directions. So, a compensation of the deviations will take place and the capability of the calculation methods for this case can be evaluated. $Case_{10}$ and $case_{11}$ should simulate the variations, in which the maximal and minimal humidity, possible with these input parameters, is reached. Here the accuracy of the calculation in extreme situations can be watched and maximal range of the deviation for the relative humidity can be estimated. $Case_{12}$ and $case_{13}$ are simulated to examine the accuracy of the calculations with increasing deviation of a parameter.

5.2 Simulation of the verification cases

Since the deviation calculation is only usable for the values of Node 1, only the simulation results for Node 1 are considered. In Fig. 5-1 to Fig. 5-13 the simulation results for the cases defined in Tab. 5-1 are shown and the mean values for the relative humidity, which are compared to the reference case, are given.

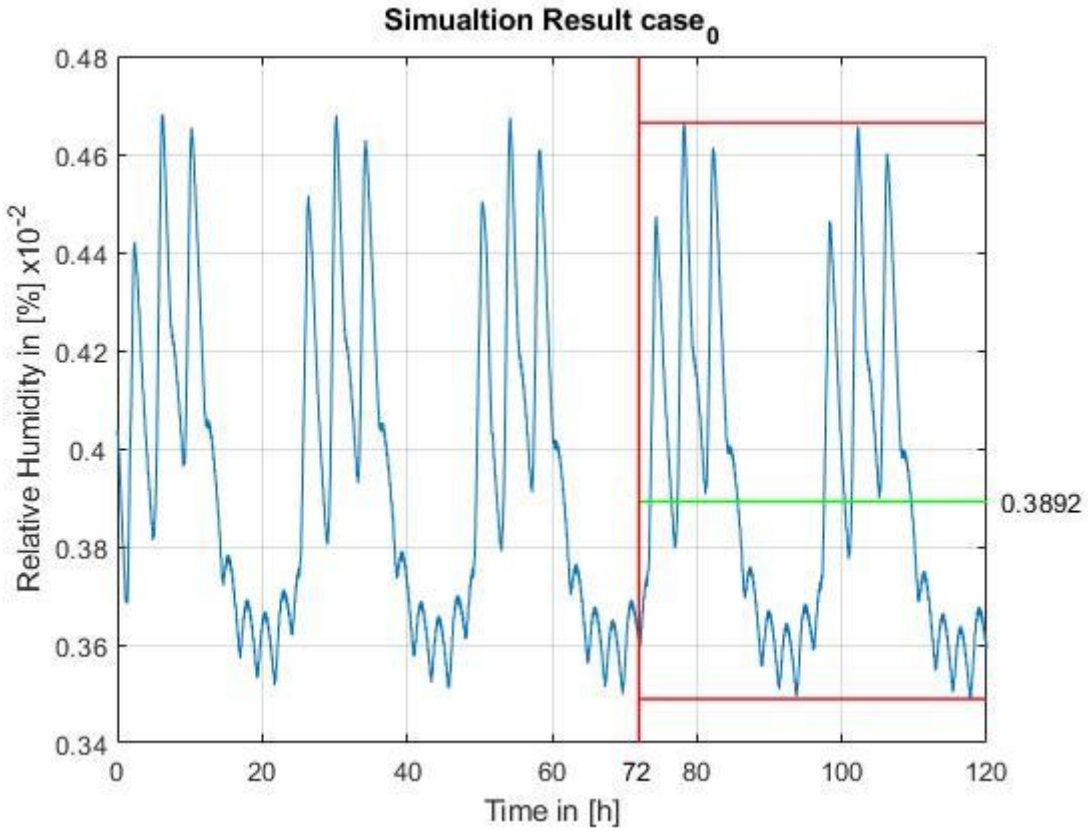

Fig. 5-1: Simulation result and mean value of the relative humidity in Node 1 for case$_0$.

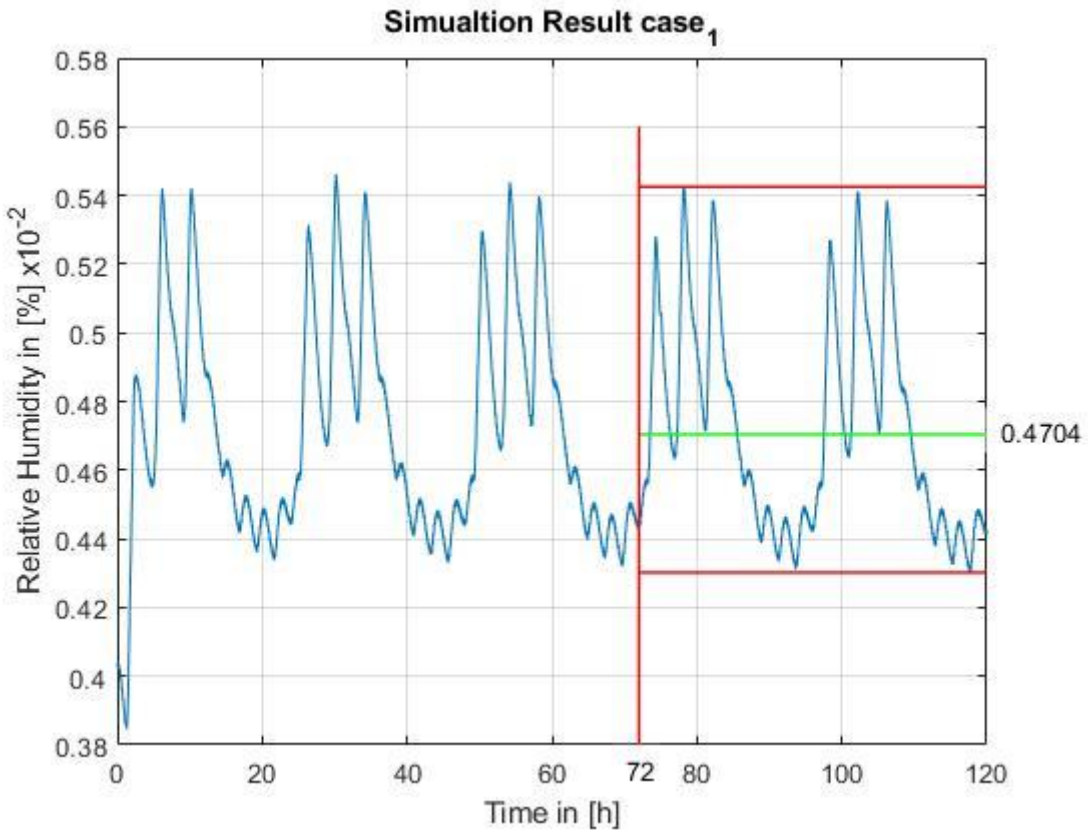

Fig. 5-2: Simulation result and mean value of the relative humidity in Node 1 for case$_1$.

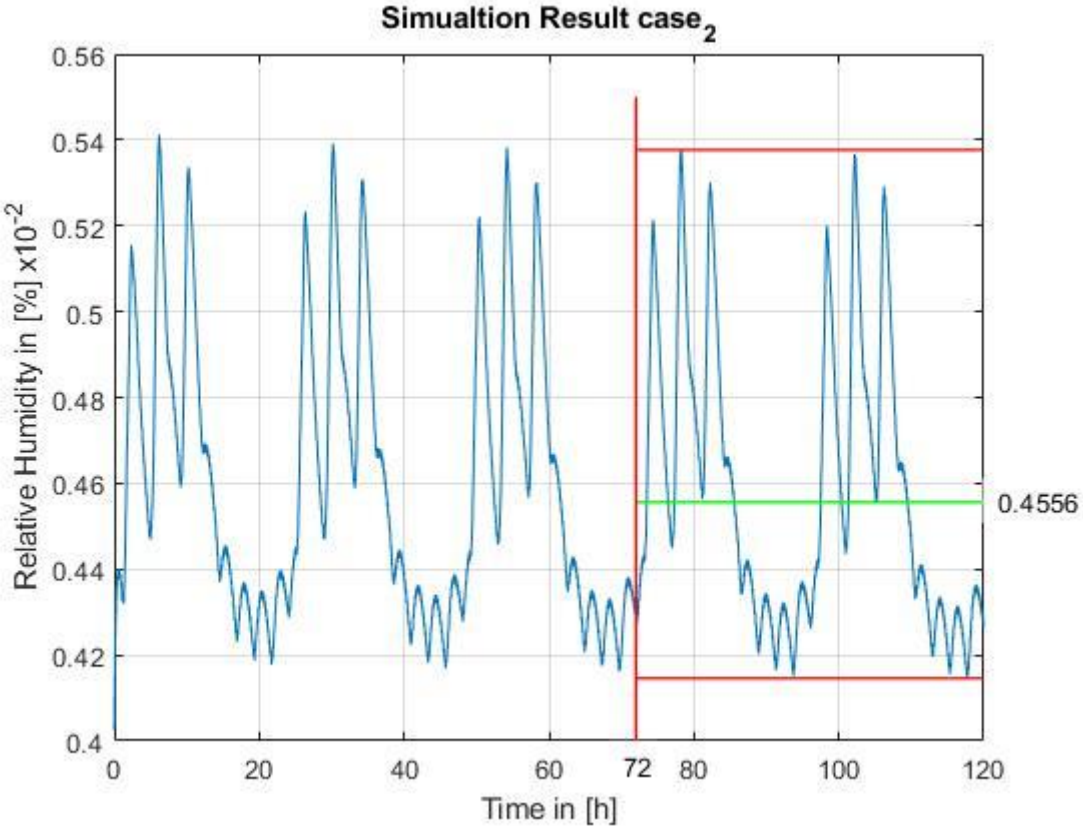

Fig. 5-3: Simulation result and mean value of the relative humidity in Node 1 for case$_2$.

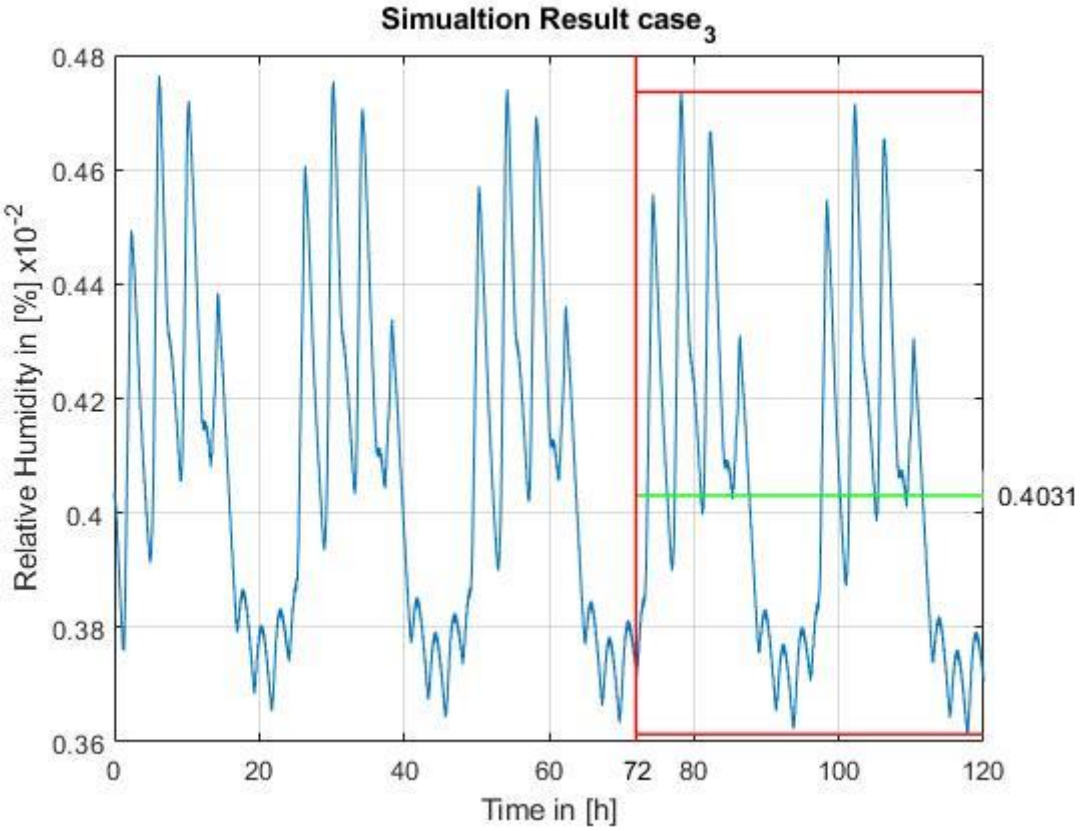

Fig. 5-4: Simulation result and mean value of the relative humidity in Node 1 for case$_3$.

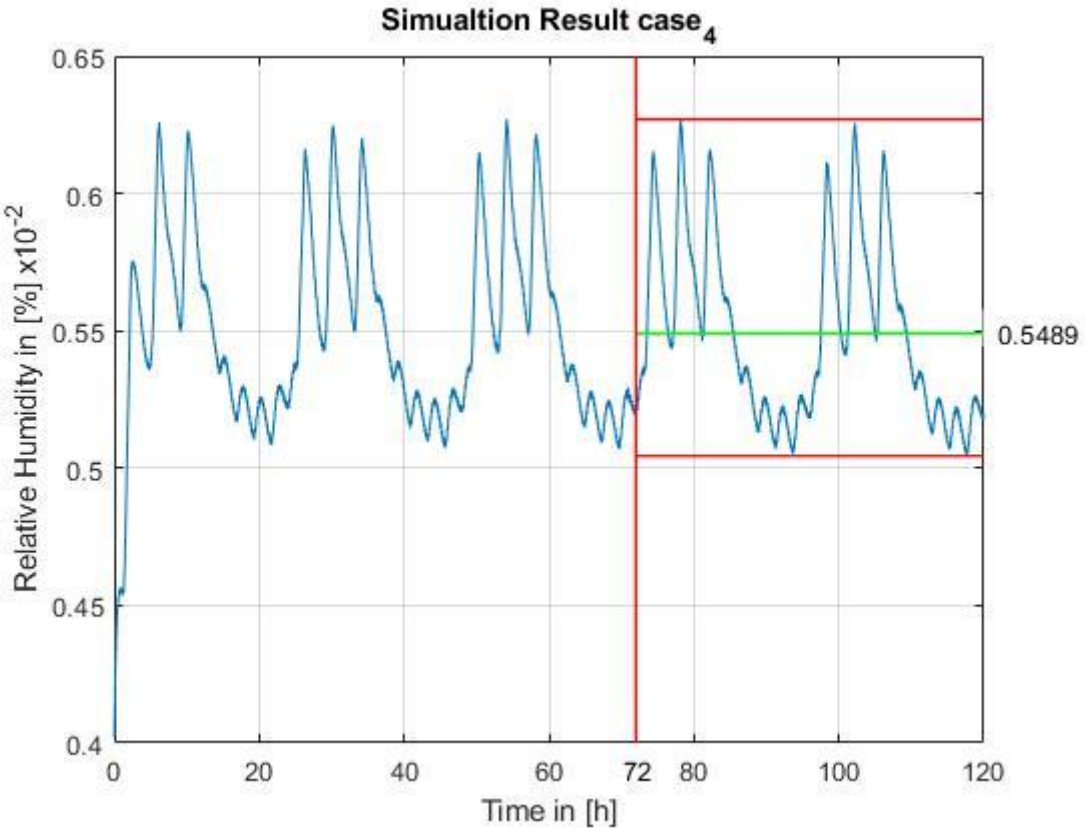

Fig. 5-5: Simulation result and mean value of the relative humidity in Node 1 for case4.

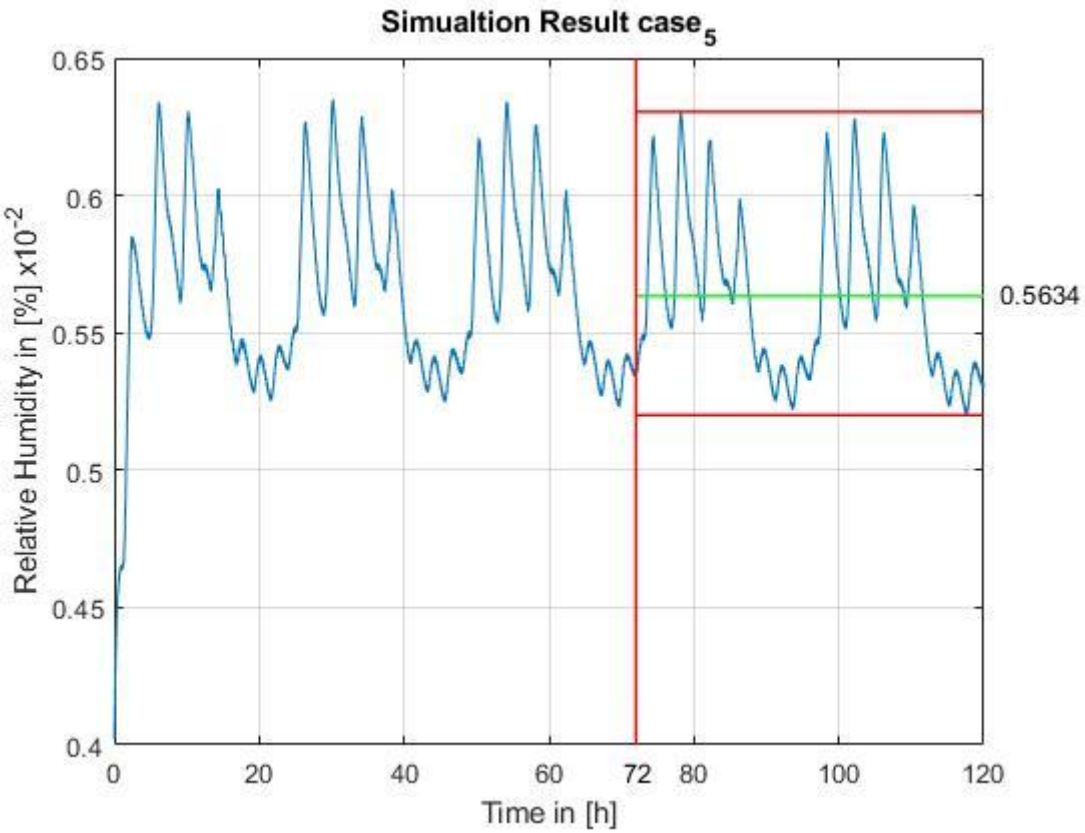

Fig. 5-6: Simulation result and mean value of the relative humidity in Node 1 for case5.

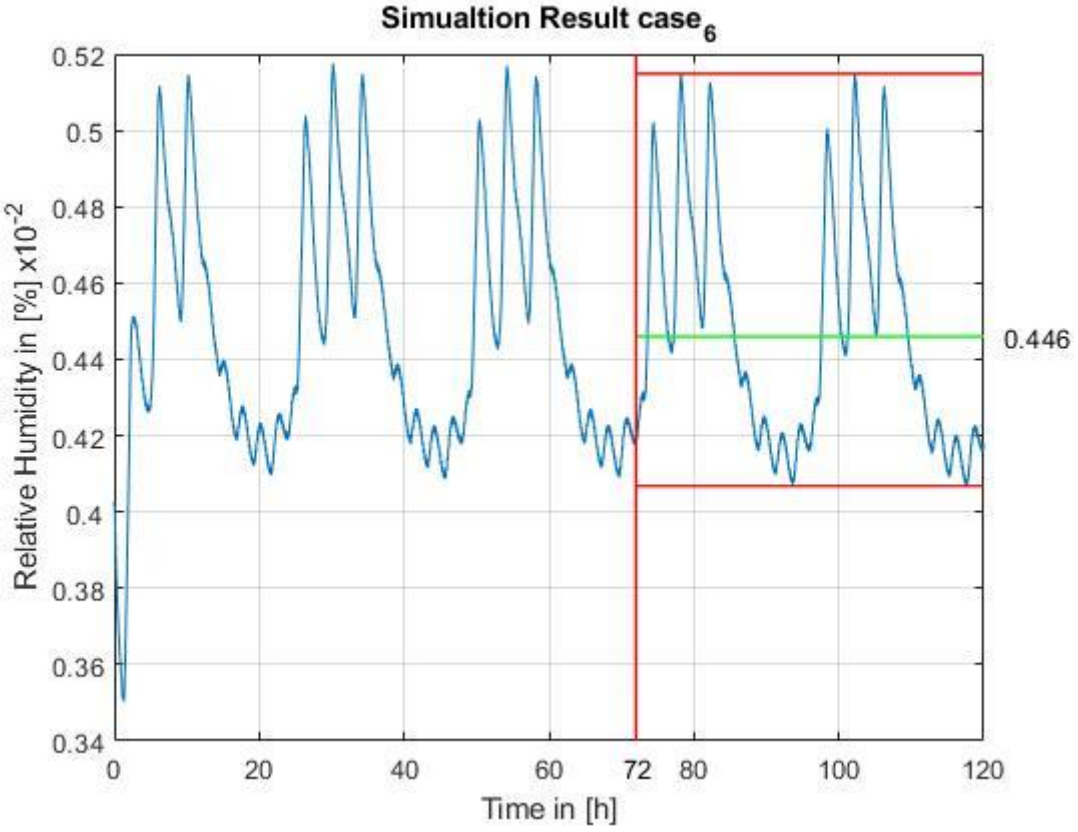

Fig. 5-7: Simulation result and mean value of the relative humidity in Node 1 for case6.

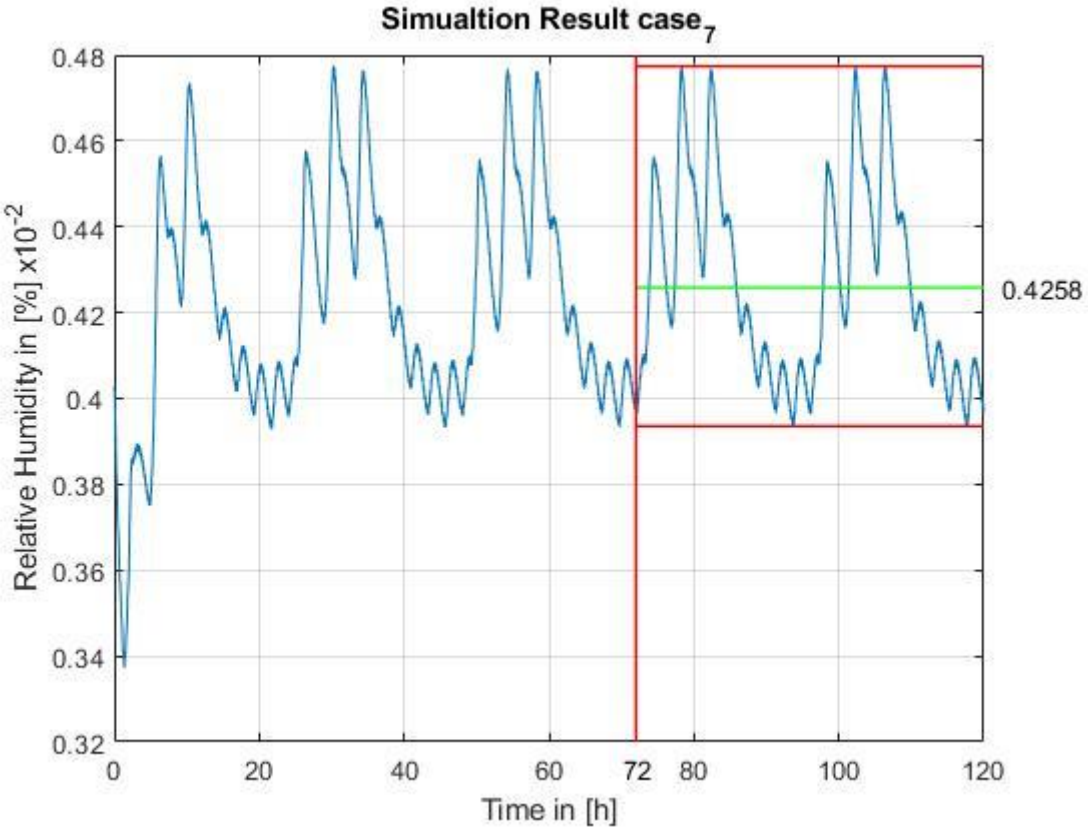

Fig. 5-8: Simulation result and mean value of the relative humidity in Node 1 for case7.

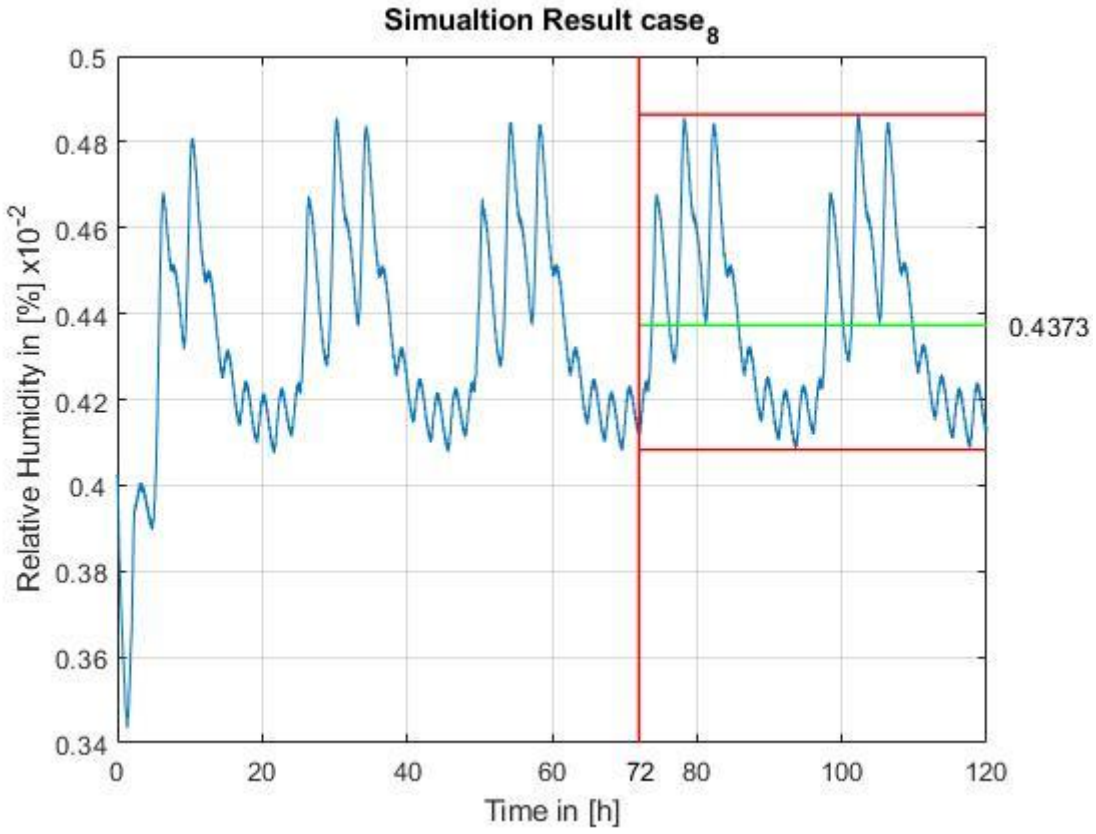

Fig. 5-9: Simulation result and mean value of the relative humidity in Node 1 for case8.

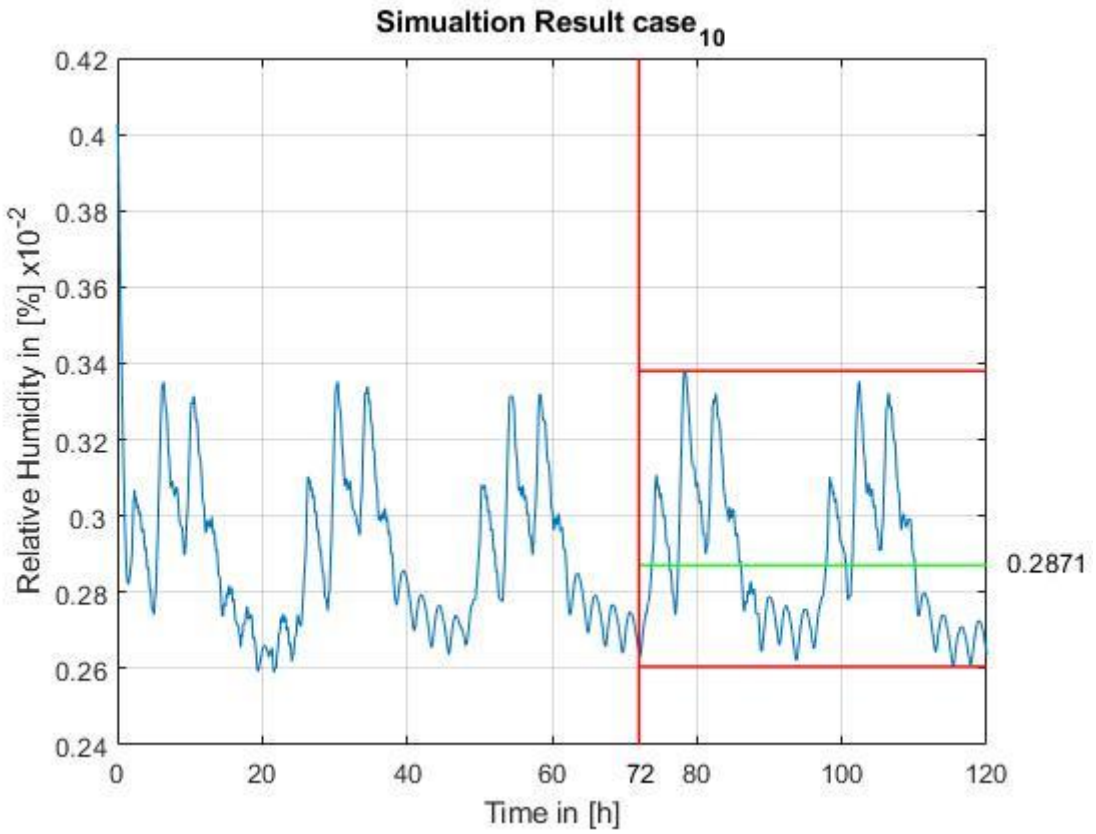

Fig. 5-10: Simulation result and mean value of the relative humidity in Node 1 for case10.

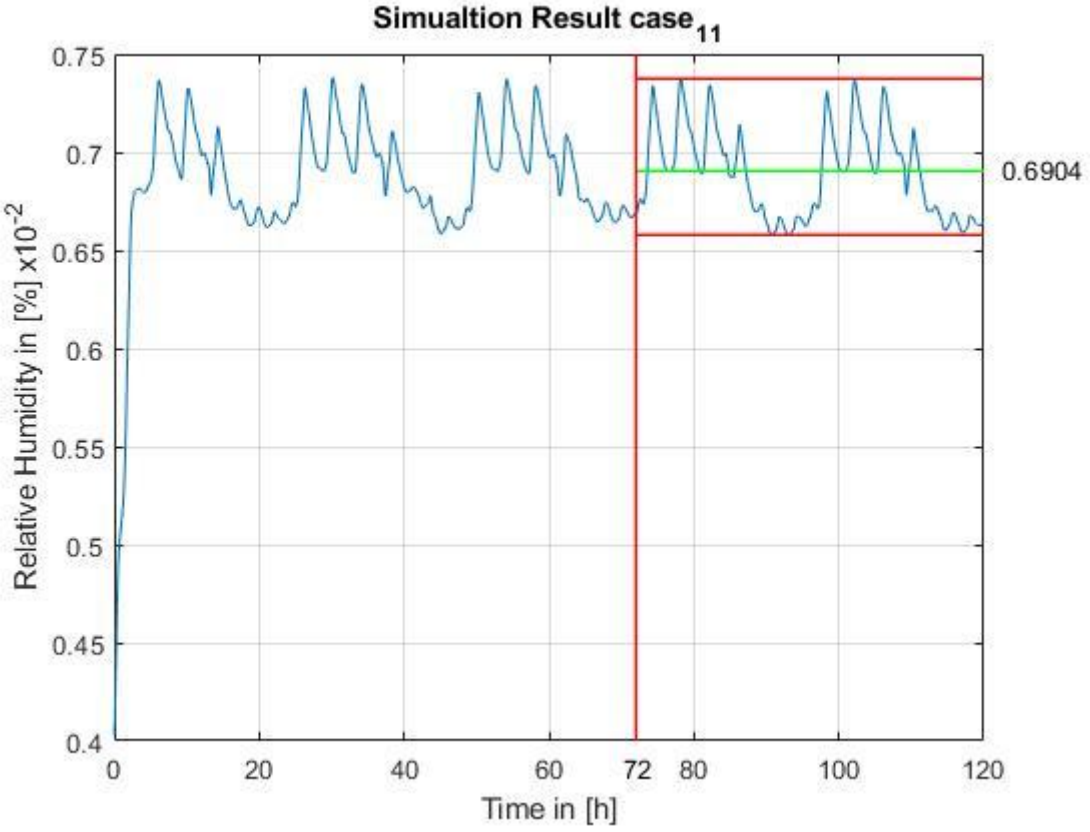

Fig. 5-11: Simulation result and mean value of the relative humidity in Node 1 for case$_{11}$.

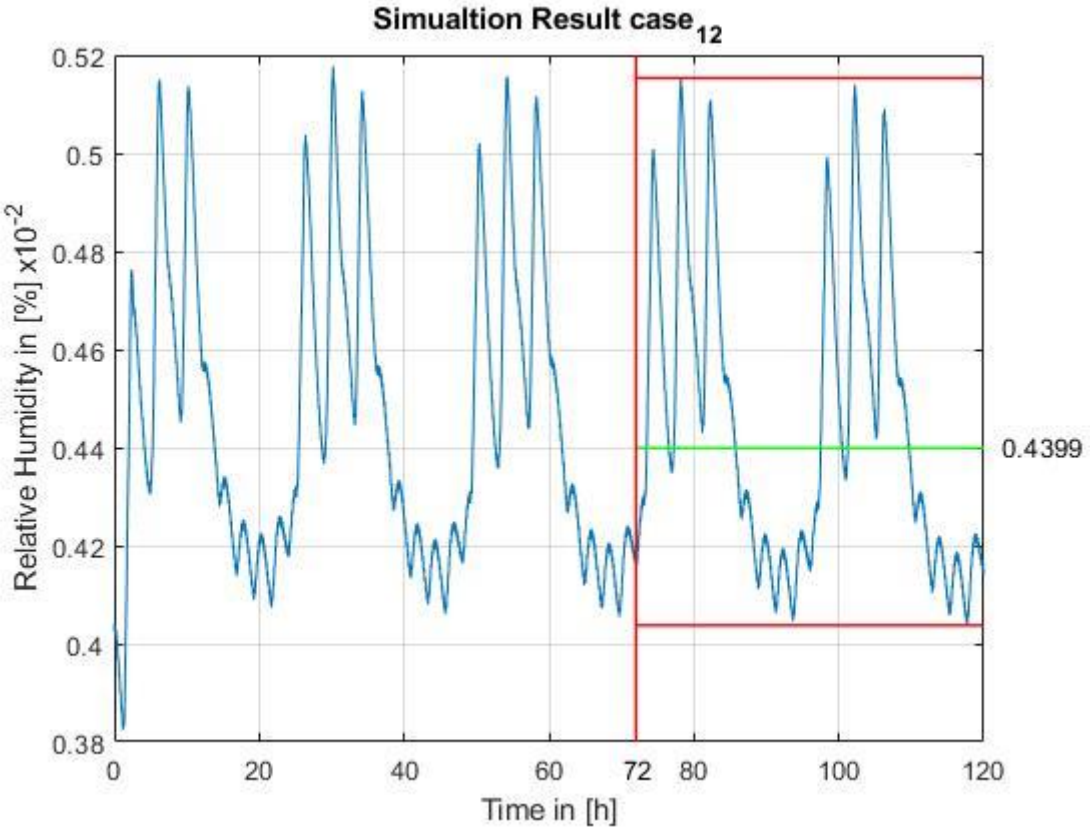

Fig. 5-12: Simulation result and mean value of the relative humidity in Node 1 for case$_{12}$.

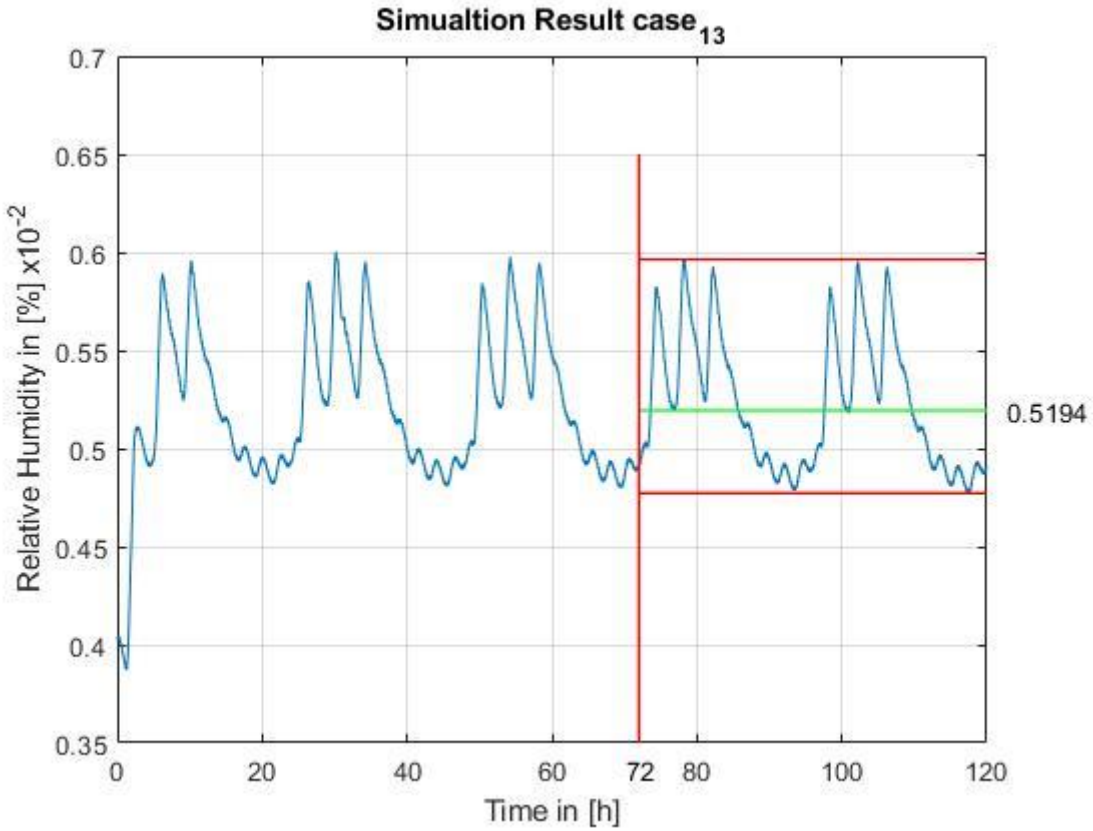

Fig. 5-13: Simulation result and mean value of the relative humidity in Node 1 for case$_{13}$.

All test cases simulated well, beside of case$_9$, which stopped with an error in the SCRA subsystem. This error was already mentioned in 3.2.3 and could not be fixed until the end of the thesis. So, this case cannot be evaluated. The mean values of the relative humidity and the resulting deviations from the reference case$_0$ are collected in Tab. 5-2.

Tab. 5-2: Overall Simulation results for the test cases.

	Case$_0$	Case$_1$	Case$_2$	Case$_3$	Case$_4$	Case$_5$	Case$_6$
Rel. Humidity [%]	38.92	47.04	45.56	40.31	54.89	56.34	44.6
Deviation from case$_0$ [%]	0	20.86	17.06	3.57	41.03	44.76	14.59

	Case$_7$	Case$_8$	Case$_9$	Case$_{10}$	Case$_{11}$	Case$_{12}$	Case$_{13}$
Rel. Humidity [%]	42.58	43.73	N.A.	28.71	69.04	43.99	51.94
Deviation from case$_0$ [%]	9.40	12.36	N.A.	-26.23	77.38	13.03	33.45

5.3 Comparison of simulation and calculation results

For all test cases the deviation values were simulated and calculated with the standard and the advanced approach using the functions developed in chapter 4.2.4 and 4.2.5. All results are collected in Tab. 5-3 and can now be compared to each other.

Tab. 5-3: Comparison of the simulation and the calculation results.

	Simulation [%]	**Calculation with standard approach [%]**	**Calculation with advanced approach [%]**
$Case_1$	20.86	14.28	21.13
$Case_2$	17.06	17.06	16.91
$Case_3$	3.57	1.74	3.62
$Case_4$	41.03	31.35	38.04
$Case_5$	44.76	33.09	41.65
$Case_6$	14.59	8.39	15.89
$Case_7$	9.40	3.16	10.76
$Case_8$	12.36	4.65	12.25
$Case_9$	N.A.	12.61	20.21
$Case_{10}$	-26.23	-22.72	-28.85
$Case_{11}$	77.38	63.29	70.94
$Case_{12}$	13.03	9.32	13.19
$Case_{13}$	33.45	27.94	33.96

In the following all test cases are evaluated and the accuracy of the calculation approaches is estimated and compared to each other.

$Case_1$ to $case_3$. In $case_1$ the advanced approach shows a very good calculating result with only +1.2 percent deviation from the simulation result, while the standard approach divers about -31.5 percent from the simulation result. Interestingly at the second case the calculation result of the standard method fits perfectly to the simulation. But also, the advanced approach result is very good with only -0.9 percent deviation to the simulation. In $case_3$ the result with the advanced approach is again much more accurate than the standard method. While the results of the simulation and the result of the advanced calculation only differs about -1.4 percent, the result of the standard calculation is over 50% lower than the simulation result. This difference can be explained with Fig. 5-14 and Fig. 5-15.

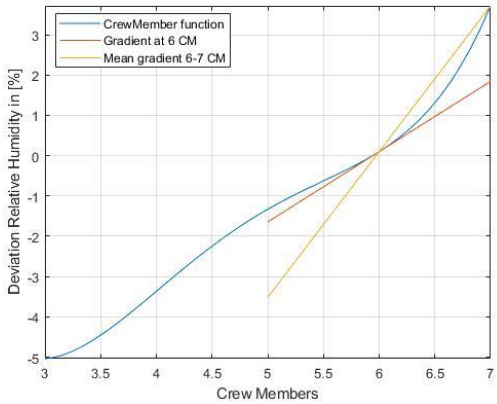

Fig. 5-14: Mean and specific gradient of the CrewMember function.

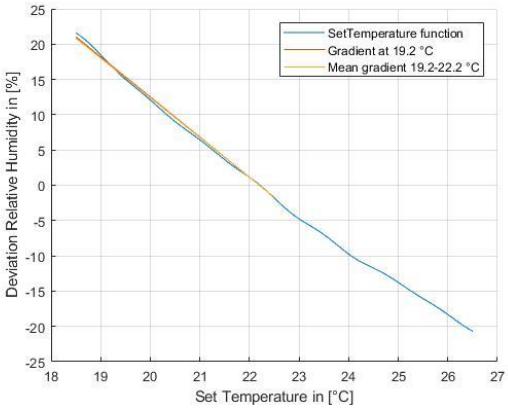

Fig. 5-15: Mean and specific gradient of the SetTemperature function.

The specific gradient at 6 crew members for the CrewMember function, which is calculated by the standard calculation when doing the partial derivation, is way too small, because the function is not linear and the gradient increases immediately after the data point for six crew members. In comparison the mean gradient takes also the gradient at 7 crew members into account and so, it is much steeper and the calculated value fits much better to the simulation result. In Fig. 5-15 the same circumstance is visualized, but with the SetTemperature function. There the results are much better, because the gradient at 19.2 °C fits nearly perfect for the calculated range. But this is just luck. Of course, the probability is higher when the function is rather linear without heavy oscillations to hit a good fitting gradient, but it is not reliable. This explains also the very good result with the standard approach in $case_2$.

$Case_4$ and $case_5$. In $case_4$ the variations of $case_1$ and $case_2$ are combined. The results show that the deviation at the calculated result with the advanced approach is about 7.3 percent lower than the simulation result. The result of the standard approach is about 23.6 percent lower compared to the simulation, which is no surprise, because the error in $case_1$ was already such big and is just inherited to this case. In $case_5$ all variations from $case_1$ to $case_3$ are combined and the percentage deviation of the advanced approach drops slightly to -6.95 percent compared to $case_4$. But it must be noted that the gap of the absolute values for the deviation of the relative humidity between the simulation and the advanced approach still increases from $case_4$ to $case_5$. The deviation of the standard approach increases compared to $case_4$ to -26.1 percent, because now the error from $case_3$ inherits to this case, too. The results of the advanced calculation compared to the simulation results implies that the multiple variation of input parameters, which influence the relative humidity in the same direction, leads to a mutual reinforcement during the simulation.

$Case_6$ to $case_9$. In these cases, the processing of the deviation of the calculations compared to the simulation is visible. In the beginning the standard calculation has a big error of -42.5 percent in $case_6$, which climbs to -66.4 percent in $case_7$ and has a small drop to -62.4 percent in $case_8$. But in $case_8$ there is no difference in the calculation of the BPA_Dummy between the two approaches, so there should be no differences in the deviation to the simulation. The Same counts for $case_9$, but for this case no simulation results can be provided. The main error of the standard approach results here in the behavior, mentioned at $case_1$ to $case_3$. The results of the advanced

calculation are much better here. It starts with a deviation of +8.9 percent at case$_6$, increases to +14,5 percent at case$_7$ but drops again to -0.89 percent at case$_8$. Here the variation of the error comes through a compensation of the calculated deviations, which is rather random. Because one parameter causes an increase in the relative humidity and another parameter a drop and both calculations have an error, the overall error in the end gets smaller.

Case$_{10}$ and case$_{11}$. In these both cases the advanced calculation delivers better results, too. But here even the advanced approach shows bigger deviations. Especially in case$_{11}$, the calculation of maximum humidity, the result for the advanced calculation deviates -8.3 percent and the result of the standard calculation deviates even -18.2 percent from the simulation results. An explanation attempt for these errors can be that with so many parameters, having an influence to increase the relative humidity, the CCAA system is absolutely over the capacity limit and the influence of the single parameters will reinforce each other, which is not respected in the calculations. In case$_{10}$, the calculation of the minimum relative humidity, the deviations are +9.9 percent for the advanced approach and -13.38 percent for the standard approach. But in this case the advanced approach has a negative deviation, which means the variations influence the results of the simulation smaller than expected by the calculation. Thus, in the case of a lower relative humidity than the nominal value, the CCAA system seems to be able to regulate the humidity better, because the system just needs to lower the performance of the condensation system and does not come to its capacity limit. Also, the interaction of the varied parameters in the simulation can be an explanation here.

Case$_{12}$ and case$_{13}$. In these two cases the advanced calculation provides good results. The deviation from the simulation result increases slightly, from 1.23 to 1.5 percent, with the big variation in the parameter. But it is not recognizable that the results will get significantly worse when using bigger deviations in the parameters, which is logical, because this approach always respects the whole varied range in the function. The standard approach is much less accurate with an error of 28.5 percent in case$_{12}$ and an error of 16.5 percent in case$_{13}$. But it is interesting to see, that the deviation from the simulation results gets not bigger, but even smaller with the bigger variation in the parameter. This can be explained with a look on the function of the coolant temperature parameter (Fig. 5-16).

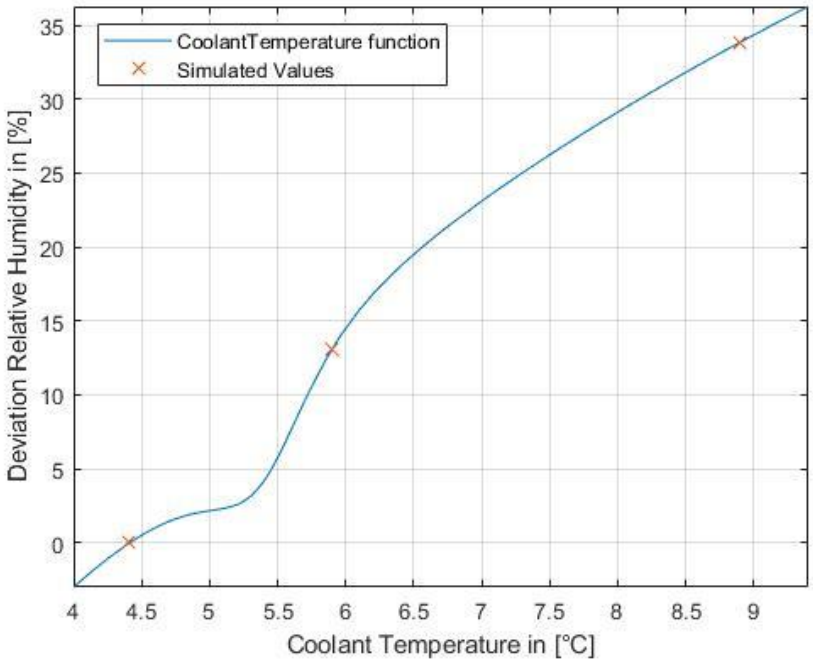

Fig. 5-16: CoolantTemperature function with the points, at which the simulation take place.

Both results of the standard approach were calculated with the gradient at 4.4 °C. Between 4.4 °C and 5.9 °C the function has a big change in the gradient, which is not respected in the calculation. From 5.9 °C to 8.9 °C the function is similar to the part at 4.4 °C. So, the big mistake in the calculation happens at the first part from 4.4 °C to 5.9 °C. After that the gradient of 4.4 °C fits roughly again to the function and the calculated values are similar to the simulation results. Hence the gradient fits again to the curve, the overall error gets smaller because the function is calculating the right deviation for this part of the simulation.

As a short conclusion it is to say, that the advanced approach delivers more accurate and overall more reliable results. The standard approach can produce accurate results in some cases, like in $case_2$, but these are rather random and not reliable.

The deviation in the results of the advanced approach, which grew bigger with more parameters varied, are owed to the influence the parameters have on each other during the simulation, which cannot be respected by the single functions. The functions of the single parameters can also cause an error, because they do not fit to the real curve of the simulation for 100 percent. But in this example the functions are fitted very accurate, so this is only a small influence on the error, as can be seen in $case_1$ to $case_3$ with a deviation of -1.4 % to 1.2 %.

6 Conclusion

6.1 Summary

In this thesis a sensitivity analysis and an error propagation for a simulation of the LSS at the ISS, which is modeled in V-HAB, is performed. Therefore, simulation parameters, which were uncertain, because of human, technologic or external uncertainties, were determined. The simulation code was modified and expanded to allow a variation of the determined parameters without changes in the code and an extended crew planner and dummy subsystems were implemented.

After that, the variation of the parameters was tested for every parameter with example simulations and the reliability of the results was examined with the help of a sensitivity analysis. Within the sensitivity analysis it was determined that the simulation can handle the modifications and performs like before the changes. Thus, the changes in the parameters influence the results in the way it was expected before. Indeed, there were two simulations which did not work an stopped with an error in the SCRA system, which could not be fixed till the end of the thesis. So, for these two cases no results are available to evaluate.

Once it was secured that the simulation works fine in the most cases an error propagation with the aim to develop a function, which can calculate the deviations caused by certain parameter changes was performed. In the course of this, different calculation methods were discussed and the best applicable one was chosen. The selected principle was adapted to the present problem and an additional modification was developed, which promised better results. As an example, an error propagation was accomplished for the relative humidity. Therefore, all input parameters, which can have an impact on the relative humidity were varied over a certain range and simulated, to get a collection of data points. With this data points functions of every input parameter were developed and processed to build the final function for the deviation. This was done for the selected calculation principle and for the additional modification of it, to make a comparison possible. As a verification some test cases were specified and as well simulated as calculated with both calculation principles, to evaluate the accuracy and reliability of the developed functions. A short example was given, how eventually occurring subsystem errors can be evaluated and respected in the error calculation.

The comparison of the resulting values showed that the standard calculation delivers rather bad results. The calculated deviation was in the most cases far away from the deviation obtained from the corresponding simulation. The few good results were rather based on randomness and not reliable. The modified calculation method produced noticeable better results. The calculated deviation compared to the simulated deviation was mostly in a similar range and moreover reliable. With the developed calculation method, it is possible to give an accurate statement, how the simulation results will deviate when varying one input parameter, and an estimation, how the simulation results will deviate when varying several simulation parameters. With this a possible deviation range of the simulation can be determined, which is from -28.85 % (Minimal relative humidity case) to +70.94 % (Maximum relative humidity case) for the calculation and from -26.23 % to +77.38 % for the simulation, which are the more accurate values. But an exact statement for the error of the simulation, compared to

the reality is hard to give, because the subsystem errors of the simulation and the working parameter of the real systems are not known. Hence it only can be said that the simulation results can deviate from the reality in the given range (-26.23 % to 77.38 %), on which the not known subsystem errors need to be added.

6.2 Discussion

In the following section an evaluation of the reached results in comparison with the given tasks is done and the results of the different parts of the thesis are rated.

Simulation modification. The input routine of the simulation was reworked, to change all necessary simulation parameters with the execution command of the simulation. Thereby a reliability and a secure repeatability is provided. Moreover, an easy extension of the input routine is ensured to add more input parameters when needed. All changes and expansion of the code, which allow the simulation of the determined variation cases were successfully implemented.

Sensitivity Analysis. Within the sensitivity analysis all added input parameters were tested for function. Besides two exceptions, which throw an error in the SCRA, all simulations worked fine. So, the simulation code is capable of working with varied parameters. The examination of the sensitivity analysis itself, showed overall comprehensible results, which fitted to the expected tendencies.

Error Propagation. For the error propagation two approaches were developed and an instruction how to perform them is given. The so named standard and the advanced approach. They were derived from the error calculation normally used for measurements or similar. In the end they both provide a function to calculate the difference in a certain value between two cases.

Verification. With the standard approach most calculating results were not comprehensible and far away from the simulation results. The good results were due to chance and not reliable, but which counts for all results of the standard approach. Although the advanced approach delivers better results than the standard approach, there is still a part of randomness and uncertainness, especially when calculating deviations, where several input parameters are changed at one time. When only one varied parameter is analyzed the results are very accurate and can be used to calculate very exact deviations, which make extra simulations for these cases redundant. When varying more than one parameter a good trend of the deviations is still identifiable, but to get exact and accurate results simulations are necessary. But with this kind of error calculating no better results are expectable, because the influence of the changed input parameters on each other during the simulation is neglected. To find reliable connections between these parameters was not possible within this thesis, because it will need a multitude of simulations, which already took place and analogical more time. Before this is done, it should be evaluated if this makes sense and is worth the time.

General error of the simulation compared to the reality. The example for the relative humidity showed that the simulation can deviate from -26.23($case_{10}$) to 77.38($case_{11}$) percent for this value compared to the reference case. The overall deviation when comparing these extreme cases could be 140 %. But this is only the deviation for the simulation cases themselves and not for the deviation to the reality, because for this case, errors of the subsystem models must be respected, too. Then

the possible error is given through the wrong working parameters, which were determined with -26.23 % to +77.38 %, and additionally the subsystem errors, which are systematic errors and can deviate the given error range in one direction. For the case that all subsystems of the simulation model conform perfect to the reality the subsystem errors fall away and the error of the simulation compared to the reality can be in the range given above. But this case is very improbably, how it is shown in chapter 4.3. To determine the exact range the simulation can deviate from the variation of the working parameters only, the error of all subsystems must be known. To get these errors, a first approach can be the comparison with test data, where the working parameters are better known, how it is done in chapter 4.3, to evaluate the quality of the subsystem model and to estimate the error of this model compared to reality. But unfortunately, such test data is only rarely available. In the end, the error of the simulation compared to the real system will be a mixture of deviating simulation parameters and a system model, which fits not perfect to reality. With the results from this thesis it only can be said that the relative humidity can deviate in a range from -26.23 % to +77.38 % from the reference case, which is also the range the results can deviate from the reality through the variation of the input parameters, but additionally this range can be shifted through errors of the subsystem models in the simulation, which are not known. Thus, the estimation of a concrete error value for the simulation compared with the reality would need the knowledge of the error of the subsystems and of the exact working parameters, which are both not known, so only a range, in which the deviation can be, is estimated.

6.3 Outlook and future work

With the approach presented in this thesis, it is possible to calculate very accurate deviations of the simulation, when varying one input parameter. Furthermore, when several input parameters are changed at one time a trend and the magnitude the results will deviate can be estimated. If an accurate deviation result is necessary, a simulation of the particular case needs still to be done. To get this ability for more values than the relative humidity the presented error propagation needs to be done for other values like the CO_2 or O_2 partial pressure.

In the future it should be evaluated, if it is rational to develop a more complex error propagation function, which respects the influence of the input parameters on each other, when more than one parameter is varied. This will need a lot of additional simulations and accordingly a lot of extra time. Before such a project is started, it must be clarified if it is necessary.

Every time a change in the simulation routine takes place, like the implementation of a new subsystem or the development of a better version of an existing one, the whole error propagation needs to be redone. Because the simulation results will change and so the fitted functions used for the deviation function will change, too. This will take place in the near future, when the Complex CDRA or the new CHX model, which are developed right now, are introduced.

Moreover, when the Complex CDRA is finished it should be tried to examine the general subsystem error, like it is showed for the Simple CDRA in this thesis, to be able to classify the occurring deviations better and estimate the influence of the simulation parameters more accurate. Furthermore, with knowledge of the subsystem error, it is also better possible to estimate the error of the simulation compared to the

reality. This should be done for all subsystems, when appropriate real test data is available.

A References

[1] C. Olthoff und J. Schnaitmann, „Website des LRT," [Online]. Available: https://www.lrt.mw.tum.de/index.php?id=110&L=0. [Zugriff am 30 08 2018].

[2] D. Pütz, Assessment of the Impacts of ACLS on the ISS Life Support System using Dynamic Simulations in V-HAB, München: TU München, 2015.

[3] M. S. Anderson, M. K. Ewert, J. F. Keener und S. A. Wagner, Life Support Baseline Values and Assumptions Document, Houston: National Aeronautics and Space Administration, 2015.

[4] D. E. Link Jr. und S. F. Balistreri Jr., Inter-Module Ventilation Changes to the International Space Station Vehicle to support integration of the International Docking Adapter and Commercial Crew Vehicles, Bellevue: ICES, 2015.

[5] A. Schweizer, „Formelsammlung und Berechnungsprogramme Anlagenbau," 08 September 2018. [Online]. Available: https://www.schweizer-fn.de/lueftung/feuchte/feuchte.php. [Zugriff am 08 09 2018].

[6] U. D. Essen, „Bauphysik-Interaktiv," 15 Januar 2005. [Online]. Available: https://www.uni-due.de/ibpm/Bauphysik-Interaktiv/luftfeuchte_1.htm. [Zugriff am 09 09 2018].

[7] Boing, Active Thermal Control System (ATCS) Overview, St. Louis: Boing.

[8] L. K. Kelsey, P. Pasadilla und T. Cognata, „Closing the Water Loop for Exploration: 2018 Status of the Brine Processor Assembly," in *ICES*, Albuquerque, 2018.

[9] K. Bockstahler, C. Matthias und J. Lucas, „Development Status of the Advanced Closed Loop System ACLS," in *ICES*, Bellevue, 2015.

[10] R. F. Coker, J. C. Knox, R. Cummings, T. Brooks und R. G. Schunk, Additional Developments in Atmosphere Revitalization Modeling and Simulation, Huntsville: NASA Marshall Space Flight Center, 2013.

[11] Y. Wang und M. D. LeVan, Adsorption Equilibrium of Carbon Dioxide and Water Vapor on Zeolites 5A and13X and Silica Gel: Pure Components, Nashville: Vanderbilt University, 2009.

[12] U. Walter, Datenanalyse und Fehlerfortpflanzung, München: TU München, 2018.

[13] M. Steger, „Fehlerrechnung zur Messdatenanalyse," Technische Universität München, 14 Februar 2018. [Online]. Available: http://zfp.cbm.bgu.tum.de/mediawiki/index.php/Fehlerrechnung_zur_Messdatenanalyse#Fehlerfortpflanzung. [Zugriff am 10 09 2018].

[14] T. M. Inc., „Mathwork Documentation - Evaluating Goodness of Fit," Mathworks, 10 September 2018. [Online]. Available:

https://de.mathworks.com/help/curvefit/evaluating-goodness-of-fit.html. [Zugriff am 10 09 2018].

[15] J. C. Knox, International Space Station Carbon Dioxide Removal Assembly Testing, NASA Marshall Space Flight Center, 2000.

B Appendices

B.1 Results for the partial pressure of O_2

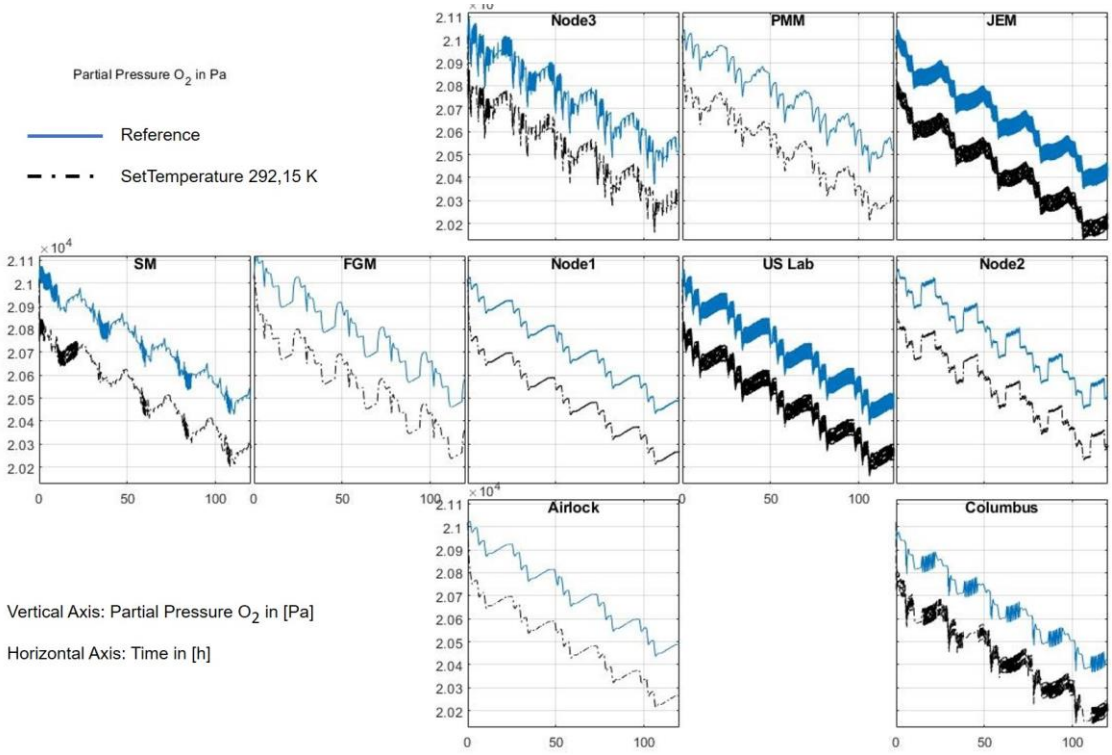

Fig. 6-1: Partial pressure of O_2 simulated with lower air temperature compared to the reference.

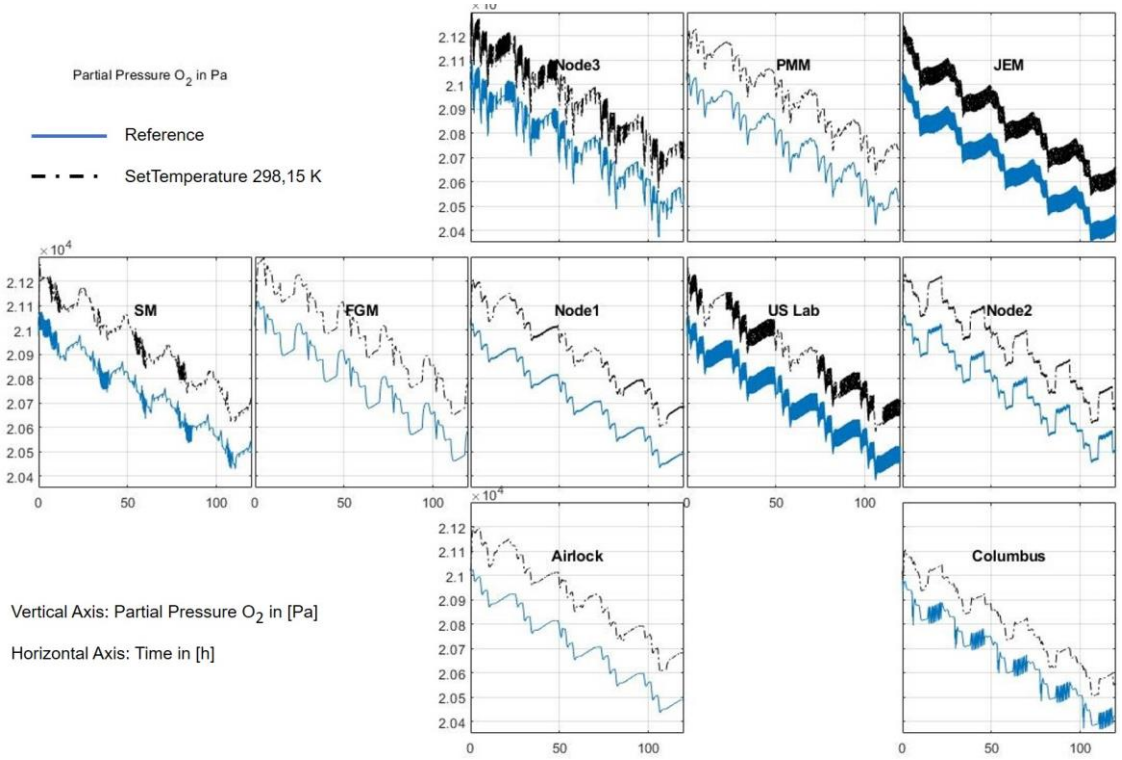

Fig. 6-2: Partial pressure of O_2 simulated with higher air temperature compared to the reference.

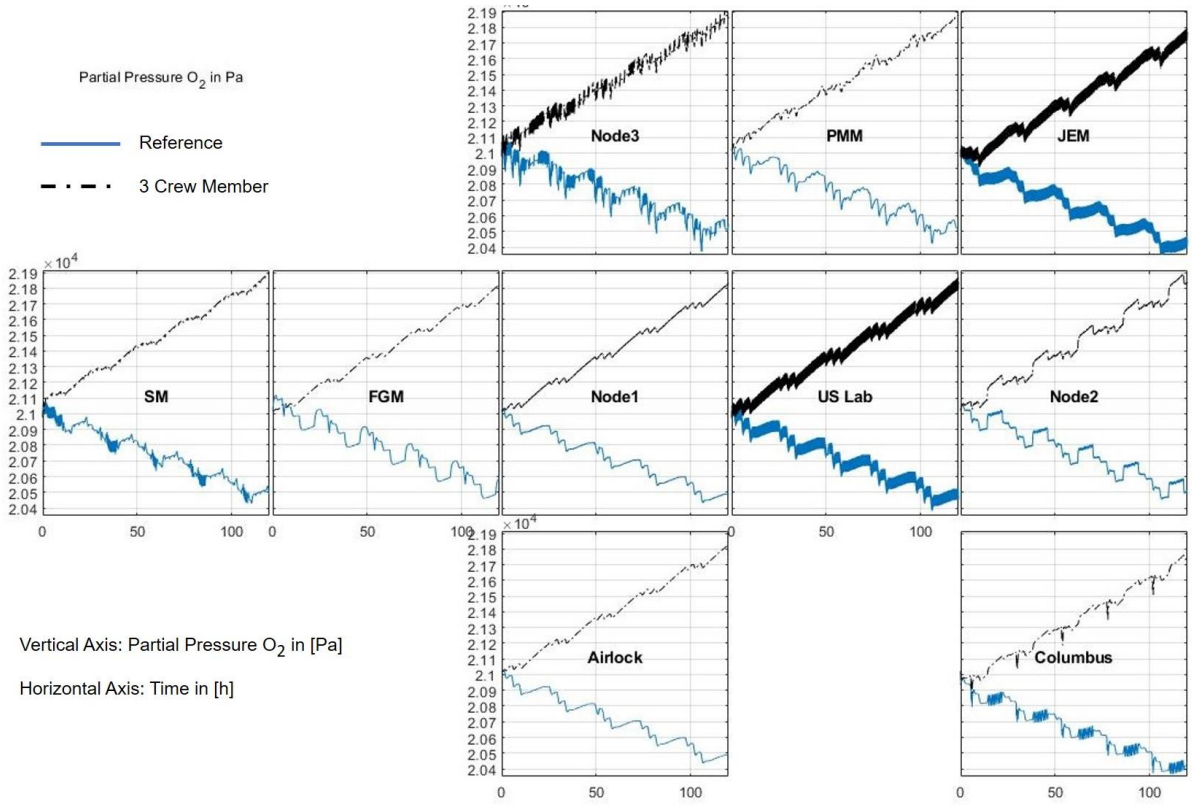

Fig. 6-3: Partial pressure of O_2 simulated 3 crew members compared to the reference.

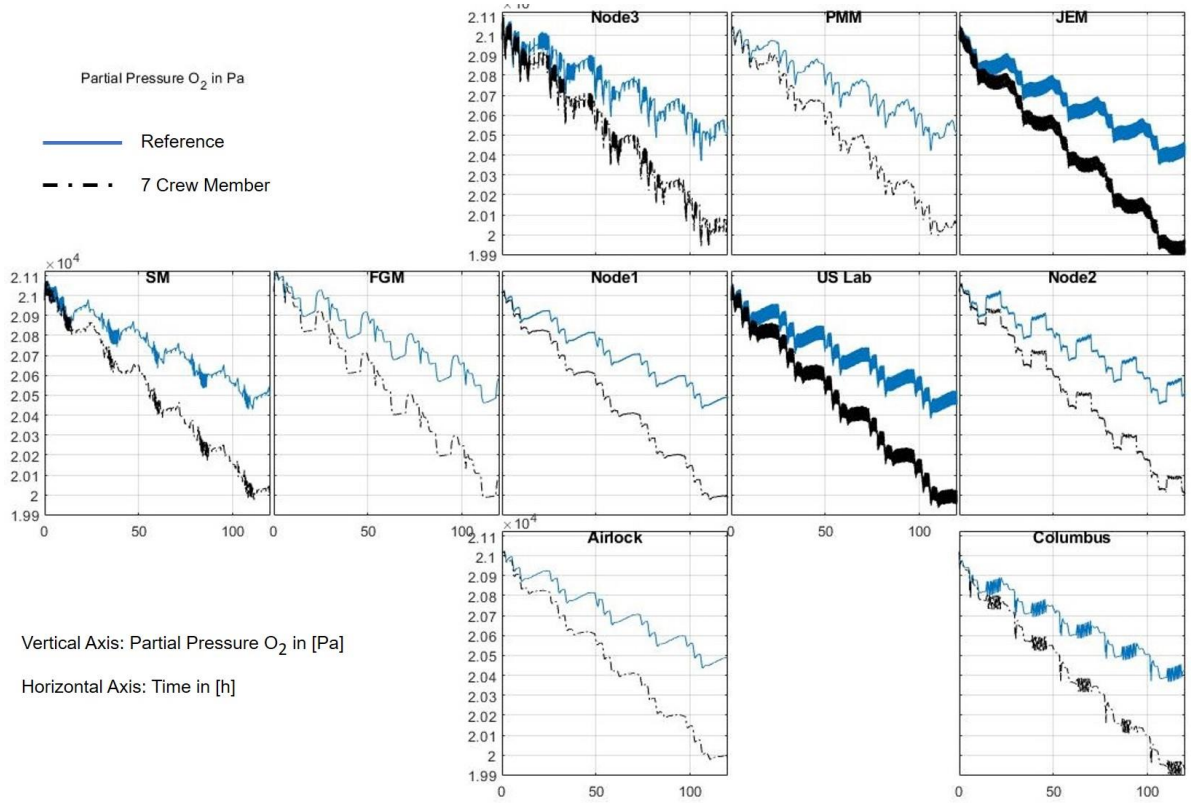

Fig. 6-4: Partial pressure of O_2 simulated with 7 crew members compared to the reference.

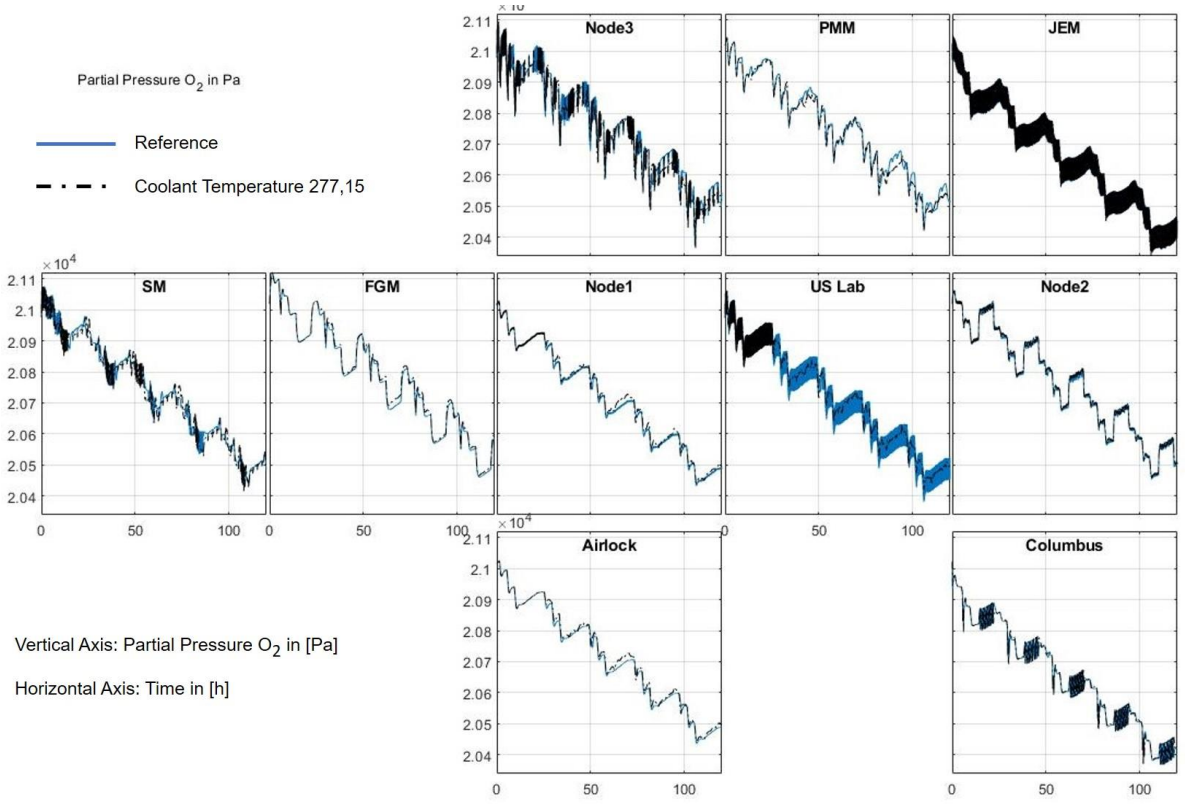

Fig. 6-5: Partial pressure of O_2 simulated with lower coolant temperature compared to the reference.

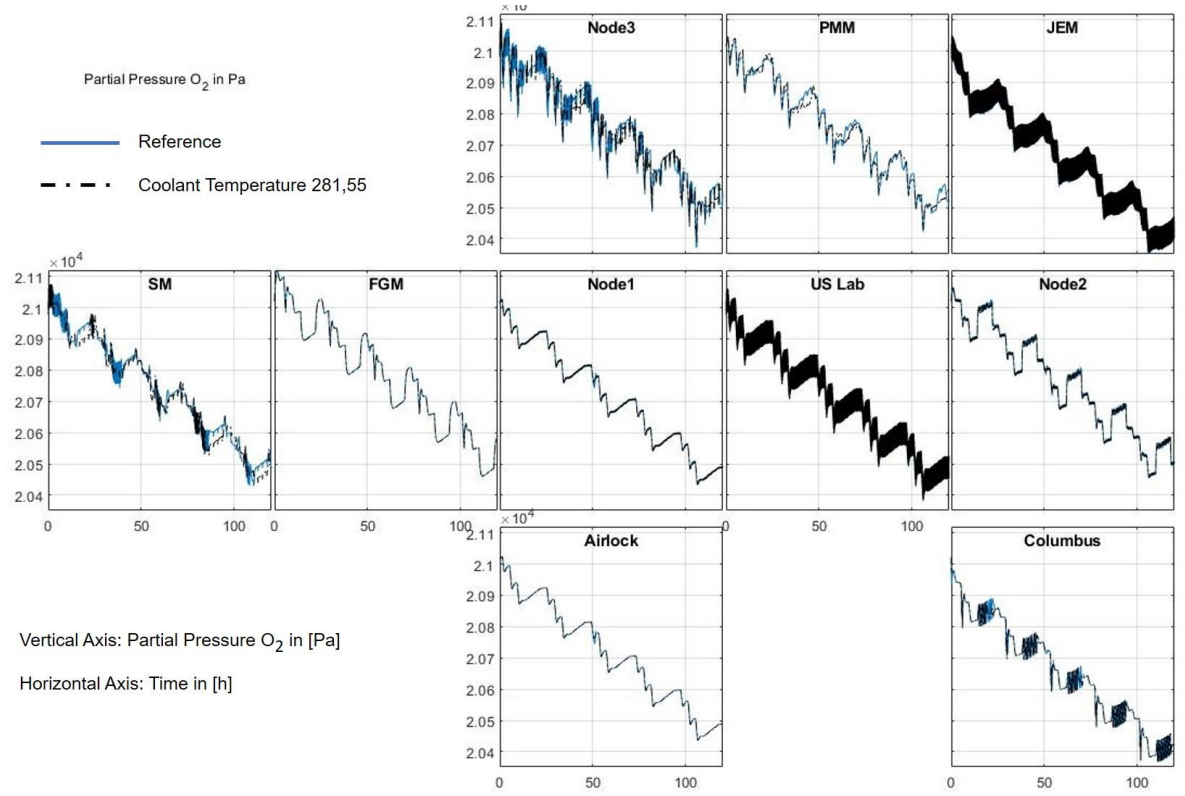

Fig. 6-6: Partial pressure of O_2 simulated with higher coolant temperature compared to the reference.

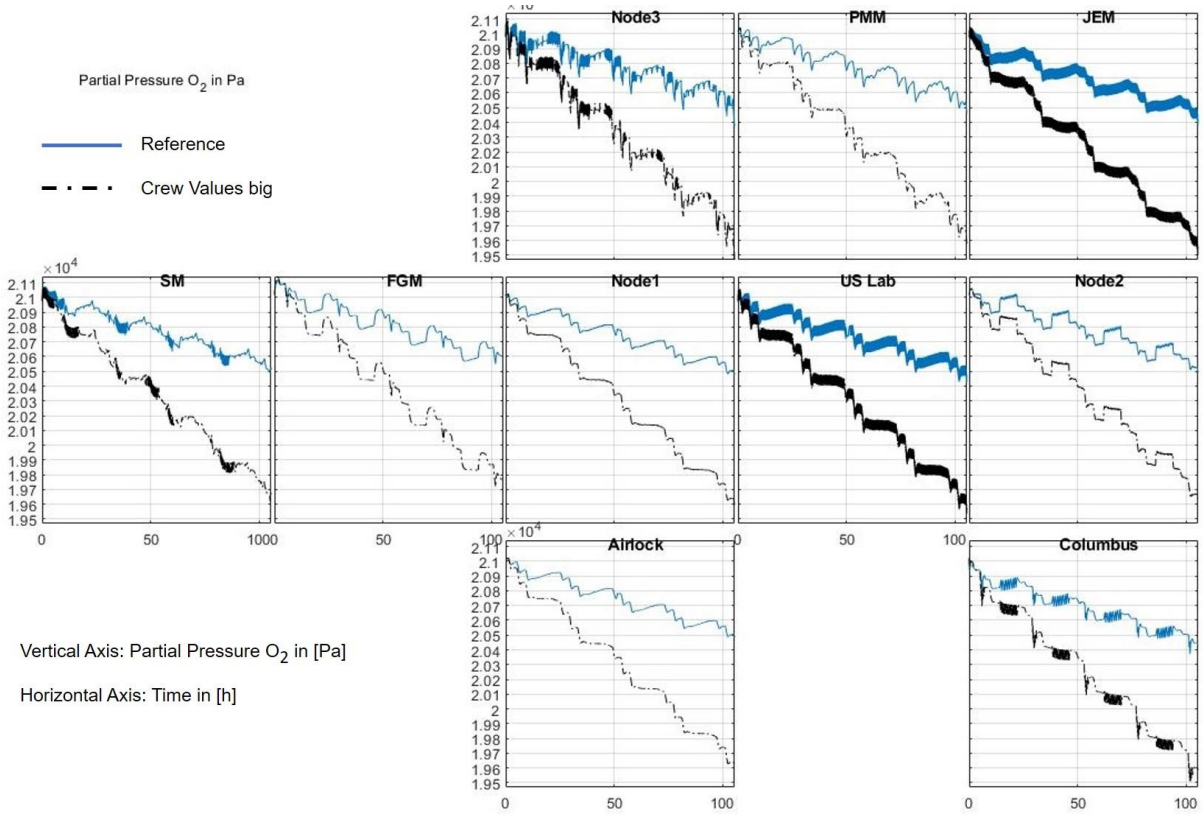

Fig. 6-7: Partial pressure of O_2 simulated with crew values big compared to the reference.

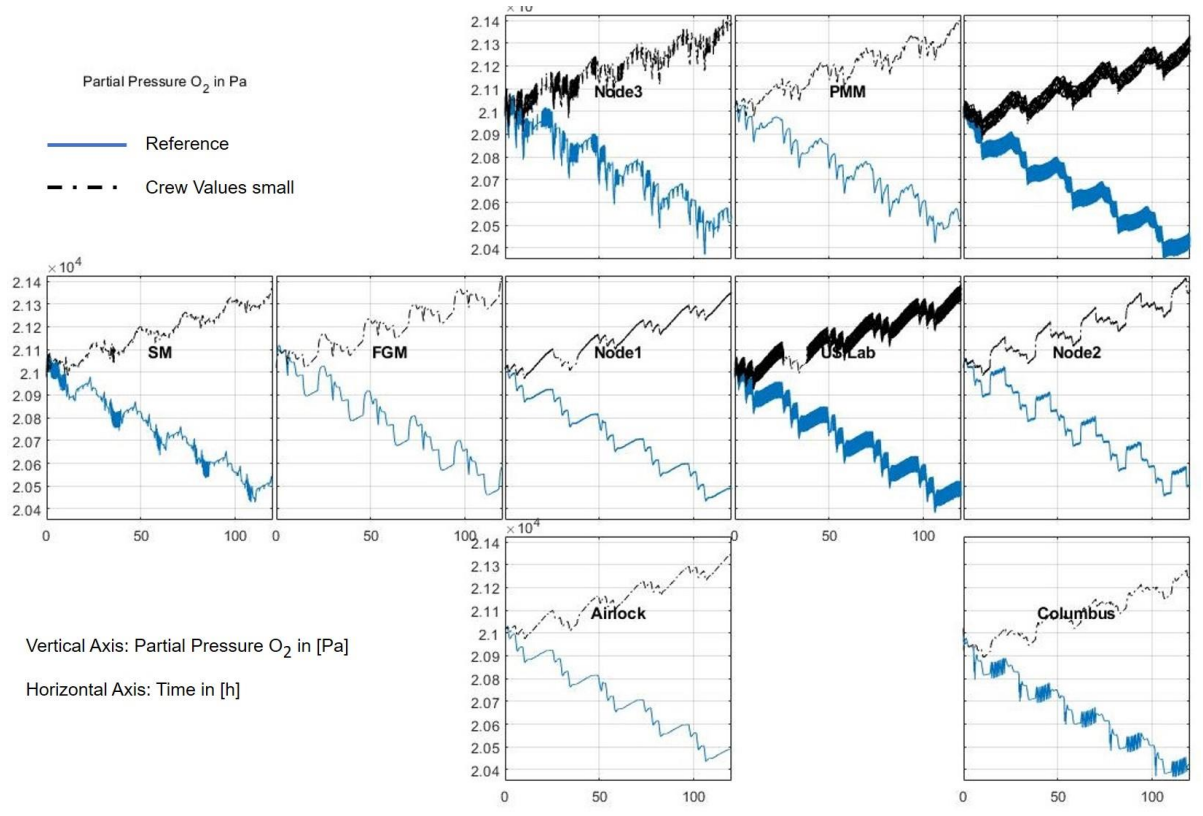

Fig. 6-8: Partial pressure of O_2 simulated with crew values small compared to the reference.

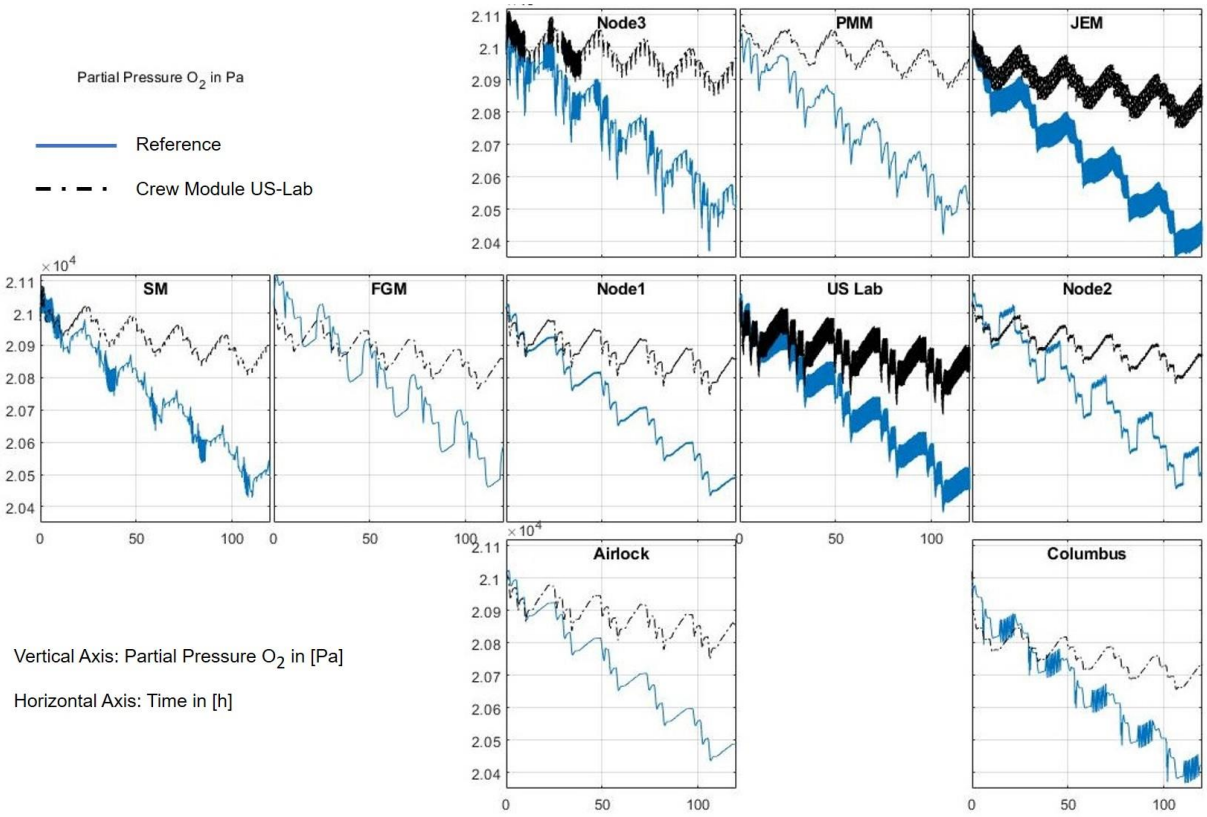

Fig. 6-9: Partial pressure of O_2 simulated with crew in US-Lab compared to the reference.

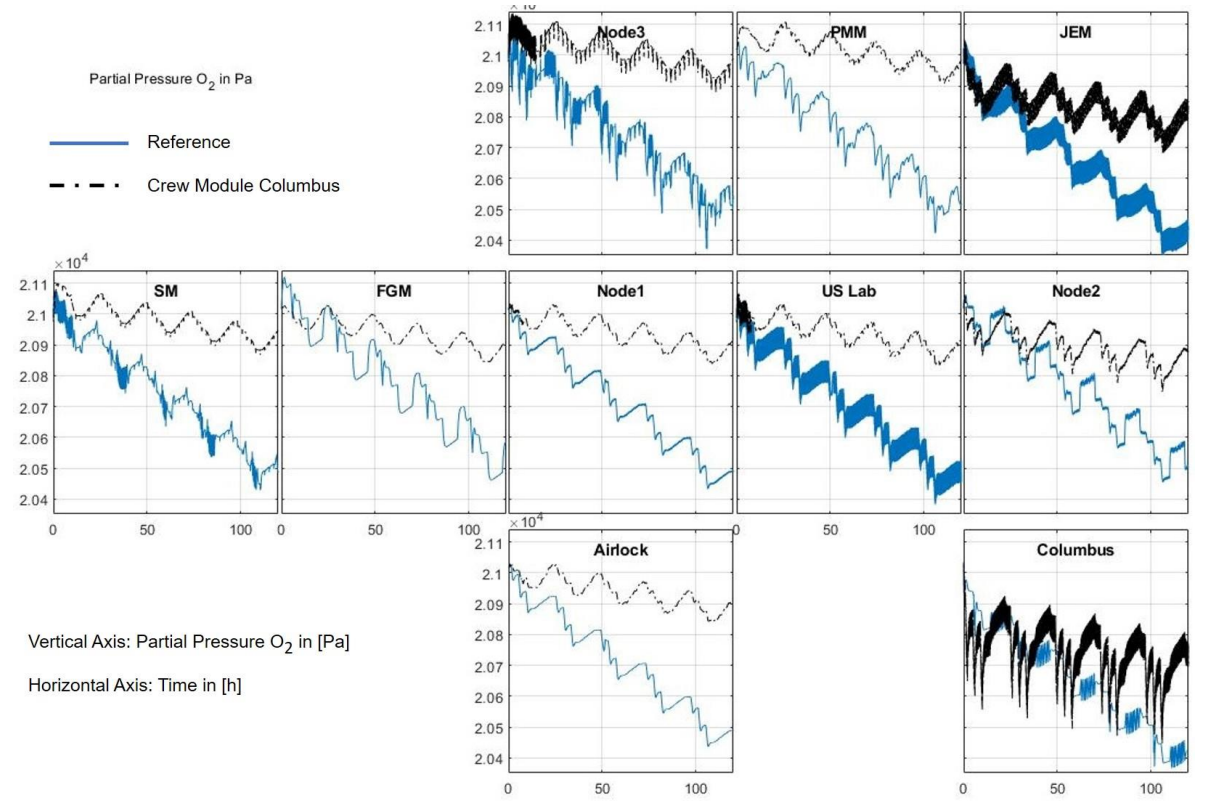

Fig. 6-10: Partial pressure of O_2 simulated with crew in Columbus compared to the reference.

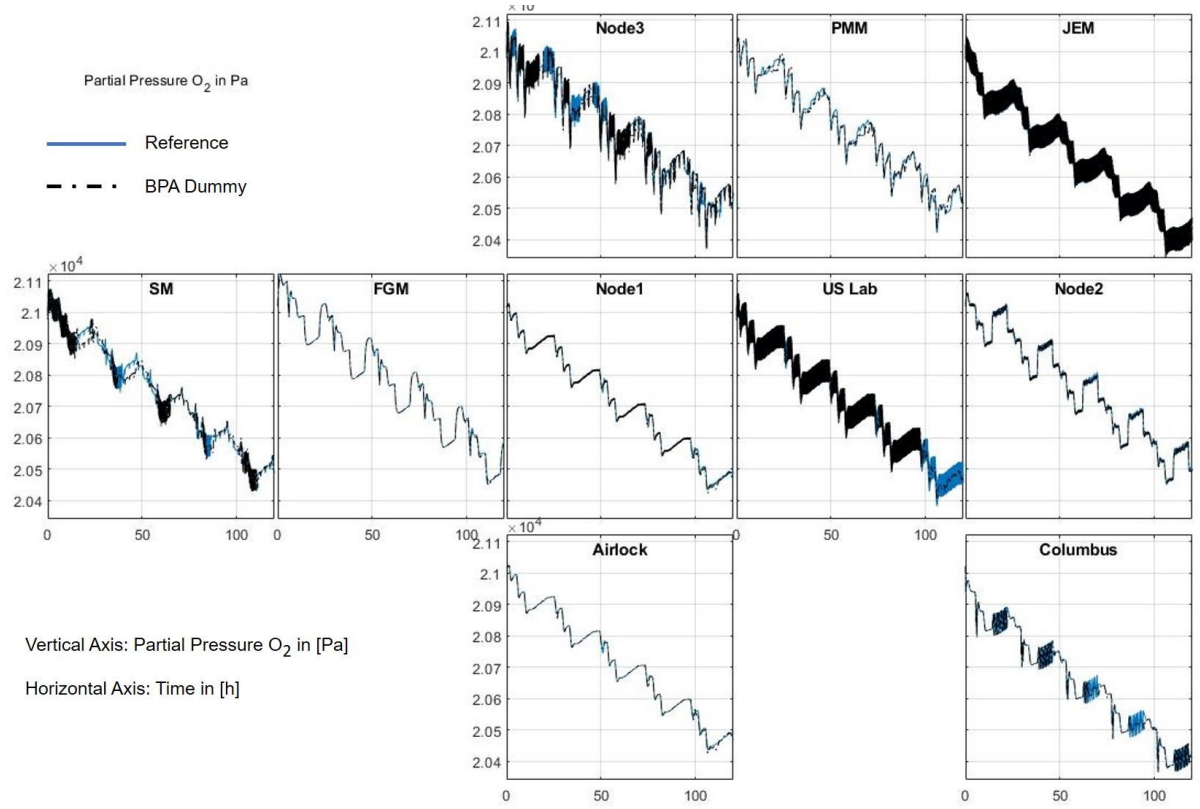

Fig. 6-11: Partial pressure of O_2 simulated with BPA Dummy compared to the reference.

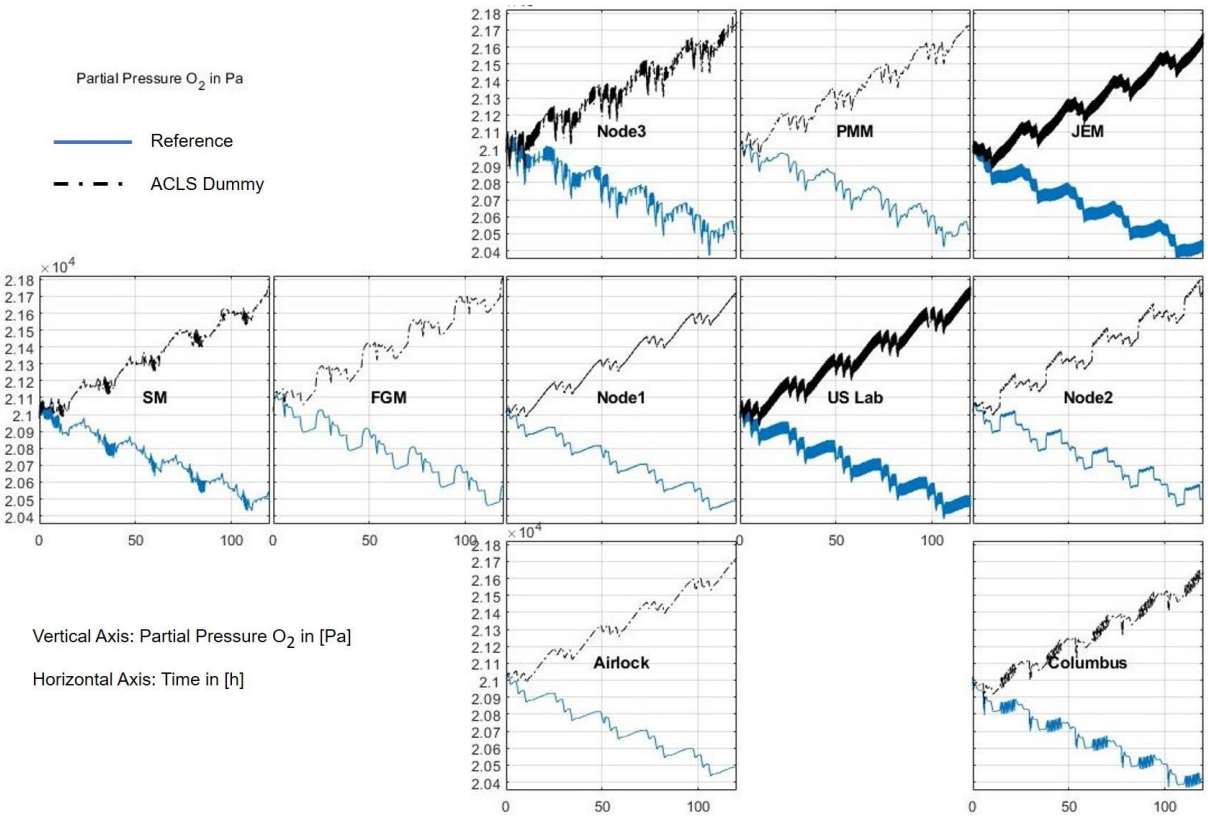

Fig. 6-12: Partial pressure of O_2 simulated with ACLS Dummy compared to the reference.

B.2 Results for the CrewModule parameter

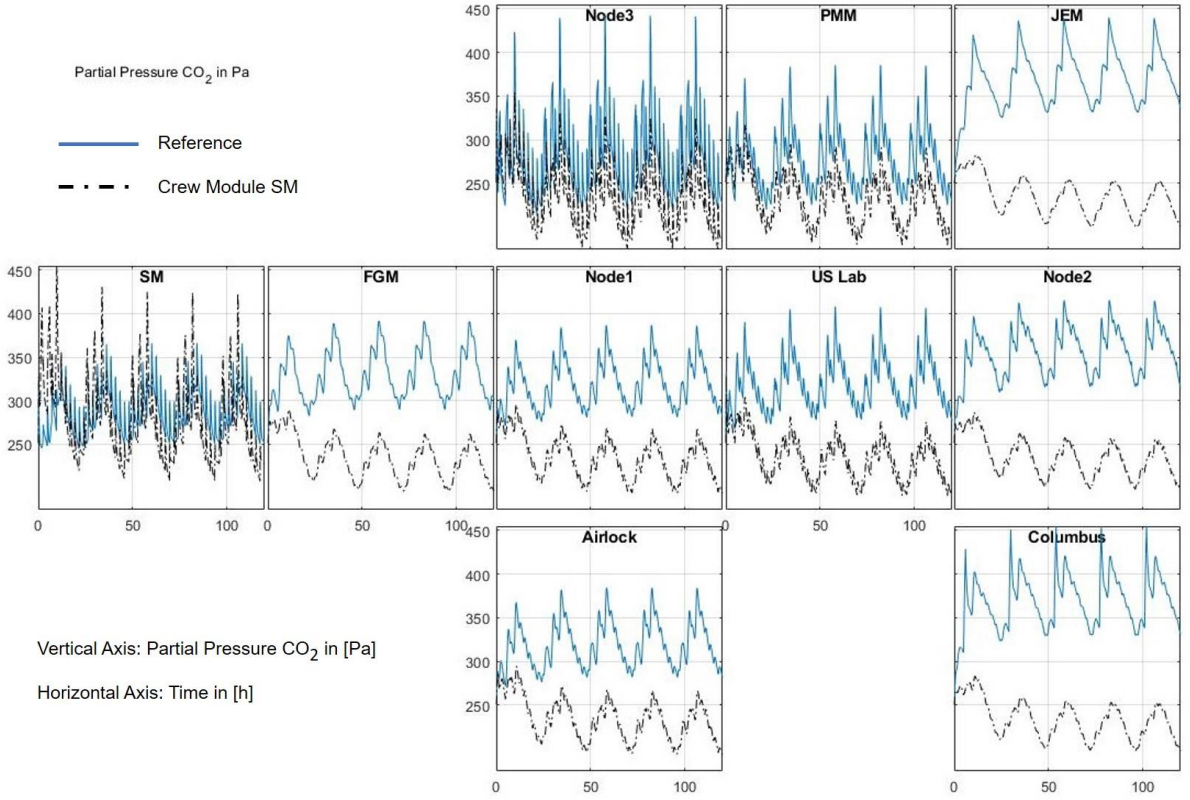

Fig. 6-13: Partial pressure of CO_2 simulated with crew in SM module compared to the reference.

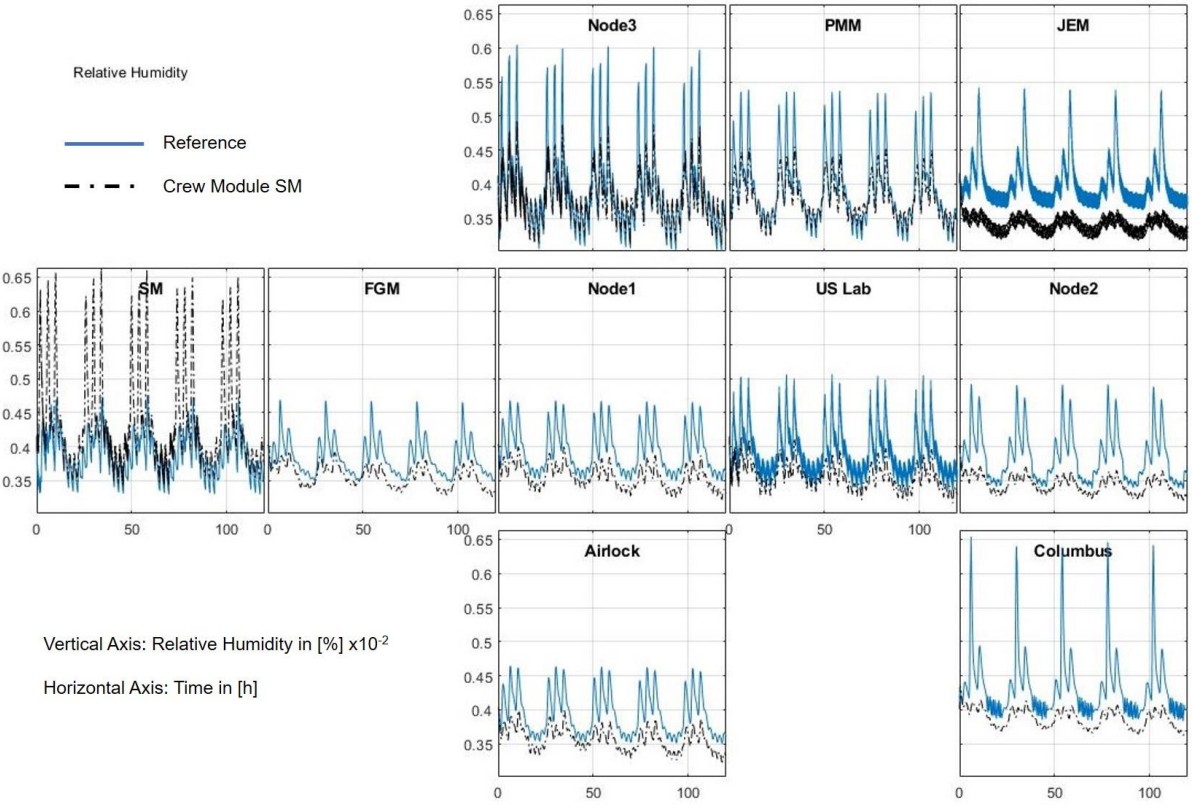

Fig. 6-14: Relative humidity simulated with crew in SM module compared to the reference.

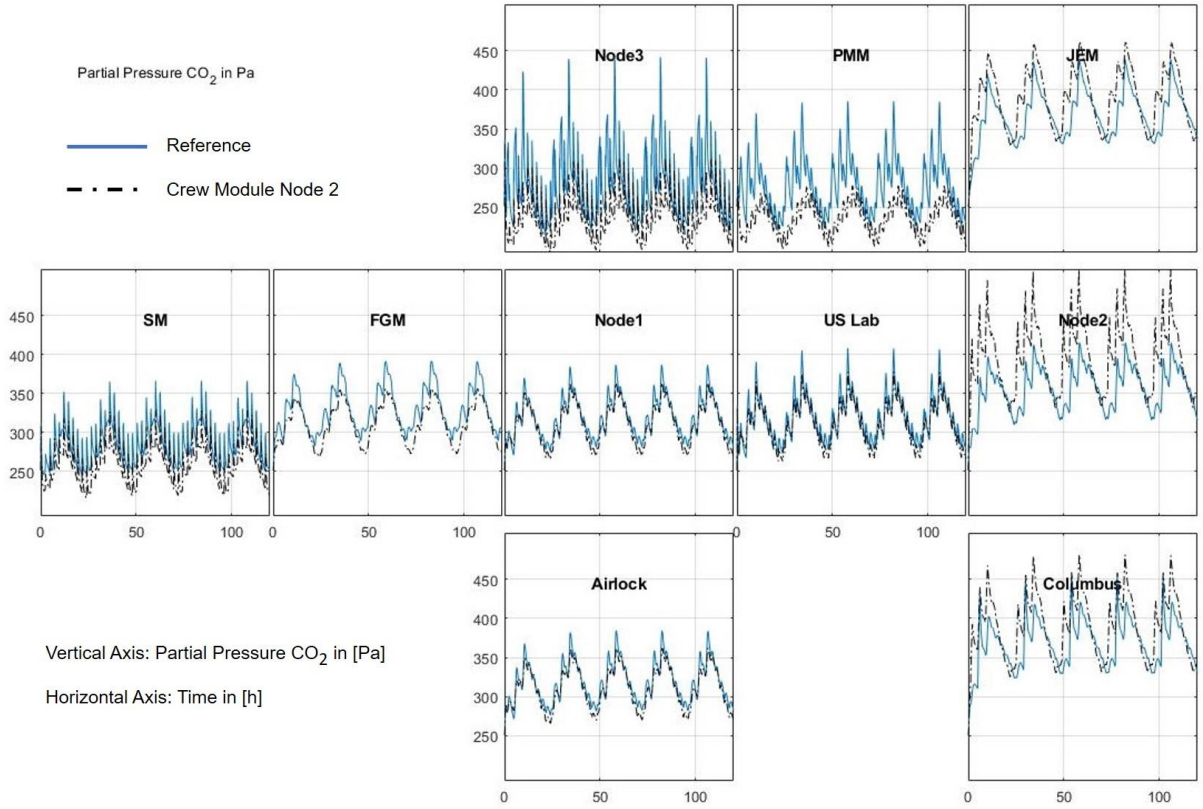

Fig. 6-15: Partial pressure of CO_2 simulated with crew in Node 2 module compared to the reference.

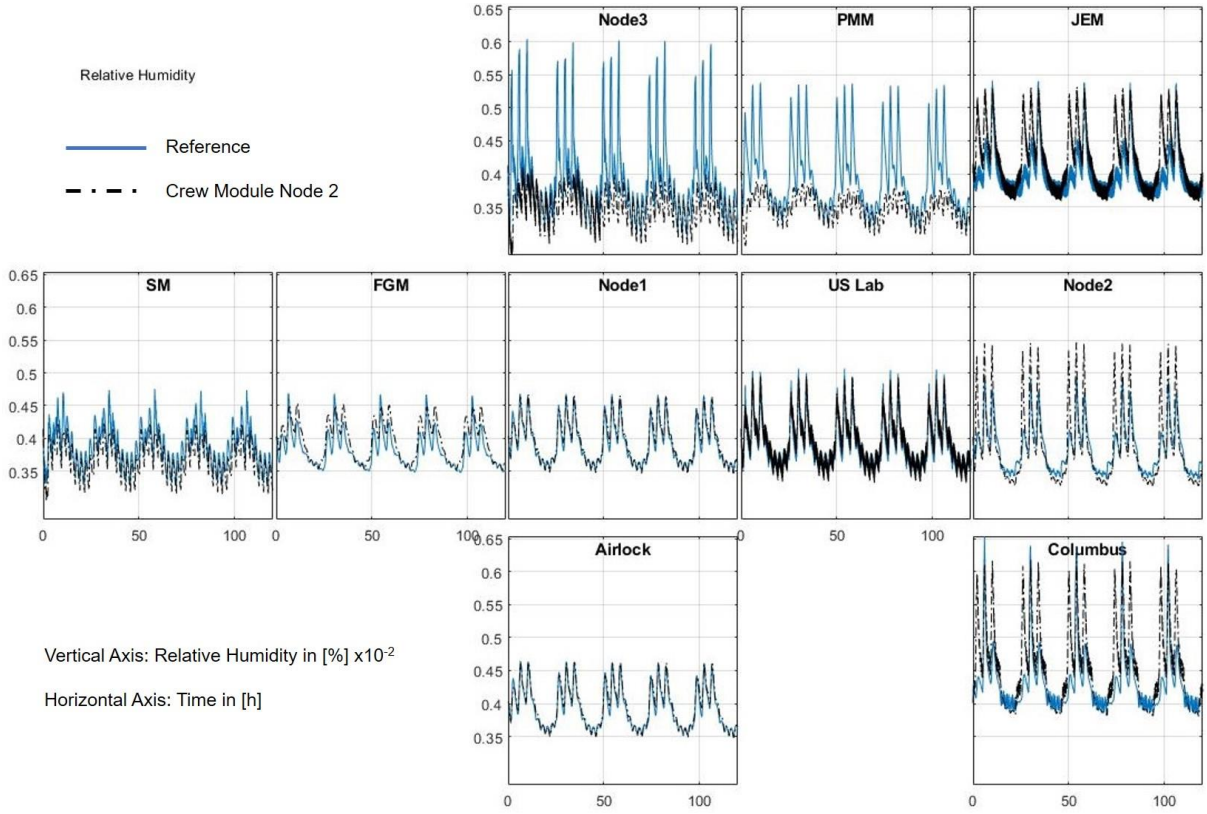

Fig. 6-16: Relative humidity simulated with crew in Node 2 module compared to the reference.

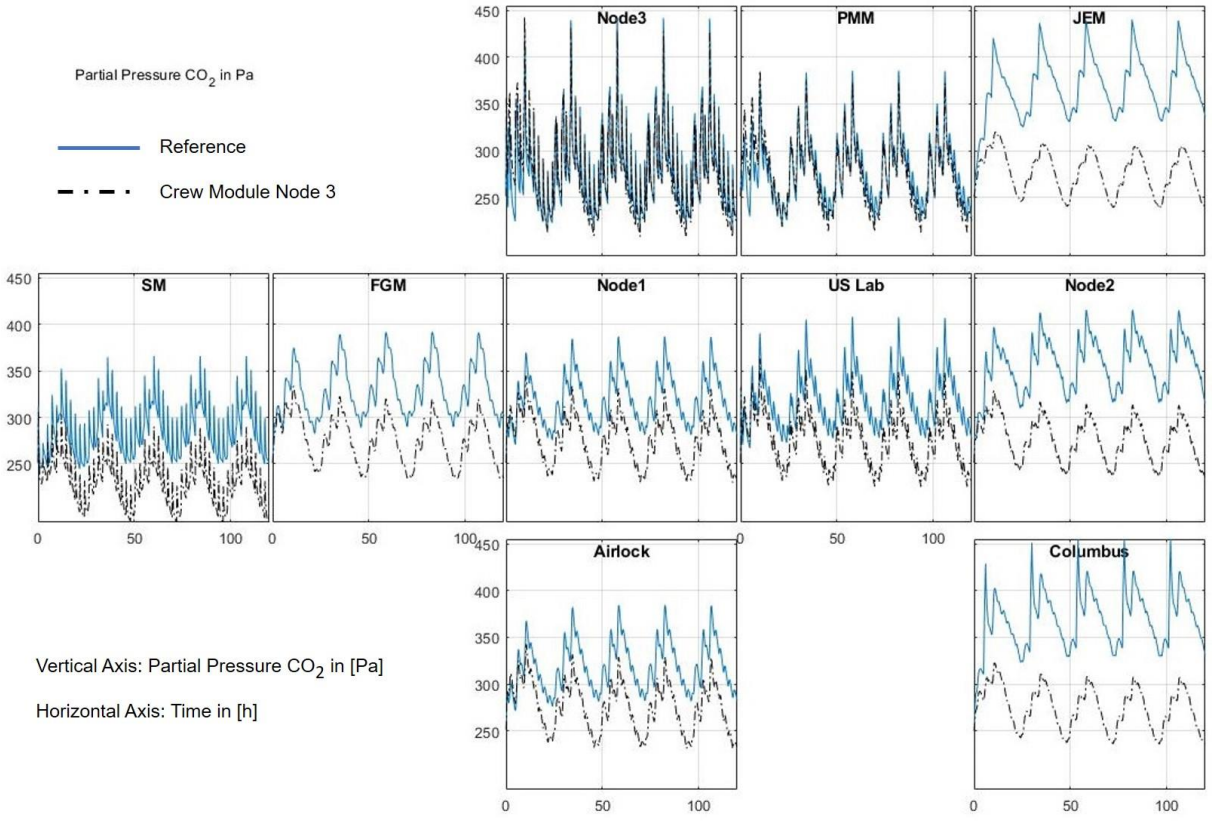

Fig. 6-17: Partial pressure of CO_2 simulated with crew in Node 3 module compared to the reference.

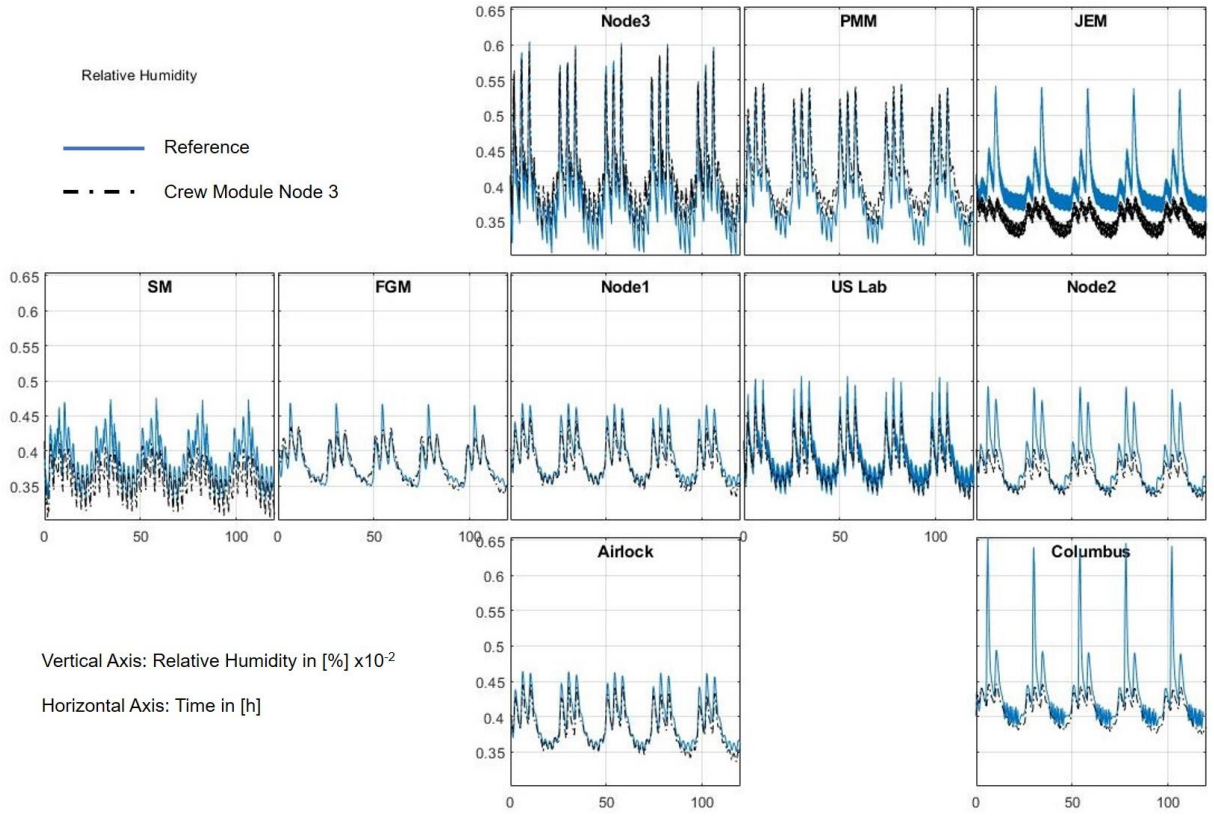

Fig. 6-18: Relative humidity simulated with crew in Node 3 module compared to the reference.

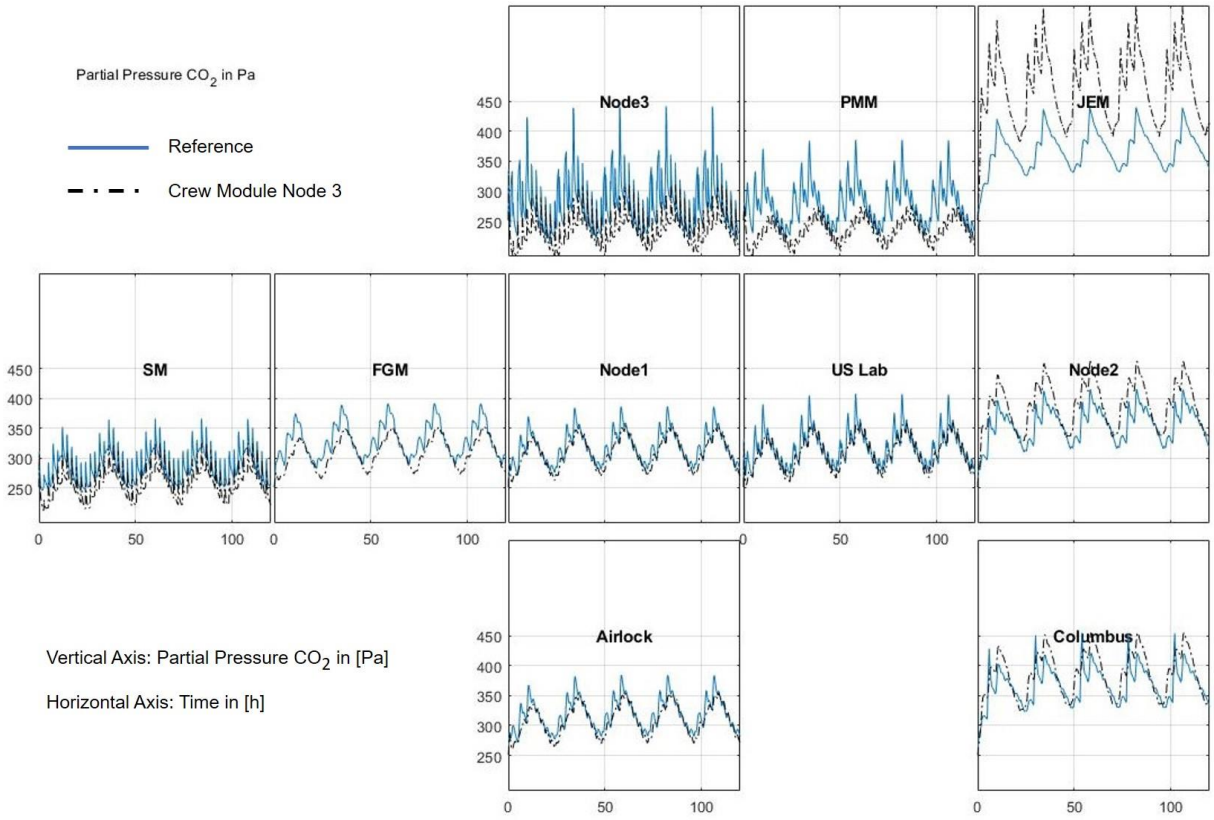

Fig. 6-19: Partial pressure of CO_2 simulated with crew in JEM module compared to the reference.

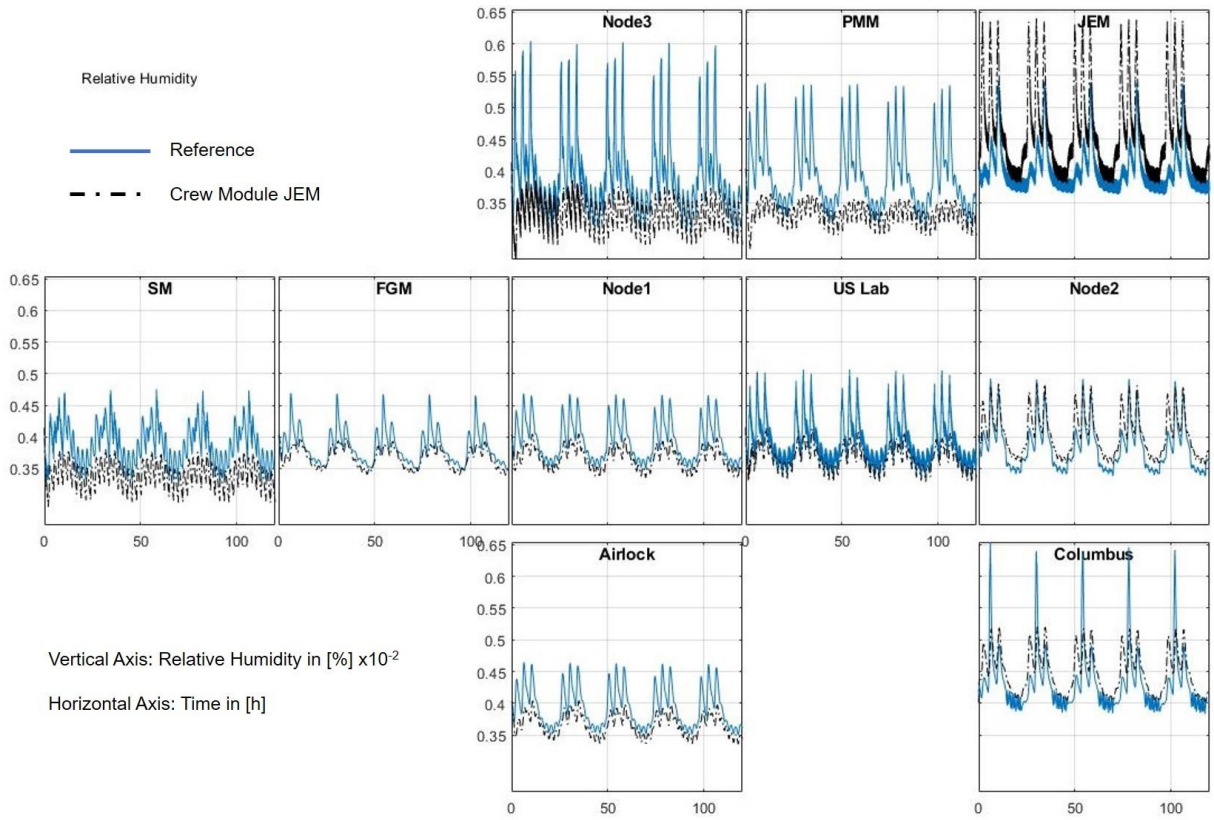

Fig. 6-20: Relative humidity simulated with crew in JEM module compared to the reference.

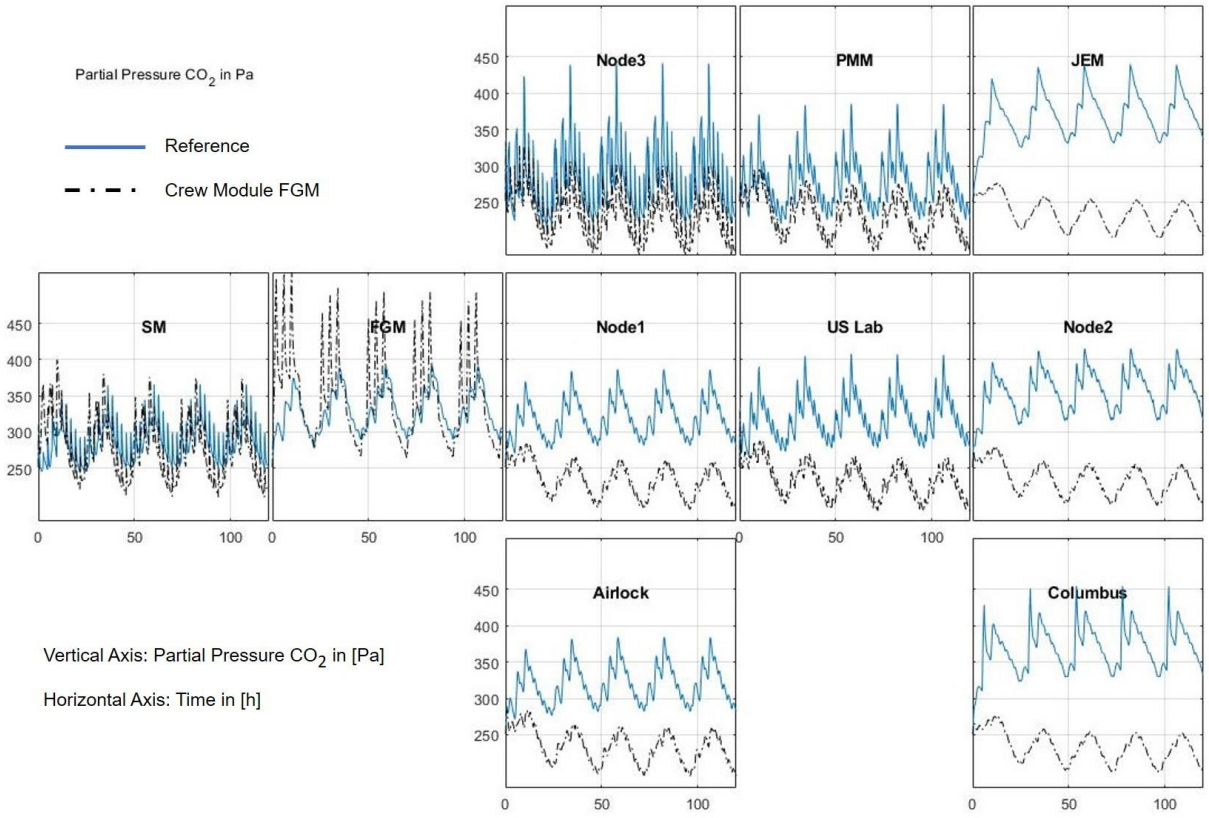

Fig. 6-21: Partial pressure of CO_2 simulated with crew in FGM module compared to the reference.